MECHANICAL RESTITUTION IN ISOLATED HUMAN MYOCARDIUM:
a study of underlying mechanisms and myocardial hypertrophy

Thesis presented to The University of London
for the degree of Doctor of Medicine
by

Ian Charles Cooper MB BS, MRCP

1990

ProQuest LLC.
789 East Eisenhower Parkway
P.O. Box 1346
Ann Arbor, MI 48106 – 1346

Abstract

The phenomenon of mechanical restitution is investigated in isolated strips of human, guinea-pig and ferret ventricular myocardium. Species differences, together with the effects of interventions known to influence the cellular handling of calcium, provide some insight into the mechanisms underlying mechanical restitution.

Mechanical restitution in human myocardium is described by three exponential processes; two recovery and one decay. The data presented support the hypothesis that the faster of the two recovery phases represents a combination of recovery of releasable calcium by the sarcoplasmic reticulum and reactivation of the slow inward current. Decay would seem to be a function of trans-sarcolemmal ionic gradients.

Hypertrophic human myocardium exhibits a slowed recovery phase of restitution. The data is compatible with the hypothesis that the sarcoplasmic reticulum of hypertrophic human myocardium has a reduced rate of uptake and an increased capacity for calcium. The time course of mechanical restitution provides a possible explanation for a cellular mechanism of pulsus alternans.

ICC 1990

To my daughter, Alice

Acknowledgements

This project would not have been possible without the joint ideas, support and encouragement of Dr MM Webb-Peploe of the Department of Cardiology, St Thomas' Hospital and Dr CH Fry of the Department of Physiology, United Medical and Dental School, St Thomas' Campus.

Dr Fry's expertise, versatility and dedication have been a constant guide to my education, thinking and practice. I have a great deal to thank him for.

The samples of of human myocardium were obtained by Mr MV Braimbridge and Mr BT Williams of the Department of Cardiothoracic Surgery. I am grateful for their co-operation in this project.

For financial assistance I thank Sterling-Winthrop Pharmaceuticals and St Thomas' Hospital Cardiac Research Fund. The latter owes its existence solely to the hard work and altruism of Dr Webb-Peploe.

I thank Dr DJ Coltart and Dr BS Jenkins for their support and Alex Crowther for his unique ability to grasp problems of all kinds and to provide sound advice on every occasion.

Finally, I would like to thank all my colleagues at St Thomas' who have provided much encouragement and friendship throughout various difficulties.

Contents

Figures

Tables

CHAPTER 1: INTRODUCTION

'But the practitioner must be prepared to meet with many cases which he will be unable to refer satisfactorily to any of these forms; for the complications of heart disease are so numerous and varied that, as we have said before, it becomes impossible to determine the exact nature of every case that may come before us. Fortunately it is unnecessary to do so, for if we can be certain that organic disease really exists, the treatment, as has been before remarked, will depend less on the nature of the valvular affection than on the vital and anatomical state of the heart itself.'

William Stokes. The Diseases of the Heart and the Aorta. 1854 Hodges and Smith, Dublin.

BACKGROUND

Failure of the heart to perform its requisite function is a common cause of morbidity and mortality and may herald the end-stage of a number of disease processes. In the clinical setting it is not always possible to distinguish the relative contribution of the different lesions giving rise to heart failure. In many cases it may be of prognostic and therapeutic importance to do so. For example, it may be important to assess myocardial contractility and to distinguish this from abnormalites of loading, geometry and valvular function. Primary heart muscle diseases producing *myocardial failure* alone are rather less common than those conditions in which myocardial failure may be a sequela. Many underlying conditions producing *pump failure* are now surgically correctable (e.g. valve replacement), but these conditions may themselves give rise to altered geometry of the ventricles and damage to the myocardium itself. Each of these may in turn become additional factors contributing to heart failure. In many cases myocardial damage may be reversible by treatment of an underlying condition, such as the relief of valve stenosis (Selzer, 1987), whereas, in other cases (e.g. in aortic regurgitation) the

damage may not be reversible, in which case valve replacement may not be as effective in dealing with the underlying problem.

The pathophysiology of myocardial failure at the cellular level in man is incompletely understood. Changes in myocardial structure and function in response to physiological and pathological stress have been described in a number of different mammalian species (Reviews: Cooper, 1987; Chilian & Marcus, 1987; Banchero, 1987; Morgan *et al*, 1987; Wikman-Coffelt *et al*, 1979; Scheuer & Buttrick, 1987). Much of this work has been on the compensatory hypertrophic response of the myocardium to increased afterload, in which important species differences have been described (Scheuer & Buttrick, 1987). Little work has been undertaken on isolated human myocardium, to date, possibly largely due to the lack of availablity of suitable samples.

The aim of this investigation is to examine the *in-vitro* properties of human myocardium from patients with different underlying cardiac disorders, and to compare these with the clinical findings and *in-vivo* measurements made in the same patients.

HYPERTROPHY

Hypertension is a common antecedent of congestive cardiac failure and may occur in up to 75% of all patients presenting with heart failure (McKee *et al*, 1971). With the reduced incidence of rheumatic fever and the increasing age of the population, there has been a change in the spectrum and natural history of valvular heart disease. Rheumatic valve lesions are becoming less common in developed countries, and non-rheumatic aortic stenosis is now an important cause of morbidity and mortality especially in elderly patients (Selzer, 1987). The hypertrophic response of the mammalian myocardium to increased afterload, such as that seen in hypertension and valvular disease has been the subject of a great deal of investigation in recent years. The thickening of the myocardium in response to increased afterload is associated with an increase in cellular protein synthesis, an increase in size of the myocyte and an increase in the number of sarcomeres. While this is beneficial at first, the increased energy demands of the hypertrophic muscle eventually out-weighs the supply of what has become a relative decrease in capillary density. Thus, with a sustained increase in afterload, a chronic energy deficit occurs, leading to a vicious circle cell death, failure to compensate and cardiac failure (Katz, 1990).

Systolic Function

The increased pressure demand induced by increasing resistance to left ventricular outflow provokes compensatory myocardial hypertrophy. Preservation of left ventricular function by this means plays an important role in the natural history of aortic stenosis. Unlike the dilated ventricle caused by volume overload, left ventricular volumes and function will remain normal in the pressure overloaded hypertrophied ventricle, until the late stages of the disease (Selzer, 1987). If the hypertrophic response is inadequate then cardiac failure is likely to develop (Gunther & Grossman, 1979), and ultimately, in patients with increasingly severe aortic stenosis left ventricular function may become depressed. When the left ventricle is no longer able to maintain an adequate cardiac output, there may be a rapid deterioration of the condition of the patient, leading to death if the stenosis is not relieved. Even in late stages, surgical relief of aortic stenosis may reverse hypertrophy and restore ventricular function to normal (Selzer, 1987); although recovery of the structural changes of the myocardium may be incomplete (Krayenbuehl *et al*, 1983 and 1989).

Myocardial hypertrophy develops in response to a number of different pathological and physiological stimuli. It is most often seen in patients with chronic systolic pressure overload but also occurs in atheletes, particularly those undertaking isometric exercise such as weight-lifting (Huston *et al*, 1985). The nature of the so-called hypertrophic response in man varies depending on the type of stimulus (Scheuer & Buttrick, 1987).

Much work has been performed on myocardial function in different mammalian models of hypertrophy. Bing *et al* (1971) induced left ventricular hypertrophy in rats by banding of the aorta. Isolated trabeculae from these animals displayed normal isometric twitch tension, prolonged time to peak tension and reduced isotonic shortening velocity. These findings were consistent with those made in hypertrophied hearts from rats with renovascular hypertension, which demonstrated normal tension development with reduced velocity of contraction in the isolated papillary muscle, and reduced velocity of circumferential fibre shortening (V_{CF}) and maximum rate of rise of tension (dP/dt max) in the isolated perfused heart (Capasso *et al*, 1981 and Schaible *et al*, 1984). In studies on chronic aortic constriction in the dog (Sasayama *et al*, 1976) and piglet (Wisenbaugh *et al*, 1983) normal ventricular function and wall stress was associated with artificially induced left ventricular hypertrophy, once it had developed. It has been suggested that when investigating contractility in animal models such as these, that time is allowed for compensatory hypertrophy to occur (Williams & Potter, 1974), bearing in mind that abrupt increase in afterload does not normally occur in pathological states in man. This problem is exemplified by the fact that depression of

contractility is seen in the intact ventricle and papillary muscles from cats after 30 days of pulmonary banding (Spann *et al*, 1972), whereas between six and twenty-four weeks contractility may return to normal (Williams & Potter, 1974). This transient impairment of the hypertrophied right ventricle has been challenged by Cooper *et al* (1981), who found no evidence of impaired right ventricular function (cardiac output and ejection fraction) in pulmonary-artery-banded cats up to sixty weeks after surgery, but did demonstrate a reduction in shortening velocity and isometric tension in papillary muscles from the same hearts. Similarly, Spann *et al* (1972) have shown that cardiac index and stroke volume may be maintained despite markedly depressed velocity of contractile element shortening (V_{CE}) in the intact ventricle and active tension and V_{CE} in isolated papillary muscles from the same hearts. In another short-term study Lecarpentier *et al* (1987) looked at guinea-pigs with left ventricular hypertrophy induced by clipping of the abdominal aorta. The animals were killed after three weeks and those with mild hypertrophy showed normal tension production whereas those with more severe hypertrophy demonstrated reduced twitch tension and reduced rate of tension development in the papillary muscle. In pulmonary–artery–banded ferrets, papillary muscles removed after 1-3 months showed reduced isometric twitch tension as well as prolonged twitch duration (Gwathmey & Morgan, 1985).

In a comparison of two different models of hypertrophy (in the rat left ventricle and the cat right ventricle), in which the degree of hypertrophy was roughly equivalent, different effects on *in vitro* indices of contractility were observed (Cooper & Tomanek, 1987). Peak isometric tension and rate of tension development was not changed in the rat, but there was an increase in the duration of active tension. In the cat model, there was a reduction in both the amount and rate of development of isometric twitch tension, and prolongation of contraction was not seen. Apart from species differences, there are a number of other differences between these two models. In one case the left ventricle was examined in the spontaneously hypertensive rat, and in the other the right ventricle was examined in the cat that had undergone pulmonary artery banding as a kitten. While the differences observed in different animal models appear to be largely consistent from one study to another, and whether these differences can be explained in terms of species differences alone, it is none the less clear that extrapolation to disease in the human is inappropriate. Indeed, it seems that models of right ventricular hypertrophy (largely that of chronic progressive pressure overload in the pulmonary banded cat) differ fundamentally from models of left ventricular hypertrophy (Cooper, 1987).

In studies on larger mammals exposed to both acute and chronic left ventricular pressure overload, in both intact hearts an *in vitro* muscle strips, contractility does not appear to be compromised in the same way. In a study on intact dogs, Sasayama *et al* (1976) described the response of the left ventricle to chronic pressure overload by ascending aortic constriction. There was initial dilation with increased wall stress, followed by gradual wall thickening and reduction in wall stress towards normal. Following these adaptations, contractility, in terms of velocity of circumferential fibre shortening (V_{CF}), returned to normal. In a more detailed study, using the same model, Sasayama *et al* (1977) found that the end-systolic left ventricular pressure/diameter relationship was shifted to the left and that end-systolic wall-stress/diameter relationship (E_{max}) was normal in hypertrophy. In the pig too, with supravalvular aortic banding, contractility (E_{max}) was unimpaired in all but the most extreme hypertrophy (Wisenbaugh *et al*, 1983).

In catheter studies on human subjects the normal relationship between left ventricular ejection fraction and V_{CF}, and wall stress is preserved in patients with aortic stenosis, suggesting that if the hypertrophic response is sufficient to maintain normal wall stress, normal contractility will be maintained (Gunter & Grossman, 1979). Similarly, Spann *et al* (1980) found normal left-ventricular-wall-stress/volume ratios in patients with aortic stenosis and no symptoms of heart failure, but reduced ratios in patients with symptomatic heart failure. Krayenbuehl *et al* (1982) found the degree of hypertrophy in patients with pure or predominant aortic stenosis to be significantly increased in those patients with a reduced normalized systolic ejection rate. Thus, in chronic pressure overload in the human being, ventricular function appears to be preserved in moderate (or early stages of) hypertrophy, but is compromised in later stages.

Thus, the literature suffers from the study of different animal models of hypertrophy in various species studied by methods of different sensitivity and at different times. It appears however, that in general the left ventricle more effectively compensates for chronic pressure overload than the right and that left ventricular function may be normal in larger mammals with mild to moderate degrees of hypertrophy. It is notable that the methods used to examine contractility both in man and in other large mammals have failed to show any impairment of ventricular function in anything but severe hypertrophy (Spann *et al*, 1980). In smaller mammals abnormalities are found in the contractility of isolated strips of myocardium in mild degrees of hypertrophy. The failure to detect any abnormalities in man may merely reflect the relative insensitivity of the methods used (Scheuer & Buttrick, 1987). Depending on how detailed an examination is made, in moderate pressure overload myocardial function in man may be

found to be relatively normal. Usually the only abnormality at this stage is a prolonged time course of contraction associated with normal tension production.

Diastolic Function

Impaired diastolic function is a consistent finding in both animal models and in patients with pressure overload. There is a decrease in the rate of relaxation and an increased time to peak relaxation in chronic left ventricular hypertrophy in the rat isolated papillary muscle (Capasso *et al*, 1981). In pulmonary–artery–banded cats the maximum rate of relaxation of the right ventricular papillary muscle is reduced (Cooper *et al*, 1981). In the papillary muscles from guinea-pigs with left ventricular hypertrophy, relaxation and the load sensitivity of relaxation is impaired in severe, but not in mild hypertrophy (Lecarpentier *et al*, 1987).

Echocardiographic studies in man have shown significant prolongation of isovolumic relaxation in left ventricular hypertrophy secondary to aortic stenosis or severe hypertension (Hanrath *et al*, 1980). In a catheter study including eight patients with hypertension, and electrocardiographic evidence of left ventricular hypertrophy, Hirota (1980) showed no difference in peak negative dP/dt compared to controls. The left ventricular systolic pressure in these patients was 156±9 mm Hg (mean±SD) and no indication was given as to the degree of hypertrophy. Inouye *et al* (1984) examined left ventricular gated blood pool scans in 39 patients with hypertension (systolic pressure 156±14 mm Hg [mean±SD], diastolic 103±5 mm Hg) and found significant impairment in ventricular filling whch was related to the degree of hypertrophy as assessed echocardiographically. Abnormalities of ventricular filling may also be found in hypertensive patients with no electrocardiographic evidence of hypertrophy (Smith *et al*, 1985). In this study, however, all eight patients with echocardiographic evidence of hypertrophy had abnormal ventricular filling as opposed to four out of twelve with no hypertrophy. Abnormalities of ventricular filling are common in hypertensive patients and it has been argued that this is in part responsible for abnormal cardiovascular reflexes in this group of patients (Fouad, 1987)

Thus, impaired relaxation and ventricular filling seem to occur early in left ventricular hypertrophy, when systolic function may remain normal (Fouad *et al*, 1980). These abnormalities can be found in man as well as smaller mammals and are related to the degree of hypertrophy.

Contractile Proteins

A possible explanation for the observed species differences in their response to increased pressure loads concerns the role of the contractile proteins. In some species the imposition of a pathologically increased afterload results in a rapid shift of the isoenzyme pattern of myosin. In the rat and rabbit, with mixed, but predominant V_1 myosin isoenzyme (having a high myosin ATPase activity) the shift is towards the V_3 isoenzyme which has decreased ATPase activity. This allows a compensatory reduction in energy expenditure at the expense of a reduced velocity of contraction. In larger mammals such as the ferret, dog, pig and man the predominant myosin isoenzyme is V_3 and no such shift has been demonstrated. (For review see Scheuer & Buttrick, 1987). The guinea-pig is an exception; like man it has predominantly a V_3 isoenzyme pattern (Clark *et al*, 1982) and may therefore be a more suitable small mammalian model of left ventricular hypertrophy in man (Lecarpentier *et al*, 1987).

It is postulated that a change in myosin isoenzyme pattern results in the observed changes in the time course of contraction of hypertrophic myocardium in some mammals, and that a lack of change in other species accounts for their apparent preservation of contractility (Wisenbaugh *et al*, 1983). The mechanism for myosin isoenzyme shift is not understood, but since myosin synthesis is under genetic control it would seem that the myocyte modifies its genetic expression in response to altered loading (Scheuer & Buttrick, 1987).

Sarcoplasmic Reticulum

Ventricular hypertrophy has been shown to be associated with abnormal function of the sarcoplasmic reticulum (SR) in a number of animal studies. In SR from the rabbit with ascending aortic constriction the rate of uptake and total binding of calcium is reduced when compared to control animals (Sordahl *et al*, 1973). This contrasts with the situation in physiological hypertrophy (illustrating one of the major differences between physiological and pathological hypertrophy) in which the SR shows increased binding and uptake of calcium (Malhotra *et al*, 1981). In severe pathological hypertrophy there is a consistant depression of calcium uptake, calcium binding and abnormal calcium ATPase activity by the SR. In mild hypertrophy in the rat, however, enhanced calcium ATPase activity and calcium uptake have been demonstrated (Limas *et al*, 1980).

Using tissue from the recipients of cardiac transplants Lindenmayer *et al* (1971) showed a reduced rate of uptake and capacity for calcium binding compared to normal animal hearts. In the same preparation Harigaya & Schwartz (1969) also showed slower rates of uptake and release than animal controls. In the absence of suitable

normal human controls it remains difficult to interpret the findings of each of these studies.

Mitochondria

In a model of left ventricular hypertrophy in the rabbit Sordahl *et al* (1973) demonstrated marked increases in mitochondrial respiratory activity in the early stages of hypertrophy, and decreases in more severe hypertrophy. Mitochondrial calcium uptake was normal in the presence of hypertrophy alone, but reduced if heart failure supervened. Similarly, mitochondrial respiration is increased in hypertrophied non-failing human hearts as compared to failing hearts without hypertrophy (Lindenmayer *et al*, 1971). So it would seem that increased mitochondrial respiratory activity may compensate for increased metabolic requirements in hypertrophy, and that failure of mitochondrial compensation coincides with the onset of clinical heart failure.

Ultrastructure

Electron-microscopic studies of human myocardium have revealed well defined cellular ultrastructural abnormalities in the myocardium from hearts with left ventricular hypertrophy (Schaper and Schaper, 1983). Myocardial cells are enlarged with large nuclei and prominent nucleoli and cytoplasmic inclusions. The mitochondria show irregular size, shape and distribution. There is a reduction in contractile material with 'thinning' of fibres. In addition there is cellular proliferation and degeneration, an increase of interstitial tissue (collagen) and cellular phagocytosis. In patients with heart failure there is a significant loss of contractile material and mitochondria combined with an increase in fibrous tissue. The reason for the increase in collagen remains largely unclear (Weber *et al*, 1987), but it does provide a possible explanation for the occurence of cardiac failure in the later stages of hypertrophy and is a major factor responsible for diastolic dysfunction (Paulus & Brutsaert, 1982).

THE ISOLATED MUSCLE PREPARATION

In a classic series of experiments Abbott and Mommaerts (1958) extended the observations made by others on muscle mechanics and contractility in skeletal muscle and in intact heart preparations, and were the first to describe 'some of the fundamental mechanical characteristics of cardiac contractility' in the isolated mammalian papillary muscle preparation. Their techniques and findings, together with the widely accepted concept of the three element model of muscle (consisting of a contractile element, a

series elastic element and a parallel elastic element), adopted by Hill (1938), were to be the basis of further studies of myocardial contractility in the isolated muscle preparation (see Yang *et al*, 1978 for review), and continue to be applied today. This has allowed investigation of the intrinsic properties of cardiac muscle to complement studies of the intact heart. Much of the early work on isolated myocardium was performed in the 1960's by Sonnenblick and co-workers (Sonnenblick, 1962), and the first detailed description of the mechanical properties of isolated human myocardium was published in 1965 (Sonnenblick *et al*, 1965). In this study human left ventricular papillary muscles were removed at the time of mitral valve replacement and mounted vertically in a muscle bath containing gassed Krebs-Ringer solution. The preparations were either whole or split papillary muscles and both isotonic and isometric contractions were studied. An increase in isometric twitch tension could be demonstrated by increasing the muscle length and with the addition of stropanthidin or noradrenalin to the bathing medium. However the classical Bowditch staircase response (Bowditch, 1871) could not be demonstrated in these preparations. This was probably due to problems of tissue viability, largely due to the poor oxygen diffusion into these large specimens (cross-sectional area: 5.5±3.9 mm^2).

The rate of diffusion of oxygen to the centre of the isolated muscle preparation is a determinant of the size of the muscle which may be used in such experiments. In guinea-pig papillary muscles, following an initial recovery, there is a gradual fall of twitch tension to a new plateau level. This is accompanied by severe histological damage to the core of the preparation, so that eventually a healthy cylinder of contractile tissue surrounds a non-contractile core (Shattock *et al*, 1983). It was suggested by Hill (1928) that the critical diameter of a preparation such as this was approximately 1.0mm. However, the 'critical diameter' depends on temperature and the rate of stimulation. It has been suggested that if the effects of increased frequency are being examined in cat papillary muscles at 38°C, then 0.6mm is the critical diameter (Koch-Weser, 1963). Certainly, loss of viable muscle tissue occuring progressively throughout experiments on isolated muscles is a significant methodological problem and should be considered particularly when serial comparative measurements are made. Nonetheless, experiments which are based upon the comparison of measurements made within a short period of time are unlikely to suffer from the problem of tissue viability, and many workers have used this preparation as a valuable investigative tool.

FORCE-INTERVAL RELATIONSHIP

Since Bowditch (1871) it has been well recognised that the interval between beats of contracting heart muscle is one of the factors which determines the strength of contraction. By observing this phenomenon in strips of frog ventricle, and by altering the external ionic environment, Niedergerke (1956) was able to conclude that the the strength of contraction in this preparation was somehow controlled by the 'concentration of calcium in a superficially located region of the heart cell' and that the staircase phenomenon might be due to a change in this calcium concentration. It was then suggested that the interval dependent changes in the force of contraction of cardiac muscle might result from changes in the *duration* of the active state as well as changes in the *degree of activation* of the muscle (Koch-Weser & Blinks, 1963). Although the underlying mechanisms for the phenomena associated with force-interval changes in contractility were unknown, Koch-Weser and Blinks, in their review of the subject in 1963, concluded that study of the force-interval relationship would continue to aid our understanding of underlying inotropic mechanisms.

Well recognised clinical manifestations of the force-interval relationship are phenomena such as: 1. premature depolarisation resulting in reduced mechanical contraction, 2. the increased contraction associated with the beat following a premature beat (post-extrasystolic potentiation) and 3. the increase in contractility resulting from an increase in heart rate (Braunwald *et al,* 1988). In addition, there is evidence that mechanical alternans may be explained in terms of the cellular processes underlying the force-interval relationship (Mahler & Rogel, 1970).

Moreover, it has been proposed that quantifying the force-interval relationship in isolated rabbit papillary muscles provides a unique index of contractility which is independent of loading (Anderson *et al*, 1973). Until this time, an ideal index of contractility had been lacking, as even V_{max} (the maximum velocity of shortening of the unloaded muscle) had been shown to be dependent on muscle length (Donald *et al*, 1972).

The ratio of the maximum rate of rise of isometric twitch tension (max dT/dt) of a post-extrasystolic beat and the steady-state beat that preceeded it (so-called force-interval ratio), and the ratio of the max dT/dt of an ectopic beat and its preceding steady state beat, are both indices which are independent of muscle length in the isolated muscle preparation (Anderson *et al*, 1976). The force interval ratio is reduced by inotropic stimuli such as the addition of isoprenaline (Anderson *et al*, 1976) or calcium

(Anderson, Manring, Arentzen *et al*, 1977) to the bathing medium. These findings have been confirmed in the intact heart in the chronically instrumented concious dog when looking at the maximum rate of rise of pressure (max dP/dt) in response to artificially paced extrasystoles (Anderson *et al*, 1976).

The force-interval ratio is also altered in pathological states. In a comparative study on the isolated papillary muscles from cats having undergone pulmonary artery constriction, approximately 18 weeks previously, the force-interval ratio was significantly greater in the hypertrophied than in the control group (Anderson, Manring, Arentzen *et al*, 1977), despite there being no difference in peak tension, time to peak tension or max dT/dt between the two groups.

In a catheter study of 42 patients between the ages of 1.5 and 20 years, the left ventricular force interval relationship was compared to ventricular function, size and wall thickness (Anderson *et al*, 1979). The force-interval ratio was increased in patients with either increased left ventricular end-diastolic diameter or increased posterior wall thickness, and reduced in those with dilated ventricles and heart failure. These changes were consistent with the qualitative changes seen in equivalent mammalian models of hypertrophy and cardiac failure. A fundamental technical difficulty in this study was the need to ensure that the pre-load of each of the pair of beats, being compared as a ratio, was identical; for, while the *ratio* should be independent of pre-load, the two *contractions* must occur with identical loading. This, of course, is not a problem in the isolated muscle preparation, but presents obvious practical difficulties in the intact heart, leading to a degree of uncertainty in determining whether changes in developed pressure or max dP/dt are due to a change in loading conditions or to a manifestation of the force-interval relationship.

MECHANICAL RESTITUTION

A more detailed appraisal of the force-frequency relationship in the intact ventricle was made by Burkhoff *et al* (1984) in the isolated perfused dog left ventricle. In their model, they extended and confirmed the observations of Braveny & Kruta (1958) who had described another manifestation of the force-interval relationship, so-called 'mechanical restitution'.

The mechanical restitution curve (MRC) describes the relationship between the size of a test beat and its preceding interval, where the muscle is stimulated at a regular steady

state and test beats are inserted at various intervals (Figure 1). When the preceding interval is short, the test beat is of low amplitude. As the interval is lengthened the amplitude of the test beats increase until a maximum is reached. Thereafter the size of the test beat will decline with lengthening intervals. These two phases of the MRC describe the increase and subsequent decrease of the capacity of the muscle to contract in relation to changes in the duration of the preceding interval.

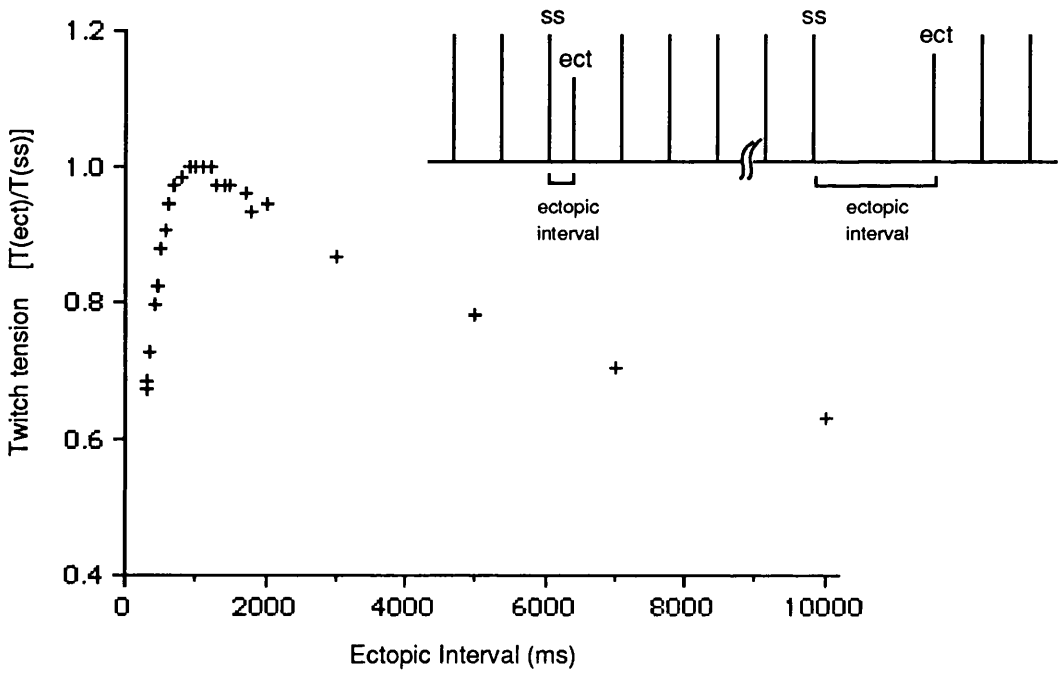

Figure 1. **The Mechanical Restitution Curve** (from a guinea-pig papillary muscle). Developed twitch tension from an ectopic stimulus (T(ect)) divided by the twitch tension of the preceding steady state beat (T(ss)) is plotted against the interval between the pair of stimuli (ectopic interval). The inset shows, in diagramatic form, a typical stimulus protocol with a steady state frequency of 1 Hz and two extra stimuli.

The MRC in isolated cat and rabbit papillary muscles was examined by Anderson, Manring and Johnson (1977). Intervals of up to 2.5 seconds were used, and the resulting curves were found to be altered by different interventions. The effect of a change in muscle length was to simply scale the magnitude of the force in the MRC. Alterations of external $[Ca^{2+}]$, addition of ouabain, histamine, noradrenalin and pentobarbitone to the medium, however, had the effect of altering both the force produced and the *shape* of the MRC.

The shape of the MRC appears to vary between species. In the rabbit the force of a test contraction reaches a maximum value with a preceding interval of 0.7 to 0.8 s (Edman & Johannson, 1976). The curve then forms a plateau and the force of contraction decays in a two phasic exponential manner with relatively long time constants. In the rat, however, maximum values are seen at 60 - 120 s, after which there is some decline in force of contraction (Ragnarsdóttir *et al*, 1982). In the dog, the MRC forms a plateau at approximately one second (Mahler & Rogel, 1970) which continues for at least up to 2.5 s (longest time interval examined) (Anderson *et al*, 1976).

In the cat there are differences in the MRC depending on the age of the animal (Maylie, 1982). The kitten MRC shows sharp rise followed by a rapid decline. Adult cat MRC, however, shows a monoexponential rise, followed by a plateau and slow decline. Similarly, in the rat the MRC shows a much faster recovery phase in 4–10 day old rats as compared to 3 month old rats (Minelli *et al*, 1985).

In Burkhoff's work on the isolated perfused isovolumically beating canine left ventricle (1984), the shape of the MRC was very similar to that found in isolated canine ventricular muscle (Anderson *et al*, 1976). The MRC in the intact ventricle of the dog showed a monoexponential rise to a plateau which continued for as long as 10–15 s. The time constant of this rising exponential phase was 189±30 ms (Yue *et al*, 1985) and it was postulated that the process described by this time constant represented the recovery of the 'calcium releaseablity' of the sarcoplasmic reticulum; this recovery process being quite distinct from the time-dependent recovery of cell membrane conductances (Elzinga *et al*, 1981). In other words, the phenomena associated with the MRC could be related to events within the myocardial cell at the ultrastructural level; events that might otherwise be impossible to examine directly.

The accepted model of excitation-contraction coupling ultimately involves the action of calcium ions on myofibrils causing muscular contraction. The source of the activating calcium remains the subject of debate. Most, however agree that activator calcium is delivered to the contractile apparatus from two main sources. Firstly, from the trans-sarcolemmal influx of Ca^{2+}, and secondly from the sarcoplasmic reticulum. The stimulus for release of Ca^{2+} from the SR may be the cellular influx of Ca^{2+} during the action potential (Fabiato & Fabiato, 1977), but the amount of Ca^{2+} available for release by the SR is a time dependent process, suggesting the presence of an intracellular circulation of Ca^{2+} which takes a finite time to recover between beats (Tritthart *et al*, 1973b). It has been suggested that it is the variation of the amount of Ca^{2+} available for release by the SR which gives the mammalian myocardium its unique ability to modify

its contractile state in response to variations in stimulus frequency (Morad & Goldman, 1973). The evidence suggesting an intracellular circulation of Ca^{2+} has lead to the widely adopted two-compartment model for activator Ca^{2+} metabolism (Edman & Jóhannson, 1976). In this model Ca^{2+} is taken up by the release compartment (presumably part of the SR) only by transfer from the uptake compartment, which itself is responsible for the sequestration of Ca^{2+} from all sources (such as the myofilaments during relaxation and Ca^{2+} entering the cell from the outside). It is the transfer from the uptake to the release compartment which is believed to be the time limiting factor, explaining the observation of a fixed time interval for attainment of an optimum contractile response (Edman & Jóhannson, 1976). The time interval of optimal contractile response seems to be independent of the stimulation rate and has been found to be in the region of 800–1000ms in rabbit papillary muscle (Edman & Jóhannson, 1976), in intact dog and cat hearts (Elzinga *et al*, 1981) and in the intact human heart (Seed *et al*, 1984).

In a study of mechanical alternans in open–chest dogs (measuring isometric tension with a strain-gauge arch sewn into the right ventricular wall) Mahler & Rogel (1970) described different time constants of restitution for the beats following large and for those following small contractions. The rate at which mechanical alternans could be induced was dependent on the restitution time constant of the muscle. In other words, if the time taken for the release compartment to reach its optimum capacity is prolonged, an optimal contractile response may not occur at heart rates above a certain level. Hence, tissue with a long time constant may develop alternans at slower rates. This, they argued, might explain the increased incidence of pulsus alternans in patients with heart disease, if there was a prolonged restitution time constant in diseased states.

Indeed, the mechanical restitution time constant was found to be prolonged in isolated myocardium obtained from patients with heart failure as compared to those without (Fry *et al*, 1983). There was also a significant negative correlation between the cinéangiographic left ventricular ejection fraction and the restitution time constant. Furthermore, the time constant was shortened by adrenalin, and lengthened by verapamil, raising the question of whether the time course of recovery of activator calcium is dependent on the recovery of membrane ionic channels rather than the accumulation of Ca^{2+} by the release compartment of the SR.

Further evidence that altered calcium handling in the myopathic hypertrophied human myocardium may be influenced by dysfunction of the sarcolemma as well as the sarcoplasmic reticulum is presented in a study of isolated myocardium obtained from

the hearts of transplant recipients (Gwathmey *et al*, 1987). In this study intracellular calcium transients were recorded with the calcium sensitive photoprotein aequorin. Both the duration of isometric contraction and of the calcium transient were found to be increased in hypertrophic myocardium. The calcium transients exhibited a biphasic pattern. The early component (similar to that seen in the monophasic transient in normal myocardium) is blocked by ryanodine (a substance known to block release of calcium from the SR). The second component, which coincides with the presence of prolonged twitch duration, is abolished by the slow inward current blocker verapamil.

SLOW INWARD CURRENT

It is now well recognised that at least two distinct voltage-gated membrane channels carry the inward currents of sodium and calcium ions during the cardiac action potential (Reuter, 1979). The first inward current (I_{Na}), carried by sodium ions, is responsible for the initial rapid upstroke of the cardiac action potential. I_{Na} may be abolished by removal of sodium ions and by tetrodotoxin (TTX). The second inward current has previously been described in multicellular preparations as a single component, or 'slow' inward current. Studies on single cells have now revealed several components of the so-called 'slow' inward current, the fastest of which has properties similar to those described for the original slow inward current. This fast component of the second inward current (I_{si}) is carried, like the original slow inward current largely by calcium ions and has slower kinetics and different voltage dependence than the faster I_{Na}. It is blocked by divalent cations such as manganese, cadmium, cobalt and nickel and the so-called calcium channel blockers such as nifedipine, verapamil and diltiazem. It is insensitive to TTX. The activation kinetics of the fast component of the second inward current in single cells appear to be much faster than had been realised from multicellular preparations (Mitchell *et al*, 1983). The explanation of this discrepancy is unclear at present, but may involve the reduced series resistance of single cells and the effects of outward currents from either the membrane recorded or from adjacent membranes.

Calcium entering the cell during the action potential is thought both to increase the intracellular pool of calcium available for myofibrillar activation and provide an important link between excitation of the cell membrane and release of calcium by the SR (Fabiato & Fabiato, 1977). Understanding of the I_{si} has been largely helped by voltage clamp studies and more recently single channels have been recorded using patch clamp techniques (Reuter, 1984).

It has been proposed that a more convenient way of studying the slow inward current is to generate so-called 'slow' (or 'slow response') action potentials (Tritthart *et al*, 1973a). Slow action potentials may be elicited by either blocking the fast inward current with TTX or artificial partial depolarisation of the cell membrane to around –50mV. At this potential the I_{Na} is inactivated and the resulting 'slow' action potential is of shorter duration, has a slower upstroke velocity and has a higher threshold of excitation than normal (Tritthart *et al*, 1973a). The upstroke velocity and overshoot of the slow action potential are both increased with increased calcium concentration and isoprenaline, and reduced by verapamil (Kohlhart *et al*, 1978), confirming the dependence of the slow action potential on I_{si}.

Fundamental biophysical theory states that if an action potential is not propagated (i.e. field stimulation is used) the ionic current (I_i) is related to the rate of change of membrane potential (dV/dt) by:

$$I_i = -C_m \; dV/dt$$

-where the constant, C_m , is the membrane capacitance.

Thus, the rate of rise of the action potential is proportional to the total ionic current flowing in the depolarising phase (Jack *et al*, 1976).

The maximum rate of rise of the action potential (max dV/dt) had been proposed as an index of sodium conductance in the normal action potential (Weidmann, 1955). Gettes and Reuter (1974) have looked at the restitution of max dV/dt in the guinea-pig papillary muscle in which the resting membrane potential was altered by changing the external potassium concentration. The time constant of recovery was approximately 20msec in the normal action potential, when the resting membrane potential was more negative than -80mV, and more than 100msec when the membrane potential was between -65 and -60mV. In the same study, voltage clamp experiments were performed and similar time constants of recovery of the slow inward current were found to the time constants of recovery of the action potential plateau duration. Despite this close relationship, and because of a dependence of the slow action potential on other factors such as the outward potassium current, Reuter (1979) has advised caution when interpreting slow action potential measurements. Malécot and Trautwein (1987) have described a close linear relationship between max dV/dt of slow action potentials and the calcium current in the single cell voltage clamp preparation in the guinea pig. It must

be pointed out, however, that in this preparation the outward current was blocked by the substitution of caesium for potassium in the internal medium. The limited specificity of the slow action potential probably restricts its use to qualitative rather than quantitative description of the slow inward current (Malécot & Trautwein, 1987).

The role of I_{si} in hypertrophic myocardium was examined by Hemwall *et al* (1984), who looked at slow action potentials in the right ventricular papillary muscles of cats with pulmonary artery banding. In this preparation the slow action potentials were of lower amplitude, slower upstroke velocity and shorter duration than those of controls. It must be said, however, that this tissue was studied 14-35 days after pulmonary artery banding and that right ventricular hypertrophy was associated with reduced isometric twitch tension.

SUMMARY AND PROPOSALS

Cardiac failure in association with increased afterload is a common problem. It would seem that the hypertrophic response is one which initially compensates for the increased demands caused by increased afterload. Eventually the myocardium may fail to compensate, marking the onset of clinical heart failure. In patients with valvular heart disease symptoms may predate the onset of myocardial failure, which itself may herald a rapid deterioration in the patient's condition.

The precise mechanism(s) by which the hypertrophic reponse occurs are unknown. There are well described alterations in myocardial structure (both gross histological and ultrastructural) and cellular function. The force-interval relationship, as manifest by the mechanical restitution curve, theoretically provides a means of examining some of the processes which occur within the cell over the brief periods between muscular contraction. The processes underlying the mechanical restitution curve have yet to be elucidated, but it has been shown that mechanical restitution is altered in pathological states and may be manipulated by agents which affect the slow inward current.

The purpose of this current investigation is to:

1. Investigate mechanical restitution in isolated strips of human myocardium obtained from patients with left-ventricular pressure overload and to compare the results with those from patients with left-ventricular volume overload and those with normal ventricles.

2. Compare the clinical status and *in-vivo* assessment of contractility with the *in-vitro* performance of isolated muscle in the same patients.

3. Investigate possible cellular mechanisms underlying mechanical restitution; in particular the relative roles of the slow inward current and the sarcoplasmic reticulum in the recovery phase of restitution.

CHAPTER 2: METHODS

CLINICAL AND CATHETER DATA

Clinical classification

All human myocardium was obtained at the time of cardiac surgery. In most cases the patients were investigated in the Department of Cardiology at St Thomas' Hospital and most operations were performed at St Thomas' Hospital. Full history and clinical examination was obtained from all patients. A recent drug history was obtained, together with details of premedication and anaesthetic agents used. Exercise tolerance was classified acording to the New York Heart Association (NYHA) classification (NYHA, 1964). Standard twelve lead resting electrocardiography, two-dimensional and Doppler echocardiography were performed in most cases.

Catheter procedure

All patients underwent cardiac catheterization before surgery. In some cases this was performed at another hospital.

In all patients catheterized at St Thomas Hospital this was performed by percutaneous catheterization of the right femoral artery and vein using the Seldinger technique (Seldinger, 1953). Premedication was not routinely prescribed. Pressures were measured using strain–gauge transducers connected via fluid-filled tubing to the intravascular catheters. The zero reference point was at the level of the sternal angle. The on–line computer provided maximum, minimum and mean pressures, and ventricular end-diastolic pressures. Simultaneous and withdrawal valve gradients (mean and peak) together with valve opening times were also available on–line. Cardiac output was estimated by the Direct Fick Method (modified by estimating oxygen consumption), the Indicator Dilution Method (using Indocyanine-green dye), and

angiographic volumes where appropriate. Valvular regurgitation was quantified angiographically according to the criteria proposed by Sellers *et al* (1964). Valve areas were calculated using Gorlin and Gorlin's formulae (Gorlin & Gorlin, 1951):

$$\text{Aortic Valve Area} = \frac{\text{Aortic valve flow (ml/sec)}}{44.5\sqrt{\text{Mean aortic gradient (mm Hg)}}}$$

$$\text{Mitral Valve Area} = \frac{\text{Mitral valve flow (ml/sec)}}{31\sqrt{\text{Mean mitral gradient (mm Hg)}}}$$

Where aortic and mitral valve areas are in cm^2.

35mm ciné left ventriculography was performed in the right anterior oblique projection at 50 frames per second. All angiograms were reveiwed and measured by myself. The projected ventriculogram was outlined on paper with a pencil and subsequently digitised using a digitising tablet (Summagraphics Corp., Los Angeles, USA) interfaced to an Apple Macintosh microcomputer. The traces were then analysed using a specially written program ('MacAngio') (Hughes *et al* 1988). The program calculates left ventricular volumes by two methods: i. using an area-length formula for the RAO projection (Kennedy *et al*, 1970), and ii. by a single-plane modification of the multiple slice method (Chapman *et al*, 1958). Mean V_{CF} was calculated, using the computer program according to the following formula:

$$\text{Mean } V_{CF} = \frac{(C_{ED} - C_{ES})}{(C_{ED} \times ET)}$$

where:

Mean V_{CF} = Mean equatorial V_{CF} during the ejection phase of left ventricular systole

C_{ED} = End diastolic circumference, in cm

C_{ES} = End systolic circumference, in cm

ET = Ejection time, in seconds

IN-VITRO EXPERIMENTS

The basic layout of the experimental apparatus is shown in Figure 2 below. Essentially, this may be divided into four components; 1. the muscle bath, 2. the stimulator, 3. isometric tension recording, and 4. transmembrane action-potential recording.

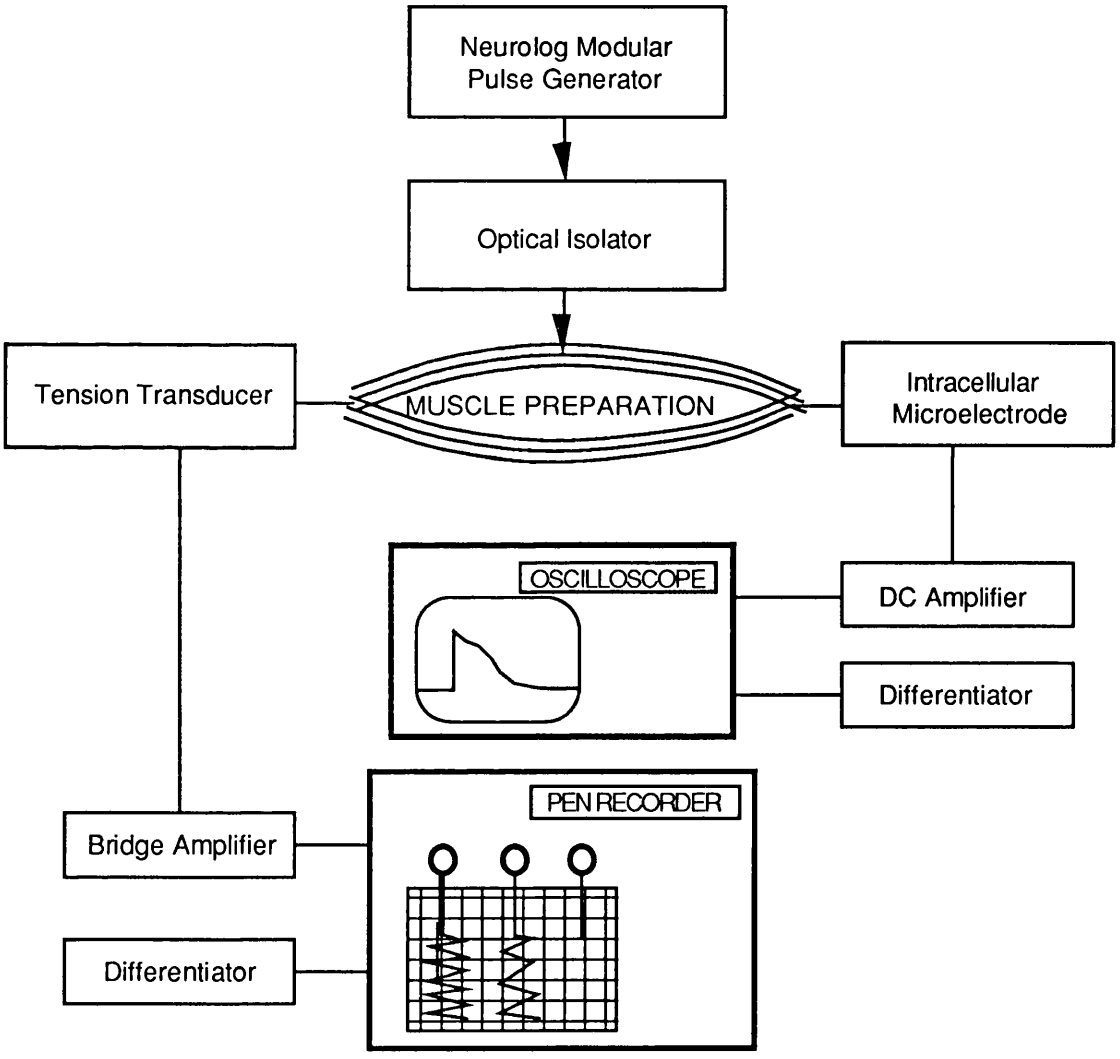

Figure 2. Layout of basic apparatus

MUSCLE PREPARATIONS

Human Tissue

All preparations of human myocardium were taken from biopsy specimens obtained at the time of cardiac surgery. Only ventricular myocardium was used. Biopsies were taken from either the subendocardial left-ventricular free wall (in the case of aortic valve replacement) or left-ventricular papillary muscle (in the case of mitral valve replacement). All biopsies were taken as soon as possible after the onset of cardio-pulmonary bypass and subsequent cardioplegia. In practice, the diseased aortic or mitral valve would be removed just prior to taking the biopsy. This procedure was approved by the ethical committee of St Thomas' Hospital. Care was taken in handling the specimen at the time of biopsy and transport as excessive stretching or crushing tended to cause irreversible damage to the tissue. Specimens were transported in modified Tyrode's solution that had been previously gassed with 95% oxygen and 5% carbon dioxide at room temperature. Transfer from the operating theatre to the physiology laboratory would typically take approximately 5–10 minutes. On two occasions specimens were stored overnight at 4°C. Following this treatment one specimen failed to contract and the other contracted very poorly. Neither of these form part of this study. Towards the end of the study some specimens were obtained from other nearby hospitals. These were transported in exactly the same way and took approximately half an hour to reach the laboratory.

Dissection of the tissue was performed under a layer of modified Tyrode's solution in a glass dish with a silcone gel base (Sylgard: 184 Silicone Elastomer Kit, Hopkin & Williams, Romford). It became clear that any undue stretching, at this stage, would have a permanent effect on the ability of the mounted preparation to contract. The specimen was therefore handled with great care (using watchmaker's forceps under direct vision with a binocular dissecting microscope). The endocardium (if present) was usually carefully stripped away (using opthalmic butterfly scissors) and the preparation pinned in two places to the silcone gel base of the dissecting dish, with fine entomology pins. (Dissecting instruments from John Weiss Ltd. London)

The objective was to cut (from the biopsy specimen) a preparation of muscle fibres which were in close parallel alignment. Two parallel cuts (see Figure 3) were made with a fine blade in such a region of the specimen to produce a strip of muscle approximately 5mm x 1mm with a "V"-shaped cross-section. 7/0 silk was then looped

under, forming a ligature around each end of the preparation before the ends were finally cut from the biopsy specimen. The silk thread was then used to tie the preparation to the fixed hook in the muscle bath (at one end) and the tension transducer hook (at the other).

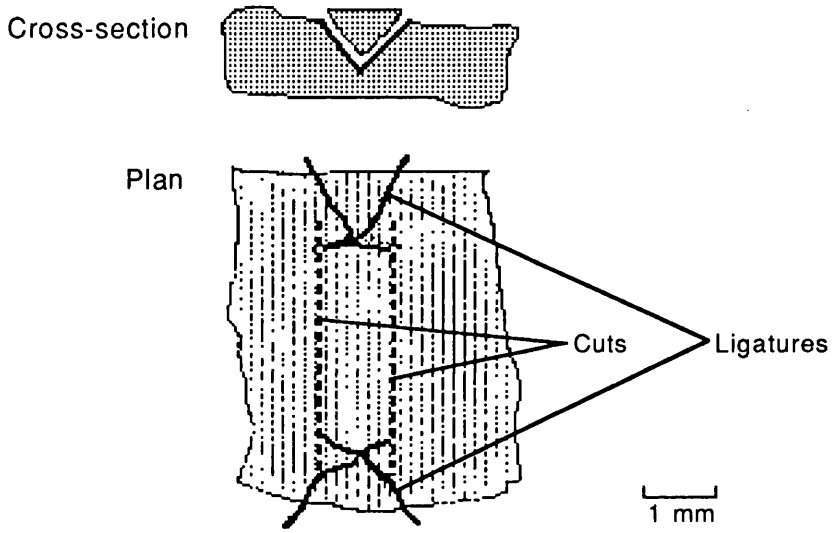

Figure 3. Dissection of muscle preparation from biopsy specimen.

Animal Tissue

For comparison with human tissue, ventricular myocardium was obtained from laboratory bred guinea-pigs and ferrets.

Guinea-pigs

The guinea-pigs were albino females weighing 250g–300g. They were killed instantly by cervical dislocation and the heart was rapidly removed. The excised heart was then placed immediately in a dissecting dish containing gassed Tyrode's solution. The right ventricle was then opened along the intraventricular septum and a suitable right-ventricular papillary muscle was indentified. A ligature was tied around each end with 7/0 silk prior to excision. The papillary muscle was then mounted in the muscle bath in the same way as the human myocardial preparation.

Ferrets

Male albino or polecat ferrets weighing 1–1.5 kg were used. They were killed by an intra-peritoneal injection of sodium pentabarbitone and the heart rapidly excised. The heart was then opened under Tyrode's solution and either a right ventricular papillary muscle or trabeculum was ligatured and excised in the same way as the guinea-pig preparation above.

THE TABLE

Mechanical vibration is a potentially serious problem when measuring tension produced by small strips of twitching muscle. External vibration is likely to cause interference with the recording, especially when small amounts of tension are produced. In addition, a more major problem is that of intracellular microelectrode stability. Long-term cellular impalement by a glass microelectrode in the twitching muscle preparation is frequently difficult to acheive. It is therefore mandatory for the preparation and the microelectrode and holder to be isolated as much as possible from the effects of external vibration. For this reason the laboratory itself was situated in the basement of the building where vibrations from passing traffic was minimal. All parts of the apparatus required to be isolated from external vibration were mounted on a steel table (61cm x 61cm) lying on the laboratory bench. The table was constructed from a sheet of bright mild steel, 13 mm thick, lying on a wooden base and supported, beneath, by Neoprene© rubber blocks (SK Bearings Ltd. Cambridge, England). Parallel aluminium bars with a 'T'-shaped cross-section were screwed onto the table to allow the muscle

bath, micromanipulators, head-stage pre-amplifiers, superfusate supply, drainage lines etc. to be clamped into position.

MUSCLE BATH

The muscle bath was constructed in Perspex according to the design shown in Figure 4. The overall dimensions were 70mm x 40mm x 15mm. The muscle strip was mounted horizontally between two stainless steel hooks; one fixed to the floor of the trough, the other to the tension transducer (Isometric Force Transducer: Gould, Hainault, Essex) (Manufacturer's specifications: range ±30g, displacement ±0.06mm, frequency response flat to 60 Hz) .

In order to allow the muscle length to be adjusted, the tension transducer itself is fixed to a micromanipulator (Prior Scientific Instruments Ltd., Bishops Stortford, England). Size of the muscle could be measured by means of a calibrated eye-piece graticule on the dissecting microscope. The flow of superfusate through the trough was approximately 12ml per minute. The trough itself had a volume of 200µl; the solution therefore being replaced once every second. The preparation was field–stimulated by a pair of platinum plate-electrodes which lie along-side the muscle.

SUPERFUSATE SYSTEM

To permit the rapid change of solution two parallel systems were used. Each superfusate reservoir consisted of a glass bottle supported, on a shelf, one metre above the muscle bath. The gassed solution passed by gravity through polyethylene tubing (internal diameter 3mm) encased in 15mm diameter tubing acting as a water jacket. Water heated by a 'Water Thermostat' water bath (Radiometer, Copenhagen) was circulated through the water jacket in a counter-current fashion to warm the Tyrode's solution on its way down. Solutions could be changed by means of a two-way Teflon tap mounted on the table adjacent to the muscle bath. The tap allowed continuous flow of solutions from each reservoir to either the muscle bath or to waste. This ensured that solutions were pre-heated and gassed before being switched to enter the bath. The tubing connecting the tap to the muscle bath was approximately 5cm long, thus a rapid (<1 second) change in superfusate in the trough was achieved.

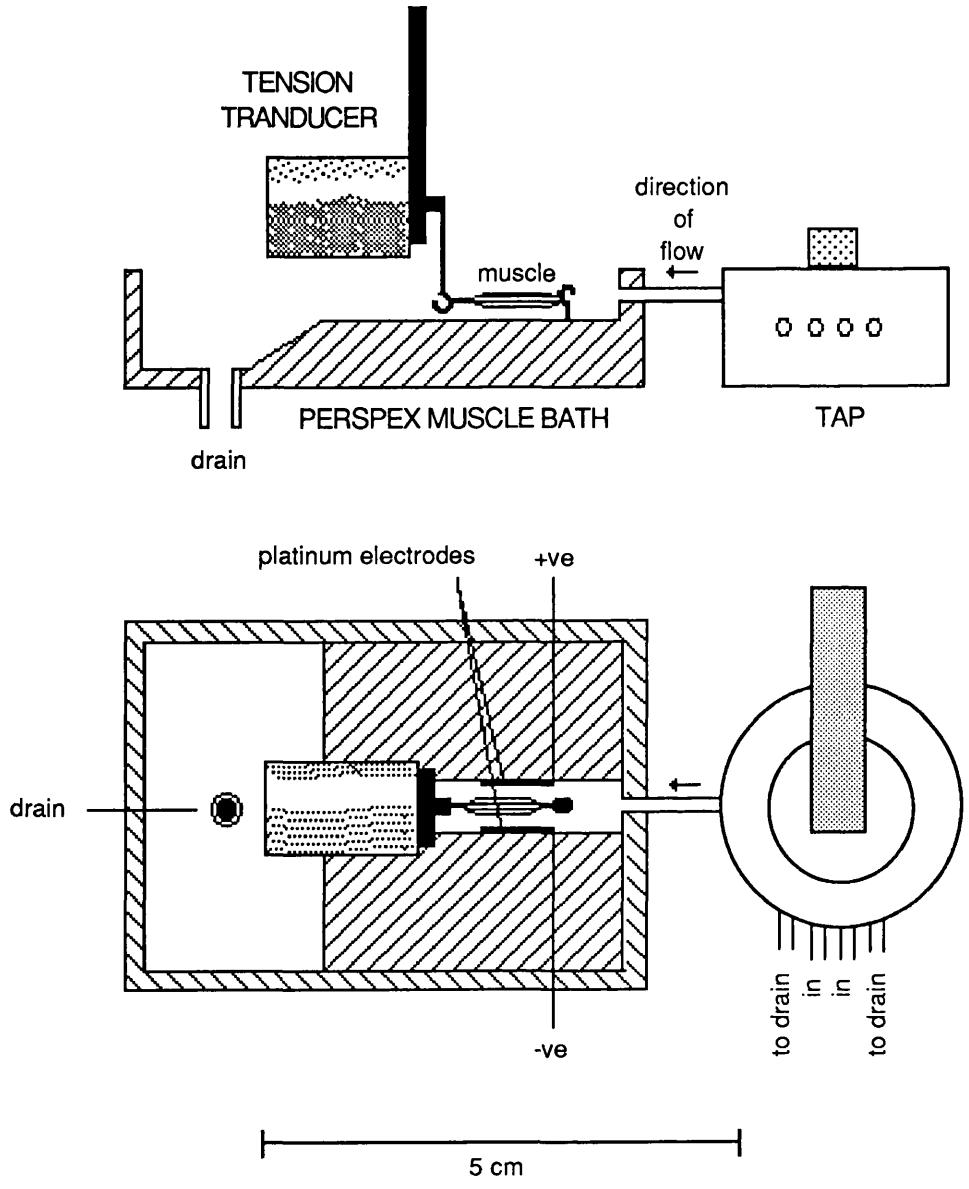

Figure 4. Diagram of the muscle bath and tap.

THE SUPERFUSATE

Unless otherwise stated, a modified Tyrode's solution, with the following composition, was used:

NaCl	118.0 mM
$NaHCO_3$	24.0 mM
$CaCl_2$	1.8 mM
$MgCl_2 \cdot 6H_2O$	1.0 mM
$NaH_2PO_4 \cdot 2H_2O$	0.4 mM
KCl	4.0 mM
Glucose	6.1 mM
Sodium pyruvate	5.0 mM

All chemicals were supplied by BDH Chemicals Ltd., Poole, England., and were of AnalaR® grade. The sodium chloride, sodium bicarbonate, glucose and pyruvate were added in powder form. All other constituents were added in the form of molar stock solutions. The solution was gassed at room temperature with a mixture of 95% oxygen and 5% carbon dioxide. The temperature of the superfusate in the muscle bath was maintained at 37 ± 0.5°C, and was monitored by a thermistor placed in the trough. The pH of the solution entering the muscle bath was 7.4 ± 0.04.

MODIFICATIONS AND ADDITIONS TO THE SUPERFUSATE

Changes in ionic concentrations

Change in $[Ca^{2+}]$

The calcium concentration was varied between 0.45 and 5.4 mmol/l in some experiments. This was achieved by adding different amounts of the molar stock solution of calcium chloride as the superfusate was made up. No correction was made for any change in osmolarity.

Change in $[K^+]$

In experiments where a stable intracellular microelectrode penetration was achieved an attempt was made to record a 'Slow' action potential. This was achieved by partially

depolarising the cell membrane by increasing the external potassium concentration. A concentration of 18mmol K^+ was often effective, but sometimes led to loss of excitability of the muscle. In these circumstances a [K^+] of 16mmol or 14 mmol was used. The potassium concentration was varied by adjusting the volume of the molar stock solution of potassium chloride added as the superfusate was made up and no correction was made for the change in osmolarity.

Addition of other compounds

The concentration used of each of the following compounds was selected as the concentration producing maximal effect in the absence of toxicity.

Adrenalin

Pharmaceutical ampoules of adrenalin (1 in 1000) were used to provide a final concenration of 1μM. (200 μl of 1:1000 adrenalin per litre of superfusate).

Caffeine

5mM caffeine was made up by dissolving the solid power (Sigma, Poole, Dorset) in the superfusate.

Diltiazem

4μM diltiazem was used. A stock solution of 0.5mM was prepared from the solid powder (Lorex Pharmaceuticals Ltd., High Wycombe, Bucks), and this was added directly to the superfusate.

Ouabain

0.5 μM ouabain was prepared by the addition of a 1mM stock solution (Sigma, Poole, Dorset).

Ryanodine

10μM Ryanodine was prepared by the addition of a stock solution (10mM) of the dissolved crystalline form (Merck Sharp and Dohme, USA)

Verapamil

2.2 nM verapamil was prepared by the addition of a stock solution (1mg/l) of the dissolved powder (Abbott Laboratories Ltd., Queenborough, Kent).

ELECTRICAL STIMULATION

Apparatus

Programmed electrical stimulation was by means of Neurolog System modules (Digitimer Ltd., Welwyn Garden City, Herts.). The modules used for the stimulation protocol which follows were:

Period Generator	NL 303
Counter (x2)	NL 603
OR gate	NL 500
Delay-Width	NL 403
Pulse Buffer	NL 510

In addition a 'Flip-Flop' circuit was specially designed to control the insertion of ectopic stimuli within a steady state train. (see *Appendix* for circuit diagram)

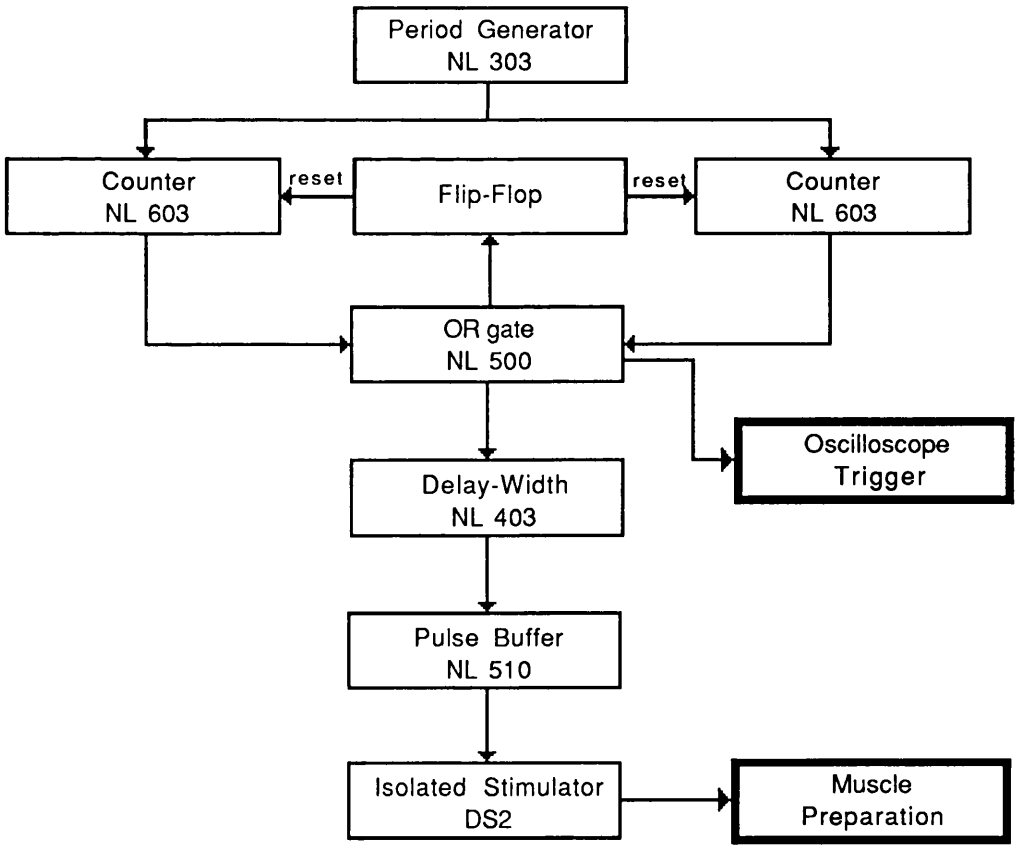

Figure 5. Neurolog Stimulator: module connections.

The output of the Neurolog System was passed into an Isolated Stimulator (DS2, Digitimer Ltd..) which controlled the stimulus strength delivered to the muscle bath. Stimulus threshold values (for pulse width and amplitude) were established for each muscle preparation. Stimulation was usually set at 50% above these values.

The interconnections of the stimulator modules are shown in Figure 5. Essentially, one of the counters was set to provide steady-state stimulation and the other varied to provide ectopic intervals of different duration. The 'flip-flop' circuit was used to switch between the two counters. The incorporation of a 'Delay-Width' module alowed the oscilloscope sweep to be triggered before the onset of the stimulus.

Restitution Protocol

The preparation was field stimulated (via platinum electrodes placed in the walls of the bath) at a steady-state rate of 1 Hz. Ectopic beats were inserted with varying preceding stimulus intervals (ectopic interval). In order to describe the relationship between the duration of the ectopic interval and parameters of twitch tension, the duration of the ectopic interval was varied from approximately 300ms to 30-60s depending on the behaviour of the tissue under experimental conditions. In practice the refractoriness of human myocardium usually prevented ectopic intervals of less than 400ms. Following steady-state stabilization between ectopic beats a further ectopic beat was inserted at an increased interval. The incremental change in the ectopic interval would depend on the slope of the relationship of twitch tension and ectopic interval at that point. A typical stimulation protocol would include ectopic intervals as follows:

300ms	500ms	1200ms	1800ms	12000ms
320ms	600ms	1300ms	2000ms	15000ms
360ms	700ms	1400ms	3000ms	20000ms
400ms	800ms	1500ms	5000ms	25000ms
440ms	900ms	1600ms	7000ms	30000ms
480ms	1100ms	1700ms	10000ms	45000ms

Figure 6 shows an example of the output of the stimulator showing the steady-state with a number of ectopic stimuli. An example of a recording of twitch tension and dT/dt during such a stimulus protocol is shown in Figure 7.

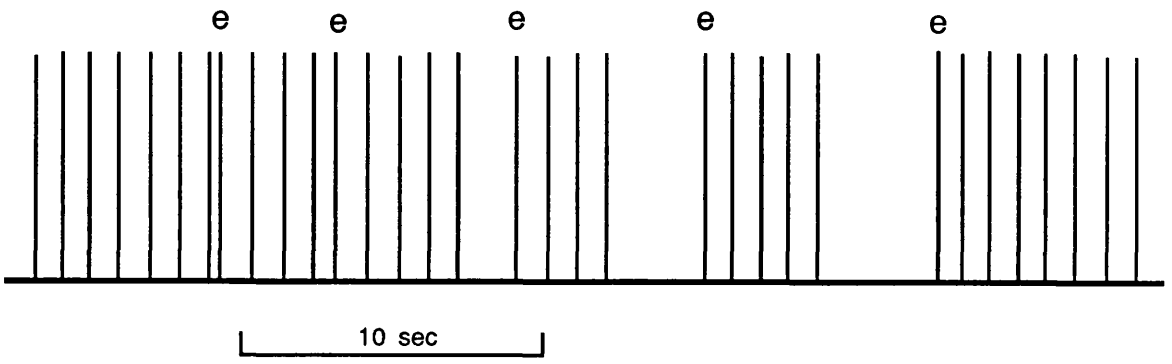

Figure 6. Diagramatic representation of stimulation protocol.
'Steady State' stimulus frequency of 1Hz with interpolated extra stimuli (e) of varying ectopic intervals.

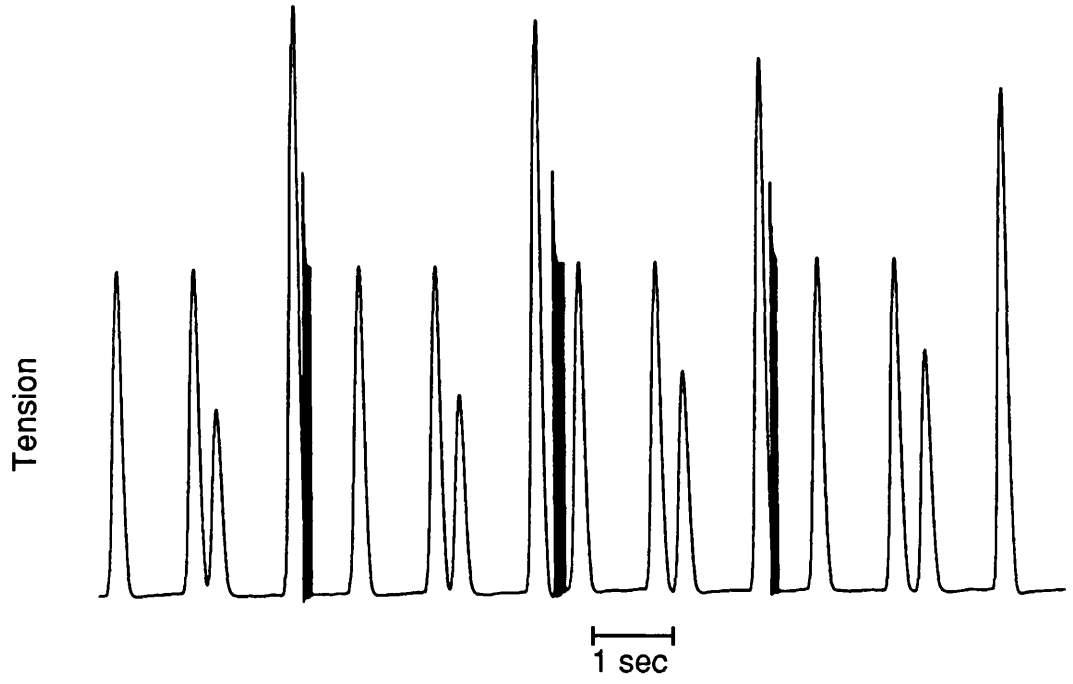

Figure 7. Pen-recorder trace of isometric twitch tension in a guinea-pig papillary muscle. Steady state stimulation (1Hz) with interpolated ectopic beats of intervals varying between 300ms and 400ms.

ISOMETRIC TENSION RECORDING

The stimulated isometric muscle preparation was allowed to stabilise in the muscle bath for at least one hour before making any recordings. Meanwhile the muscle length was increased progressively to achieve 'L max' (the length at which maximum developed tension occurs; see Figure 8). All experiments on that tissue were subsequently performed at this length (L max).

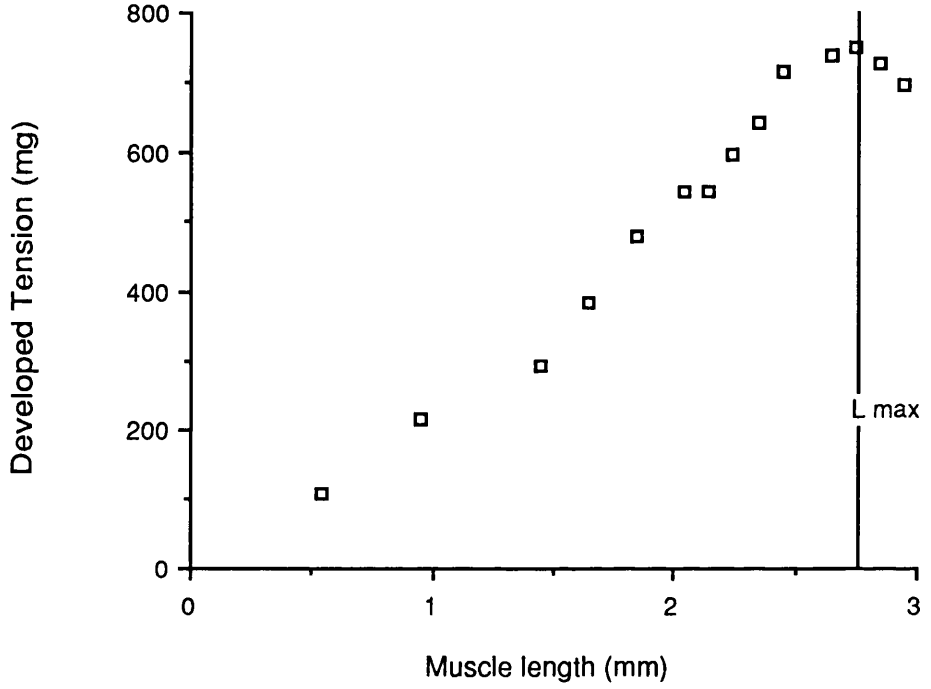

Figure 8. Length tension relationship in a guinea-pig papillary muscle

The isometric force transducer formed one limb of a Wheatstone bridge circuit. (see *Appendix* for bridge amplifier circuit diagram) The output from the bridge amplifier was passed through a 15 Hz filter to a pen recorder to display twitch tension. The same signal was passed to a differentiator (see *Appendix* for circuit diagram), to provide the first differential of tension with respect to time (dT/dt). Both the twitch tension signal and dT/dt were displayed via two "General Purpose" DC amplifiers (Model 13-4615-10; Gould, Hainault, Essex) on a three channel pressure-ink recorder (Model 2400S; Gould). The pen-recorder frequency response was 30Hz ± 2% at 100mm amplitude, and 50Hz ± 2% at 50mm amplitude (manufacturers specification).

Calibration of the entire tension recording system was carried out by suspending lengths of solder of known weight on the tension transducer hook. The differentiator amplifier was calibrated by passing a triangular waveform from a signal generator directly into the differentiator input and varying the rate of change of the signal voltage. In both cases calibration with the paper recorder was performed. Curves for both twitch tension and dT/dt are shown in Figures 9 & 10.

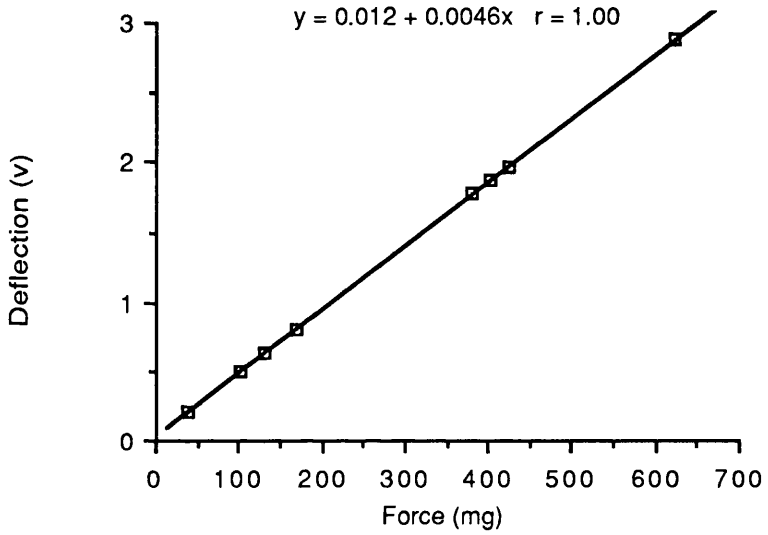

Figure 9. Calibration of Tension Transducer

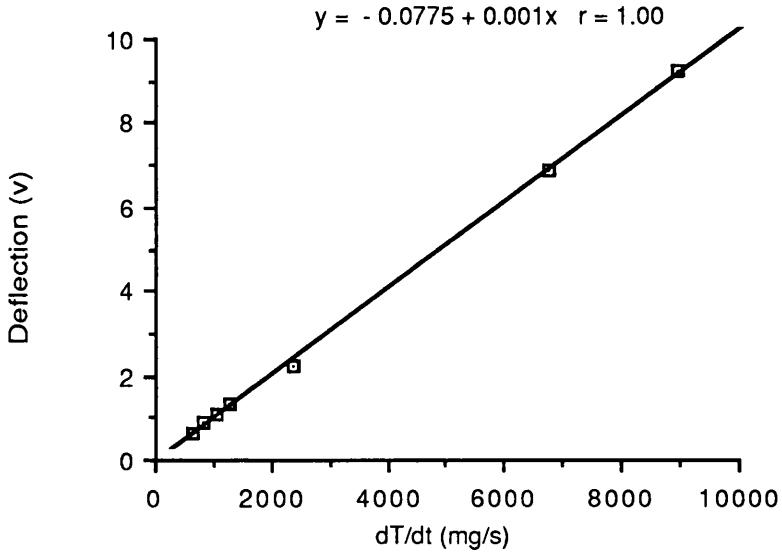

Figure 10. Calibration of First Derivative of Tension (dT/dt)

TRANS-MEMBRANE ACTION POTENTIAL RECORDING

Microelectrode

Trans-membrane potentials were recorded using standard microelectrode technique (see Purves, 1981). Glass microelectrodes were pulled from GC150F borosilicate glass tubing (Clark Electromedical Instruments, Reading) on a vertical microelectrode puller (Searle Bioscience, Sheerness, Kent). This particular type of capillary tubing contains a fine glass thread running throughout its length in order to facilitate filling.

The distal 2cm of coating was removed, from 5 cm lengths of 100μm diameter Diamel-coated silver wire (Goodfellow Metals Ltd., Cambridge, England), by scraping with a scalpel blade held perpendicular to the wire. This exposed section of silver wire was then coated with silver chloride, by electrolysis against a silver cathode in a solution of 0.1M HCl and 0.1M KCl.

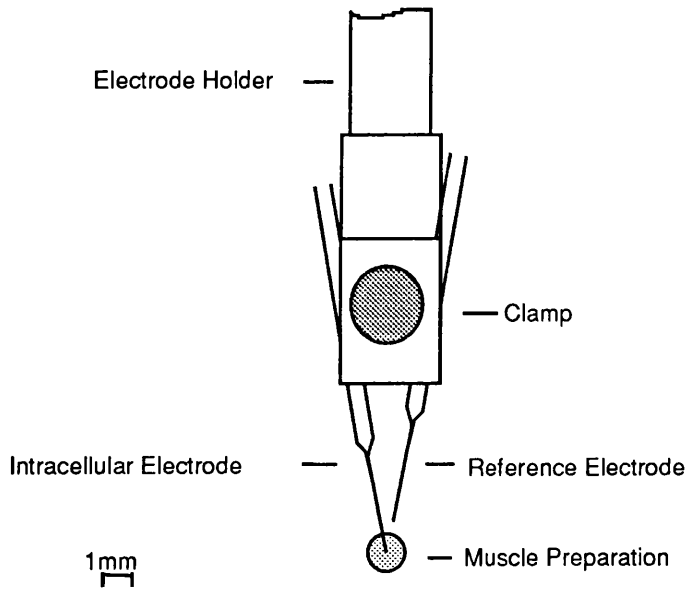

Figure 11. Arrangement of intracellular and reference micro-electrodes

The glass electrodes were filled with 3M potassium chloride and the silver chloride coated silver wire was threaded into the capillary tube. The resistance of such an electrode was between 10MΩ and 20MΩ.

The intra cellular and reference electrodes were each prepared in this way, and were clamped to a single micromanipulator holder (see Figure 11). Cellular penetration was acheived by a combination of slowly advancing the intracelluar electode with the micromanipulator and gently tapping the top of the electrode holder.

Pre-amplifier

The microelectrodes were connected by short shielded cables to a high-impedence-input pre-amplifier with a fixed gain of x10 (for circuit diagram see *Appendix*). The frequency response of the pre-amplifier is shown in Figure 12, and was flat to 4 kHz.

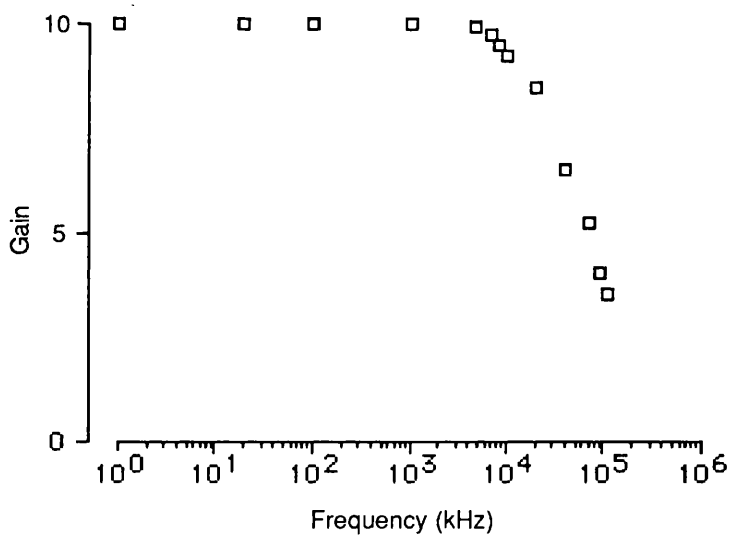

Figure 12. Frequency response of the action potential pre-amplifier with a 20MΩ input resistance. The frequency response is flat to 4 KHz.

External electrical interference via the connections between the microelectrodes and the pre-amplifier were minimised by positioning the pre–amplifier as close as possible to the preparation and surrounding this and the muscle bath by a grounded 13 x 10 x 10cm aluminium mesh Faraday cage.

Differentiator

The pre-amplifier DC output was passed to one of two differentiator circuits (depending on the range of values of dV/dt to be measured). Normal trans-membrane action potentials were associated with values of dV/dt in the 'fast' range (i.e. 100–200 Vs^{-1}). The so-called 'slow' action potenials produced a value of dV/dt in the region of 2–10 Vs^{-1}. Calibration curves of these two ciruits ('fast' and 'slow') are shown in Figures 13 and 14.

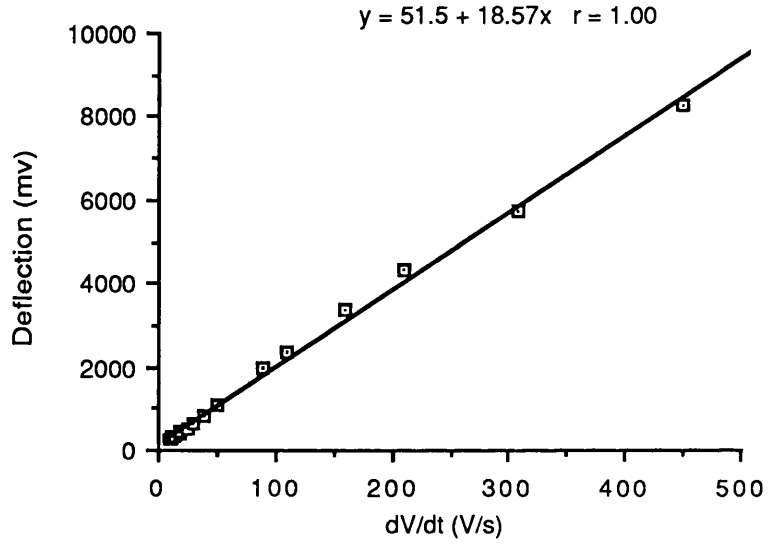

Figure 13. Calibration of Action Potential Differentiator (Fast)

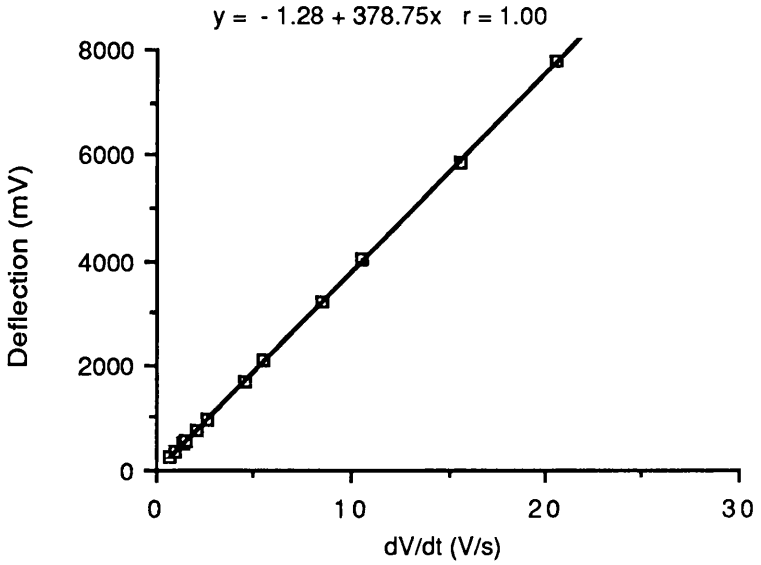

Figure 14. Calibration of Action Potential Differentiator (slow)

Display and Measurement

Both the pre-amplifier output and its derivative (dV/dt) were displayed on a two-channel Digital Storage Oscilloscope (Model 1425; Gould). Direct measurements from the stored display were possible with a remote Waveform Processor with X-Y cursor control (Type 125; Gould). Transmembrane potential could be measured to the nearest 0.7mV, giving rise to a potential error of <0.5% in normal action potentials. Action potential duration was measured to the nearest 0.5ms, producing a possible error of < 0.1%.

Permanent records of these digital plots, with a facility to produce high quality printouts was achieved by use of the RS423 interface of the oscilloscope. The digital plot could be uploaded as a text file onto an Apple Macintosh microcomputer (Apple Computer Inc., Cupertino, California, USA), using commercially available communications software ('Jazz' integrated software, Lotus, USA) via the communications port. The x—y coordinates could then be plotted using the graph plotting facility in 'Jazz'. Subsequent editing and the addition of legends was acheived by using one of the Macintosh drawing programs (e.g. MacDraw or MacPaint). A typical digitised record is seen in Figure 15.

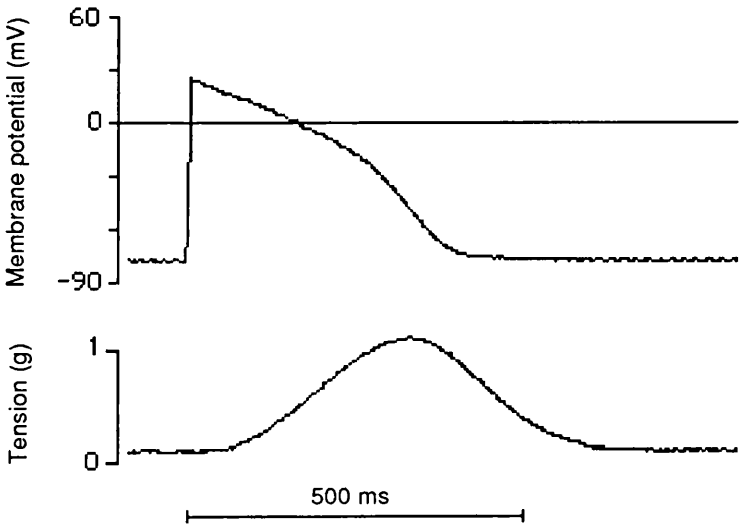

Figure 15. Digitised record of simulaneous trans-membrane action potential and twitch tension (Human left-ventricular outflow tract)

Measurement of twitch tension parameters

The height of the twitch tension trace was measured directly from the pen-recorder paper with a transparent ruler graduated in millimeters. Developed tension was measured from the baseline to the peak of the twitch (see Figure 16). Where the ectopic beat was premature, and overlay the relaxation of the preceding steady-state beat, the magnitude of the twitch tension was taken as the developed tension by that beat (see Figure 17). It is estimated that the error of these measurements is approximately ± 0.5%. Time to peak tension was measured from the onset of the upstroke of the dT/dt trace to the peak of the tension trace with a paper speed of 100mm per second. The accuracy of these measurements was to within 5msec (i.e. an error of less than 1% in human experiments). Maximum dT/dt and minimum dT/dt were taken from the height of the trace.

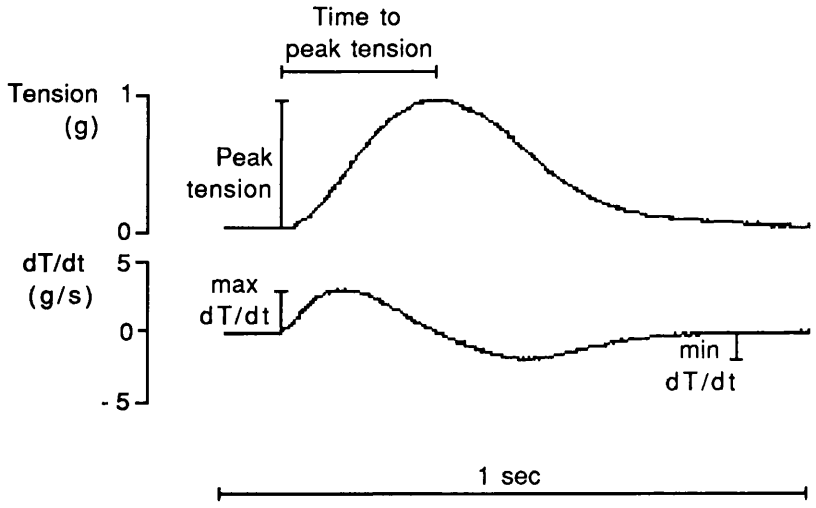

Figure 16. Digitised record of twitch tension and dT/dt from a preparation of human myocardium showing the measurement of: Peak Tension, Time to Peak Tension and Maximum positive dT/dt.

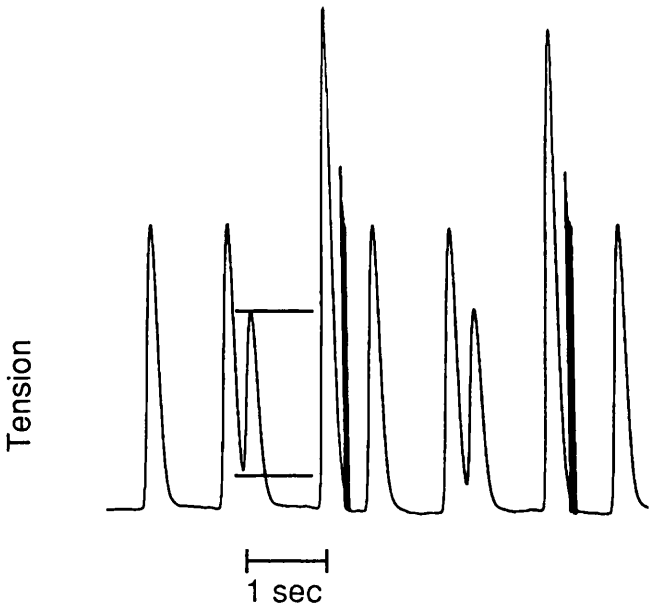

Figure 17. Recording of isometric twitch tension in guinea-pig papillary muscle. 'Developed tension' in the premature beat is measured between the horizontal lines indicated.

Measurement of action potential parameters

Measurements were made directly from the stored digital image on the oscilloscope screen using X-Y cursor control and digital output operated by the Waveform Processor key-pad.

The following measurements were made: resting membrane potential (mV), overshoot (mV), time to 90% repolarisation and maximum positive dV/dt (see Figures 18 and 19).

90% repolarisation was taken as 90% of the distance between the overshoot and resting potential. (Where the overshoot = 0% repolarisation, and resting potential = 100% repolarisation.) Time to 90% repolarisation was therefore the interval from the onset of the action potential to the point at which the membrane potential is 90% repolarised.

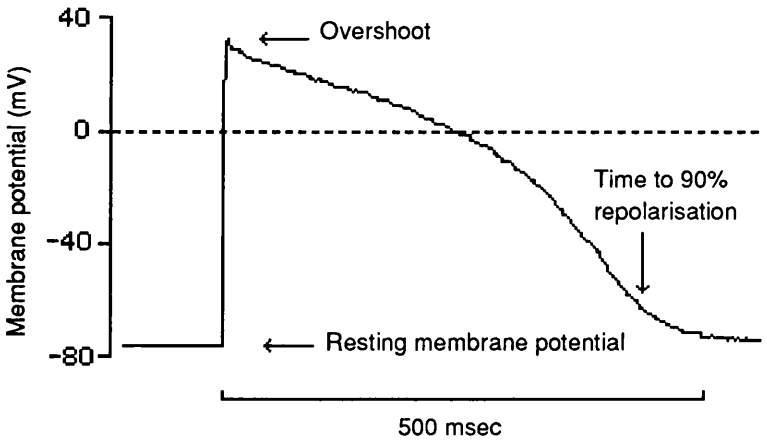

Figure 18. Digitised record of a human ventricular action potential showing measurement of resting membrane potential overshoot and time to 90% repolarisation.

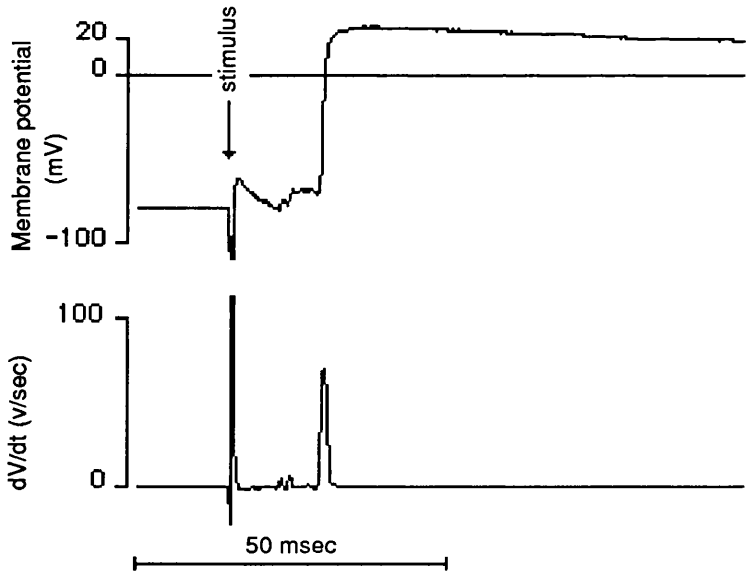

Figure 19. Digitised record of a human ventricular action potential upstroke and its first derivative with respect to time (dV/dt). The stimulus artefact is clearly seen, and preceeds the max dV/dt spike.

DATA STORAGE AND ANALYSIS

Parameters of isometric twitch tension were recorded in the steady state and ectopic twitches according to the protocol above. Trans-membrane action-potentials were recorded, whenever possible, in the steady state for each intervention. Slow action-potential maximum dV/dt were recorded in both the steady state and in ectopic beats according to the stimulation protocol above.

The data from each experiment was then entered into a specially designed microcomputer spreadsheet template (written personally using Jazz integrated software (Lotus, USA) on an Apple Macintosh microcomputer) and saved for future analysis and plotting. The spreadsheet was designed to list values from steady-state and ectopic beats. The ratio of values (ectopic/steady state) from each pair was then calculated and could be plotted against the ectopic interval. An example of this kind of plot for twitch tension is seen in Figure 20. The curve described by the relationship of twitch tension and the ectopic interval has been termed the 'Mechanical Restitution Curve', and represents the time course of the recovery and subsequent decay of twitch tension between beats of varying intervals. Similar curves may be plotted using action-potential parameters.

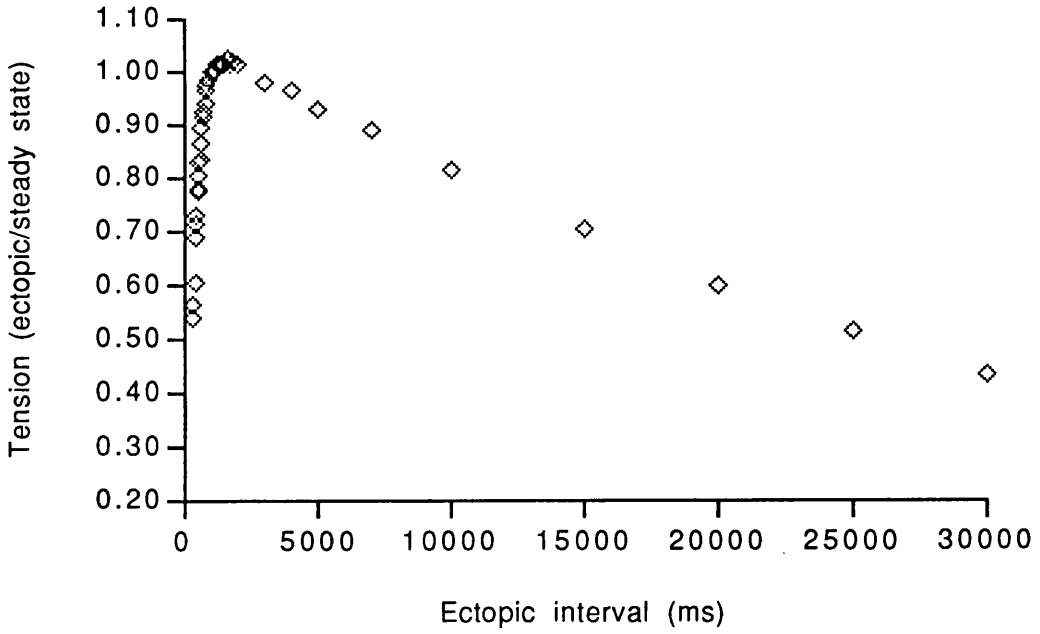

Figure 20. Mechanical Restitution Curve - Guinea-pig papillary muscle.

The recovery and subsequent decay (of twitch tension) described by the mechanical restitution curve are assumed to represent a number of underlying biological processes each with an independent exponential time course. In simple terms, the recovery in Figure 21 resembles a monoexponential process which is somewhat faster than that of the decay.

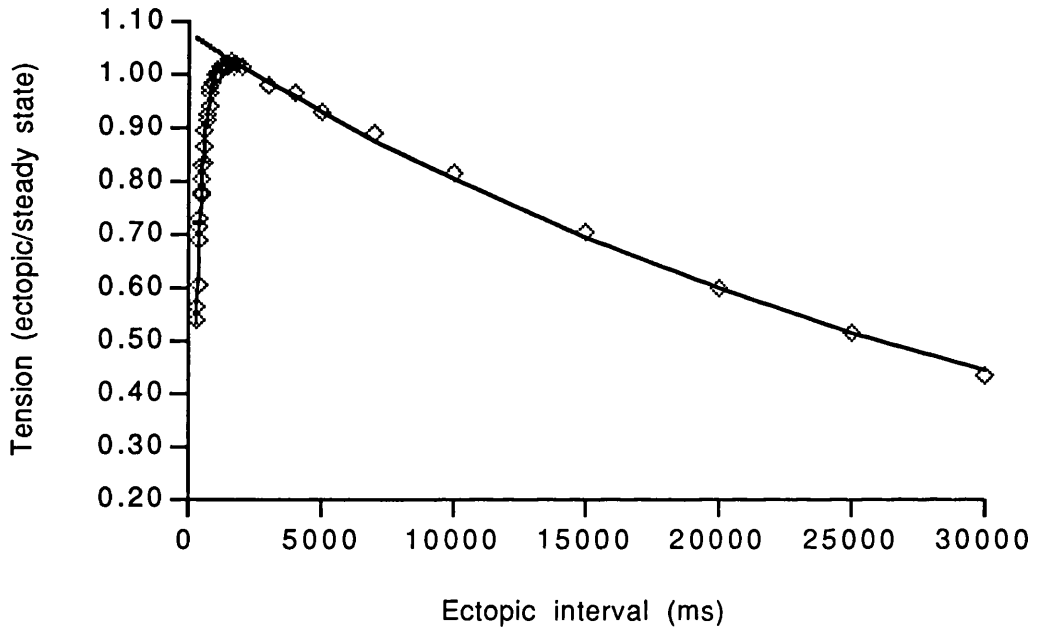

Figure 21. Mechanical restitution curve: showing two exponential curves fitted using 'Curve Stripping' spreadsheet.

In order to quantify the exponential processes underlying mechanical restitution, the time constant and capacity of each exponential would have to be derived from each curve. In other words multiple simultaneous exponential functions would have to be fitted to the data. Since it is assumed that these exponential functions are simultaneous (as opposed to serial), iterative computations are necessary to derive the different components. A procedure know as 'Curve Stripping' (see below) was adopted to fit multiple exponential functions to the experimental data. This was performed with the help of a specially written spreadsheet template; written personally on Jazz integrated software on an Apple Macintosh microcomputer (see *Appendix*). The spreadsheet allowed curve stripping in a rapid interactive manner, so that at each stage in the analysis a plot of the original data together with the fitted curves could be viewed (Figure 21). In addition, the spreadsheet calculated the variance (from the sum of the squares of the differences of the data and fitted curves) for each set of data, giving an index of the goodness-of-fit. All mechanical restitution curves were analysed in this way.

CURVE STRIPPING

A multiple exponential function may be described by the following equation:

$$y = a + A\ e^{-t/\tau_1} + B\ e^{-t/\tau_2} + C\ e^{-t/\tau_3} \ldots\ldots\ldots\ldots \text{ etc}$$

where:

a = asymptotic value

t = time (on the x axis)

A, B, C etc = intercept on the y axis of each exponential curve

τ_1, τ_2, τ_3 etc = time constants of each exponential curve

In the example above the formula represents three decaying exponentials. If the first two functions were exponential recovery processes then the formula would be:

$$y = a + A\ (1- e^{-t/\tau_1}) + B\ (1- e^{-t/\tau_2}) + C\ e^{-t/\tau_3}$$

An example of how such an equation containing two exponential functions (simultaneous recovery and decay processes) may be shown to fit the data in Figure 21 above, is plotted in Figure 22 below.

The practice of curve stripping involves deriving, from the data, each of the individual exponential functions (e.g. A $(1- e^{-t/\tau_1})$) in turn. The first step is to calculate the slowest time constant. In the example above, the natural logarithmic transform of the twitch tension at the longest ectopic intervals is regressed by the least squares method and the asymptotic value (a) adjusted to acheive the best linear fit. Having derived the slope and intercept of this line, the time constant (τ) is given by the negative reciprocal of the slope.

The curve described by this 'slowest' exponential is then extrapolated to shorter time intervals. Where the data begin to deviate from this extrapolated curve, the difference

between the two is measured (vertical lines in Figure 23) and this difference is then linearised (using a natural logarithmic transform) to derive a second exponential curve (Figure 24). Again, if the data at even shorter time intervals deviate from extrapolation of this second curve, further curves may be derived in the same manner. In other words, starting with the slowest exponential, curve stripping allows faster exponentials to be stripped one-by-one from the data. Each of the faster exponentials is therefore regarded as a decaying exponential with the preceeding exponential curve as its asymptote.

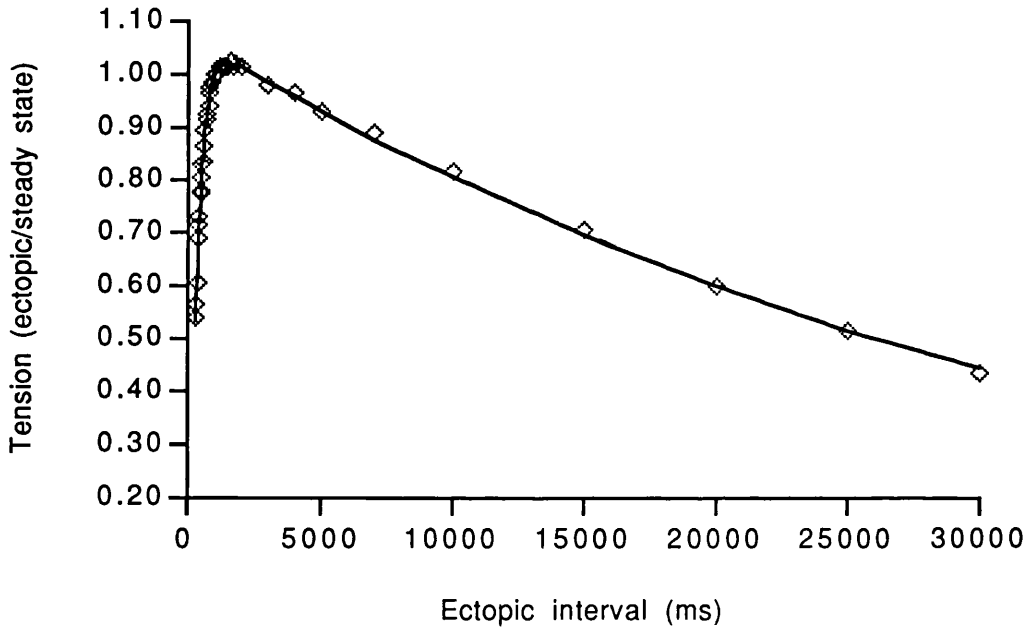

Figure 22. Mechanical restitution curve: showing plot of curve describing two exponential functions fitted with the 'Curve Stripping' spreadsheet.

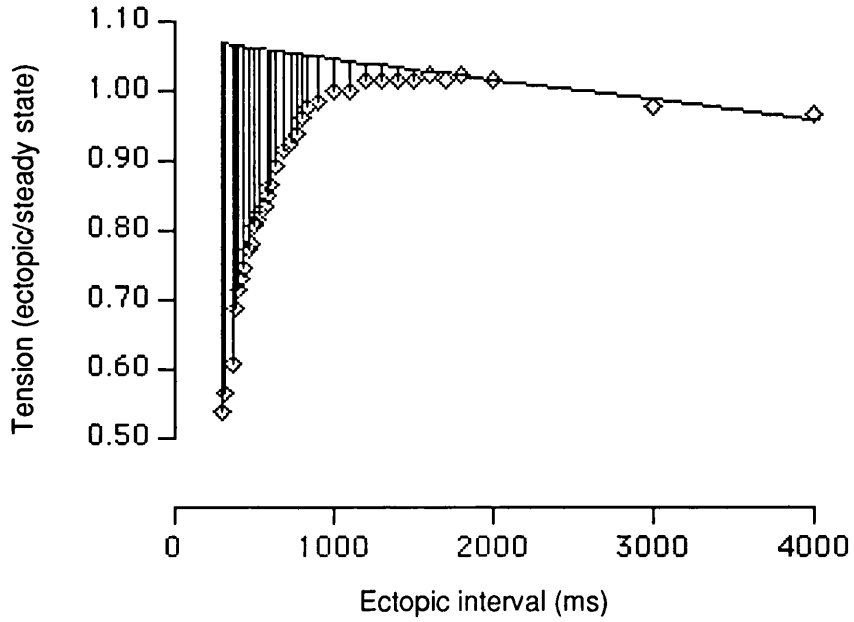

Figure 23. Mechanical restitution curve: The extrapolated decay curve is shown. The vertical lines represent the difference between the data points and the first extrapolated curve.

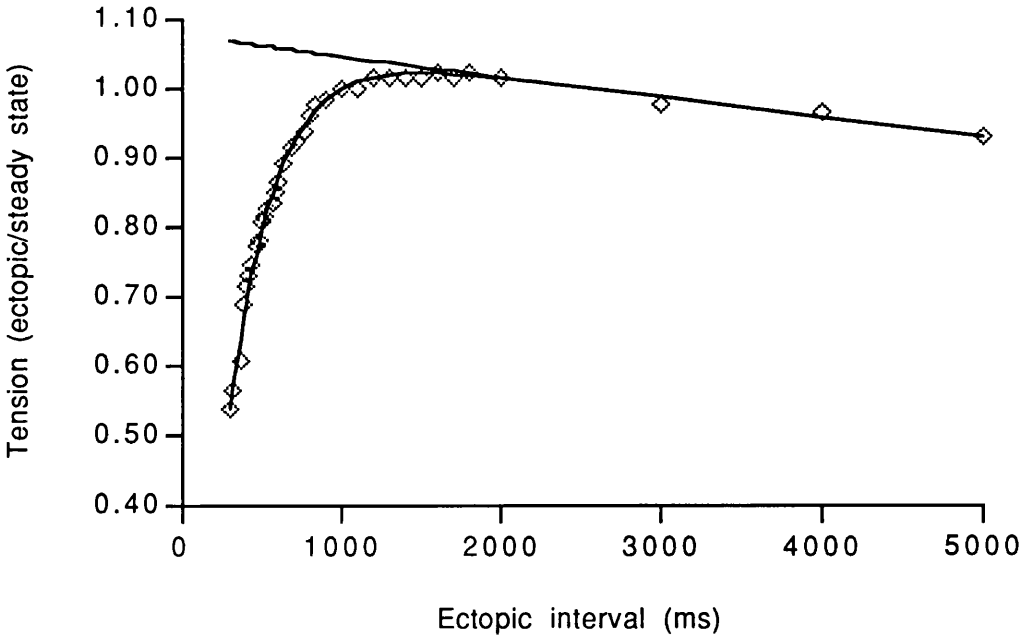

Figure 24. Mechanical restitution curve: A second exponential curve has been fitted to the recovery phase of the data.

STATISTICS

Simple statistical calculations were performed on a spreadsheet template written personally on Jazz integrated software on an Apple Macintosh microcomputer. Formulae were taken from Swinscow (1983). This spreadsheet allowed rapid insertion of data from other spreadsheets and produced a scatter plot of two columns of data, simple descriptive statistics, both paired and unpaired Student's t tests, least squares regression analysis and χ^2 tests. More complicated statistical computations were performed using Statworks™ software (Heyden & Son Ltd, London) and Statview 512™ on an Apple Macintosh microcomputer (BrainPower, Inc., Calabasas, California, USA) (verified by the authors to an accuracy of twelve decimal places using an IBM 370 and SPSS).

Values are expressed in *Results* as mean ± standard error unless otherwise stated. In many cases the data was clearly non-parametric and the average was expressed as a median and interquartile range. Frequently, no assumption was made as to the normality of distribution of the data, and on these occasions the relevant non-parametric tests have been performed to compare samples (e.g. Mann-Whitney U test, Wilcoxon signed rank test on paired data, Kruskal and Wallis rank-sum test and Kendall's rank correlation).

CHAPTER 3: RESULTS

HUMAN IN-VITRO DATA

Preparations

Biopsy specimens of human adult ventricular myocardium were obtained at the time of cardiac surgery from 58 patients. Biopsies were taken from either the left-ventricular outflow tract sub-endocardial myocardium (total 36), or left-ventricular papillary muscle (total 22). Table 1 compares the size and weights of preparations obtained from each site. Papillary muscle biopsies were very much larger than those from the ventricular wall and fibre alignment tended to be more parallel. Consequently dissection of the papillary muscle was somewhat easier and the preparations were slightly longer.

Table 1. Size and weight of human ventricular myocardium preparations.

	LV WALL n = 36	PAPILLARY n =22	
Weight (mg)	5.71±0.65	8.86±1.45	p< 0.05
Length (mm)	3.97±0.20	4.71±0.34	p< 0.05
Diameter(mm)	1.23±0.06	1.37±0.11	ns

LV wall = left-ventricular outflow tract sub-endocardial myocardium.
(mean ± standard error. Student's unpaired t-test)

Having been mounted in the muscle bath, the preparations were stimulated and generally took about one hour to recover function to a steady state. Those preparations

which recovered sufficiently to proceed usually continued to twitch in response to stimuli for several hours, or until an intervention was performed which caused irreversible damage to the tissue. In the measurement of isometric twitch parameters and restitution time constants which follow, there were no differences between the performance of muscle preparations obtained from the different sites and no further distinction will be made between the two groups.

Isometric twitch parameters

Control

A summary of isometric twitch parameters in all in-vitro preparations of human myocardium are presented in Table 2. Twitch tension is expressed as kilo-Newtons per kilogram of tissue (kN kg^{-1}).

Table 2. Isometric twitch parameters in normal Tyrode's solution. n=58

Tension (kN kg^{-1})	Time to peak tension (ms)	dT/dt max (kN kg^{-1} s^{-1})	dT/dt min (kN kg^{-1} s^{-1})
0.83±0.18	299.87±6.00	4.14±0.93	-2.91±0.72

Values are expressed as mean ± standard error

Interventions

i. Changes in $[Ca^{2+}]$

Alterations in $[Ca^{2+}]$ of the superfusing Tyrode's medium were shown to affect twitch tension parameters and the results are summarized in Table 3. A dose-response effect of $[Ca^{2+}]$ on twitch tension, time to peak tension, maximum dT/dt and minimum dT/dt can be seen from Table 3 and Figure 25.

Table 3. Human myocardium: The effect of changes in $[Ca^{2+}]$ on isometric twitch parameters.

$[Ca^{2+}]$ (mmol/l)	Tension (kN kg^{-1})	Time to peak Tens. (ms)	dT/dt max (kN kg^{-1} s^{-1})	dT/dt min (kN kg^{-1} s^{-1})
0.9 (n=5)	0.59±0.26 $p < 0.05$	316.00±19.65 ns	3.09±1.35 $p < 0.05$	-2.59±1.14 ns
1.8 (n=13)	0.69±0.21	293.46±8.50	4.02±1.30	-2.77±0.87
3.6 (n=9)	1.02±0.34 $p < 0.01$	279.44±8.01 ns	5.93±1.96 $p < 0.05$	-5.13±1.99 $p < 0.01$
5.4 (n=9)	1.01±0.33 $p < 0.01$	285.56±6.69 ns	7.23±2.09 $p < 0.01$	-4.8±1.75 $p < 0.01$

Values are expressed as mean ± standard error

Significance tested (for comparison with 1.8 mmol $[Ca^{2+}]$) using Wilcoxon test on paired samples

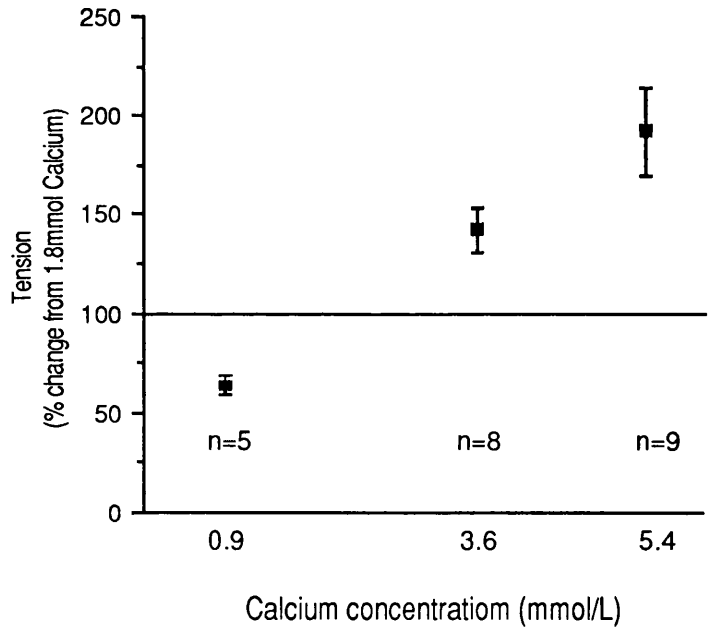

Figure 25. Calcium dose-response for twitch tension in human myocardium

ii. Adrenalin

Fifteen interventions were performed with 1μM adrenalin. The results are presented in Table 4. Adrenalin significantly increased peak isometric twitch tension, dT/dt max and dT/dt min, and reduced the time to peak tension.

Table 4. Human myocardium: Isometric twitch parameters in Tyrode's solution containing 1μM Adrenalin. n=15

Tension ($kN\ kg^{-1}$)	Time to peak tension (ms)	dT/dt max ($kN\ kg^{-1}\ s^{-1}$)	dT/dt min ($kN\ kg^{-1}\ s^{-1}$)
1.78±0.70	255.47±9.72	10.35±3.48	-10.47±5.13
(1.37±0.64)	(308±13.56)	(6.92±2.83)	(-4.93±5.13)
$p < 0.01$	$p < 0.01$	$p < 0.01$	$p < 0.01$

Values are expressed as mean ± standard error. Paired values (normal Tyrode's solution) are in brackets.
Significance tested using Wilcoxon test on paired samples

iii. Ouabain

Eleven interventions were performed with 0.5 μM ouabain and the results are presented in Table 5. Ouabain significantly increased peak isometric twitch tension, dT/dt max and dT/dt min.

Table 5. Human myocardium: Isometric twitch parameters in Tyrode's solution containing 0.5 μM Ouabain. n=11

Tension ($kN\ kg^{-1}$)	Time to peak tension (ms)	dT/dt max ($kN\ kg^{-1}\ s^{-1}$)	dT/dt min ($kN\ kg^{-1}\ s^{-1}$)
0.90±0.34	304.00±17.98	5.08±1.97	-3.11±1.24
(0.70±0.31)	(305.9±16.81)	(4.07±1.65)	(-2.30±0.78)
$p < 0.05$	ns	$p < 0.05$	$p < 0.05$

Values are expressed as mean ± standard error. Paired values (normal Tyrode's solution) are in brackets.
Significance tested using Wilcoxon test on paired samples

iv. Verapamil

Six interventions were performed with 2.2 nM verapamil and the results are presented in Table 6. Verapamil significantly reduced peak isometric twitch tension and dT/dt min, but did not affect dT/dt max.

Table 6. Human myocardium: Isometric twitch parameters in Tyrode's solution containing 2.2 nM Verapamil. n=6

Tension ($kN\ kg^{-1}$)	Time to peak tension (ms)	dT/dt max ($kN\ kg^{-1}\ s^{-1}$)	dT/dt min ($kN\ kg^{-1}\ s^{-1}$)
0.38±0.12	290.83±10.20	2.57±0.61	-1.54±0.47
(1.00±0.33)	(295.00±5.63)	(6.05±2.23)	(-3.42±1.07)
$p < 0.025$	ns	ns	$p < 0.05$

Values are expressed as mean ± standard error. Paired values (normal Tyrode's solution) are in brackets.
Significance tested using Wilcoxon test on paired samples

v. Ryanodine

Five interventions were performed with 10μM Ryanodine and the results are presented in Table 7. Ryanodine significantly reduced peak isometric twitch tension. The differential of twitch tension was not recorded in these experiments due to failure of part of the circuitry at the time.

Table 7. Human myocardium: Isometric twitch parameters in Tyrode's solution containing Ryanodine. n=5

Tension ($kN\ kg^{-1}$)	Time to peak tension (ms)	dT/dt max ($kN\ kg^{-1}\ s^{-1}$)	dT/dt min ($kN\ kg^{-1}\ s^{-1}$)
0.59±0.24	289.00±9.67	not measured	not measured
(1.23±0.39)	(261.67±9.72)		
$p < 0.05$	ns		

Values are expressed as mean ± standard error. Paired values (normal Tyrode's solution) are in brackets.
Significance tested using Wilcoxon test on paired samples

Mechanical Restitution

Mechanical restitution data was obtained from all fifty-eight human myocardial preparations in normal Tyrode's solution. In all cases the data was sufficient to construct a 'Mechanical Restitution Curve'.

The decay time constant was derived by curve stripping in the manner already described. In human ventricular myocardium the decay phase was extremely slow (almost plateau like) and it was impossible to predict the asymptotic value by linearising the data. In general, the data conformed as well to an asymptote of zero, as it did to any other value less than one. It was therefore assumed to be the same in all human experiments, and, for convenience, a valve of zero was used.

Having derived the decay time constant (by assuming an asymptotic value of zero), it became clear that a single exponential could not adequately describe the recovery phase in most cases (c.f. Methods: Curve Stripping). In other words, a logarithmic transform of the entire recovery phase did not produce a linear relationship between twitch tension and the ectopic interval. It was apparent, during the curve-striping routine, that recovery of twitch tension was more accurately described by two distinct exponential phases. The interactive nature of the curve-stripping spreadsheet requires the operator to select, by visual criteria, how many exponential functions to fit to the experimental data in each case. In nine cases it was clear from linearisation of the recovery phase that a single exponential would fit so well that an attempt to fit a second would be both unjustified and largely impossible. In most cases (49/58 [84%]), however, two recovery phase exponential functions were fitted to the data.

In order to justify this approach, data from sixteen consecutive experiments were analysed by fitting both mono-exponential and bi-exponential functions to the recovery phase. In two of these it was impossible to fit more than one rising exponential. In the remaining fourteen a comparison was made between the 'goodness-of-fit' of two and three exponentials on the same data (including the decay phase). The 'goodness-of-fit' of the derived curves to the data was expressed as the variance. The variance of curves fitted with three exponentials was 0.002 ± 0.0004 (mean±SEM); and with two exponentials was 0.027 ± 0.005. The variances within individual experiments were compared as a ratio and the significance of the difference derived from tables of the F-distribution. In every case the difference was highly significant ($p < 0.001$), indicating that a better fit was achieved by three rather than two exponential functions.

Since three exponential phases describe the majority of human mechanical restitution data, three separate time constants are derived and are designated $\tau_1 - \tau_3$ ("τ" being the Greek letter "Tau"). τ_1 describes the first (fast) rising phase, τ_2 the second (slow) rising phase, and τ_3 the decay phase. The intercepts of each of the three curves (i.e. the extrapolated value of twitch tension at an ectopic interval of zero milliseconds) are designated 'A', 'B' and 'C', for curves 1, 2 and 3 respectively.

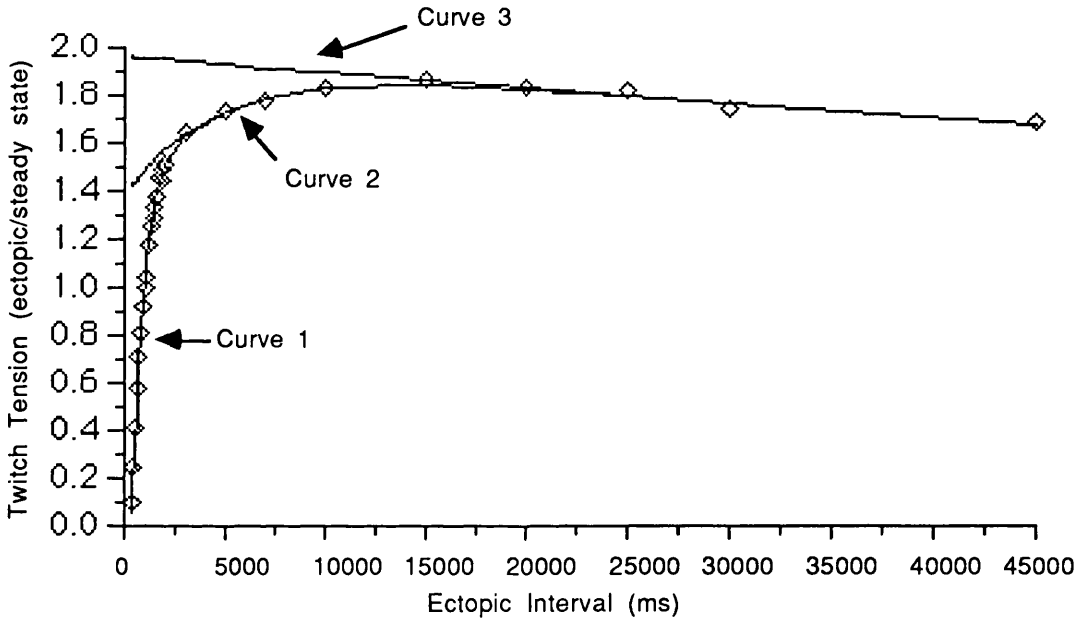

Figure 26. Three exponential curves extrapolated over data from a single experiment. Curves 1, 2 and 3 have time constants τ_1, τ_2 and τ_3 respectively.

Figure 26 shows how these three exponential curves are fitted to the data. When the curve stripping procedure is performed the first time constant and intercept to be derived are τ_3 and C (from Curve 3). Values for τ_3 were obtained in all but four cases. Where it was impossible to ascribe a value to τ_3, because the curve was clearly flat at long time intervals, a very high value (or infinity) was assumed for τ_3. In this case the value does not appear in the overall mean, but a very high value is used for the purposes of non-parametric comparison. In ten cases it was possible to fit only a single rising exponential rather than two. The rising time constant was then designated τ_1, and those curves were said to have no τ_2.

Control

The values of the time constants and intercepts of mechanical restitution for all preparations of human myocardium are shown in Tables 8 and 9. The intercepts are expressed as the median and interquartile range because the distribution of 'A' is exremely skewed. This would appear largely to be due to the inaccuracy inherent in estimating the intercept on the y-axis of 'Curve 1'.

Table 8. Time constants of mechanical restitution of human myocardium in normal Tyrode's solution. n=58

τ_1 (ms)	τ_2 (s)	τ_3 (s)
456.14 ± 32.64	4.10 ± 4.46	194.4 ± 215.6

(Mean ± standard error)

Table 9. Intercepts of mechanical restitution of human myocardium in normal Tyrode's solution. n=58

A	B	C
2.00 (1.42-2.75)	0.56 (0.34-0.80)	1.46 (1.27-1.67)

(Median and interquartile range)

Interventions

i. Changes in $[Ca^{2+}]$

The effects of changes in superfusate $[Ca^{2+}]$ on the mechanical restitution time constants and intercepts are summarized in Tables 10 and 11 and Figures 27 to 30. τ_1 was not affected by changes in $[Ca^{2+}]$. There were, however, dose-response effects of changes in $[Ca^{2+}]$ on both τ_2 and τ_3. With increasing $[Ca^{2+}]$ there is a prolongation of both the second rising phase of recovery (τ_2) and the decay phase (τ_3). The value of the

decay phase intercept (C) was significantly higher at both 3.6 and 5.4 mmol/l $[Ca^{2+}]$ when compared to 1.8 mmol/l.

Table 10. The effect of changes in $[Ca^{2+}]$ on the mechanical restitution time constants of human myocardium.

$[Ca^{2+}]$ (mmol/l)	τ_1 (ms)	τ_2 (s)	τ_3 (s)
0.9 (n=5)	481.53 ± 55.33 ns	3.38 ± 0.75 ns	199.9 ± 70.4 ns
1.8 (n=13)	386.73 ± 41.07	4.02 ± 0.96	221.2 ± 47.1
3.6 (n=8)	488.14 ± 88.12 ns	6.26 ± 1.21 ns	282.0 ± 53.5 $p < 0.01$
5.4 (n=9)	450.60 ± 73.89 ns	7.36 ± 2.11 $p < 0.05$	449.0 ± 136.3 $p < 0.01$

Significance tested (for comparison with 1.8 mmol $[Ca^{2+}]$) using Wilcoxon test on paired samples. (Mean ± standard error)

Table 11. The effect of changes in $[Ca^{2+}]$ on the intercepts of mechanical restitution of human myocardium.

$[Ca^{2+}]$ (mmol/l)	A	B	C
0.9 (n=5)	1.62 (1.22-1.85) ns	0.17 (0.13-0.25) ns	1.28 (1.23-1.34) ns
1.8 (n=13)	2.38 (1.61-2.57)	0.62 (0.36-0.74)	1.35 (1.25-1.61)
3.6 (n=8)	1.99 (1.56-2.25) ns	0.53 (0.41-0.81) ns	1.57 (1.37-1.68) $p < 0.025$
5.4 (n=9)	2.12 (1.57-2.83) ns	0.63 (0.24-1.14) ns	1.59 (1.25-2.24) $p < 0.05$

Wilcoxon test on paired samples. (Median and interquartile range)

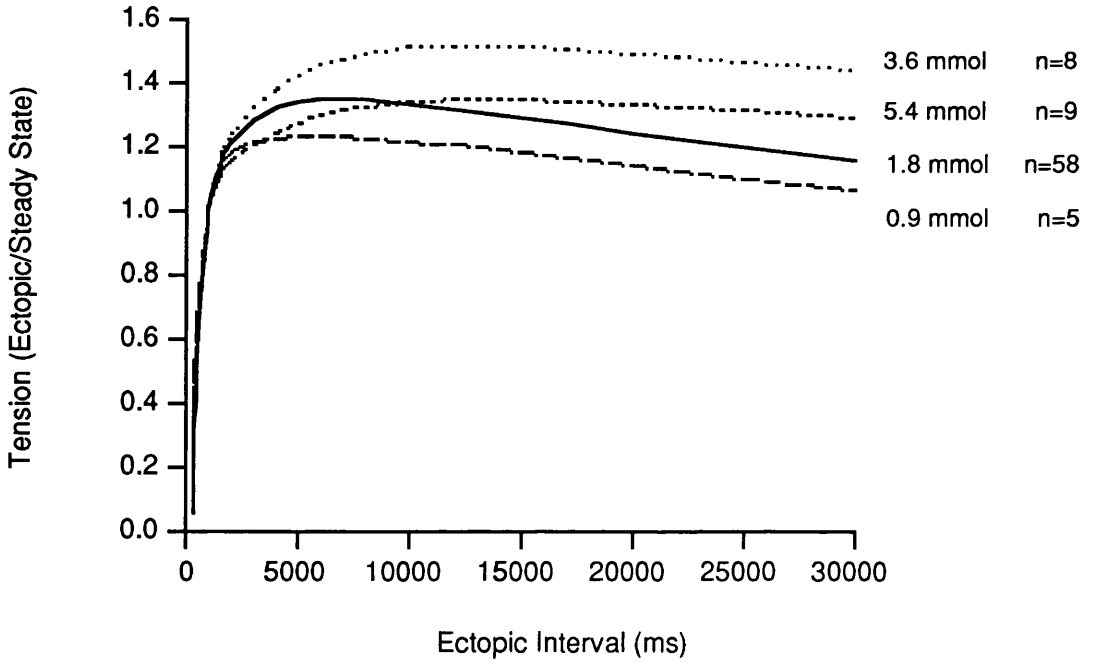

Figure 27. Mechanical restitution curves derived from the combined data of several experiments at different [Ca^{2+}].

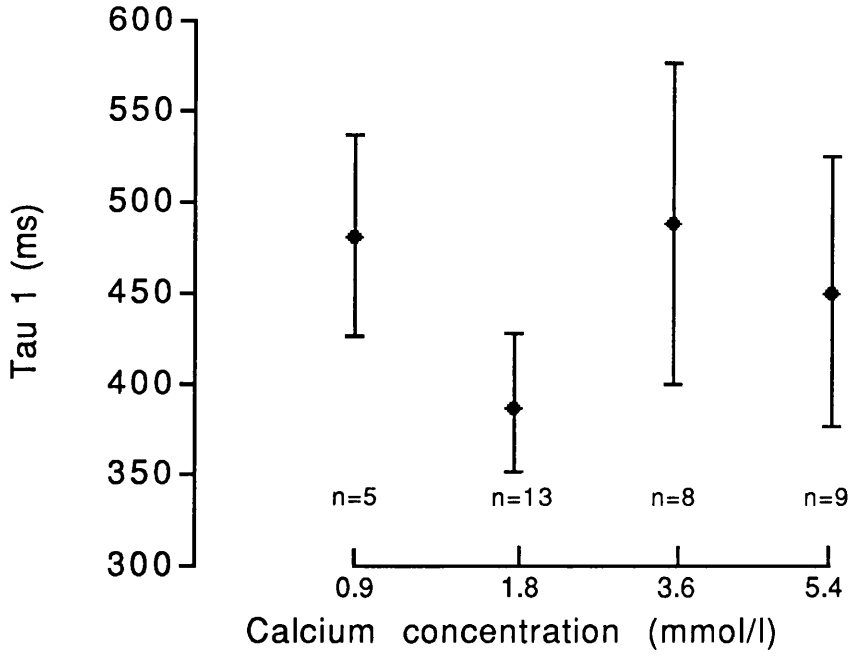

Figure 28. Calcium dose-response of τ_1 in human myocardium

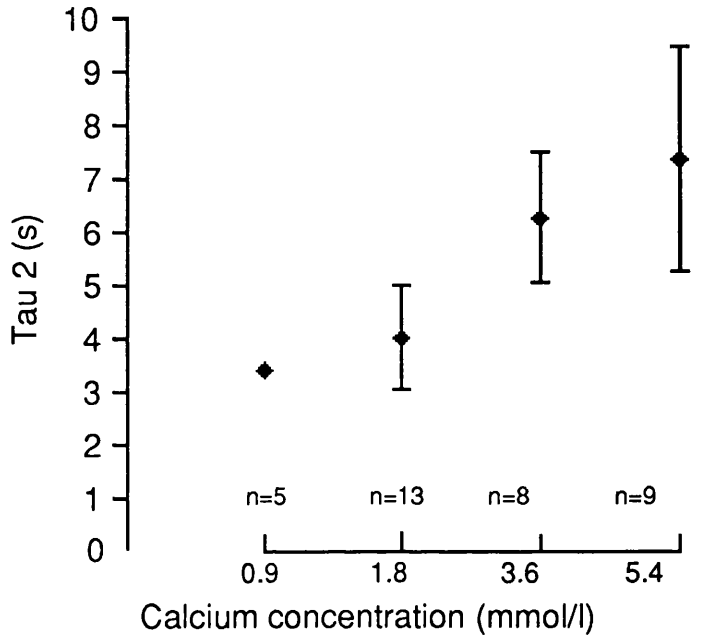

Figure 29. Calcium dose-response of τ_2 in human myocardium

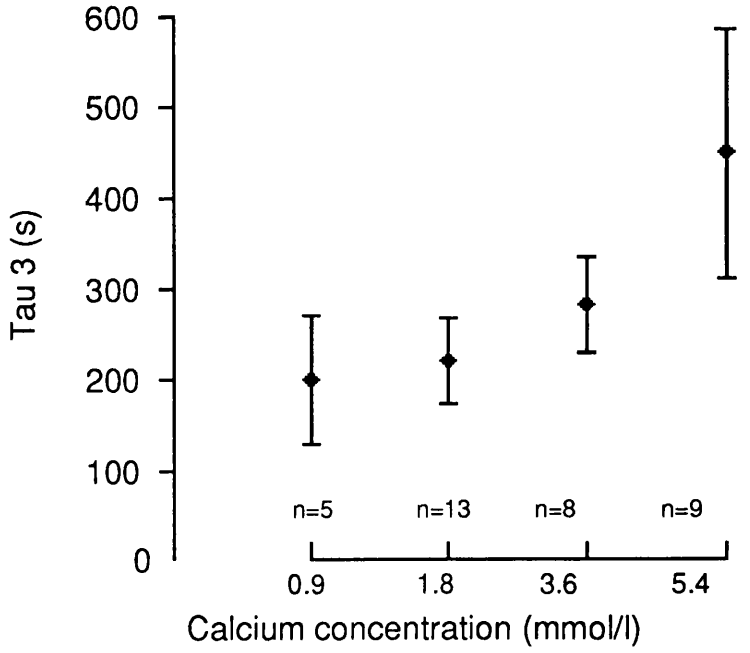

Figure 30. Calcium dose-response of τ_3 in human myocardium

ii. Adrenalin

Eight experiments were performed in the presence of 1μM adrenalin and the results are presented in Tables 12 and 13. Adrenalin is shown to abbreviate τ_1 and to have no affect on τ_2 or τ_3. There was no effect on the intercept values. The abbreviation of τ_1 is clearly seen in the lower part of Figure 31.

Table 12. Time constants of mechanical restitution of human myocardium in 1μM adrenalin. n=8

τ_1 (ms)	τ_2 (s)	τ_3 (s)
330.65 ± 48.89	5.17 ± 1.88	179.8 ± 44.3
(561.02 ± 79.67)	(4.86 ± 0.83)	(264.1 ± 63.3)
$p < 0.05$	ns	ns

(Mean ± standard error)
Significance tested using Wilcoxon test on paired samples. Paired control values are given in brackets.

Table 13. Intercepts of mechanical restitution of human myocardium in 1μM adrenalin. n=8

A	B	C
1.97 (1.58-4.46)	0.52 (0.35-0.66)	1.42 (1.28-1.57)
[1.60 (1.22-2.34)]	[0.57 (0.46-0.67)]	[1.63(1.26-1.82)]
ns	ns	ns

(Median and interquartile range)
Significance tested using Wilcoxon test on paired samples. Paired control values are given in brackets.

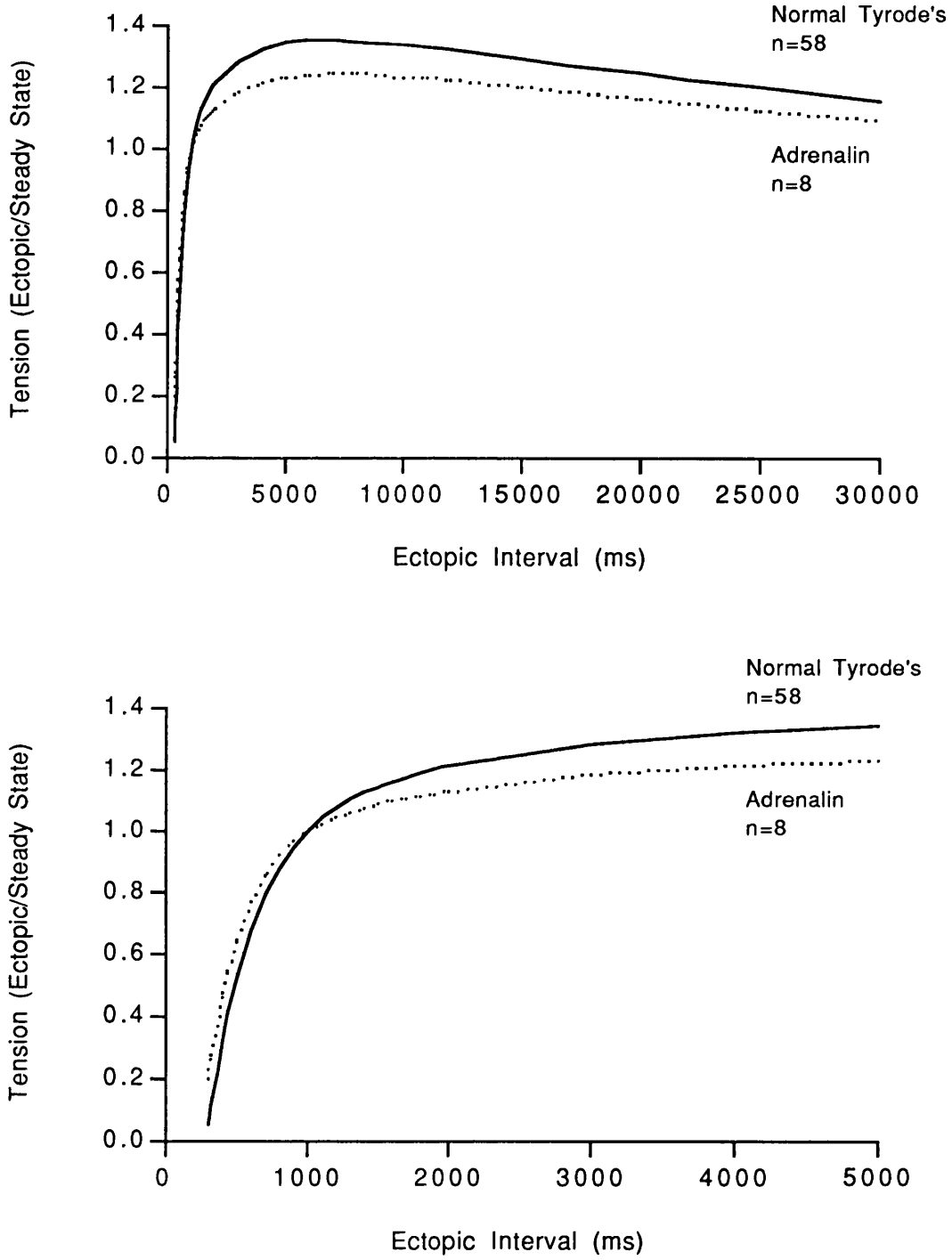

Figure 31. Mechanical restitution curves derived from the combined data of several experiments showing the effect of 1μM adrenalin. The lower panel shows the same data as the upper, but on an expanded time scale to demonstrate shorter ectopic intervals.

iii. Ouabain

Six experiments were performed in the presence of 0.5 μM ouabain and the results are presented in Tables 14 and 15. Ouabain significantly prolonged both τ_1 and τ_3, but the increase in τ_2 did not reach significance at the 5% level. There was a significant increase in the 'C' intercept which is well illustrated by the separation of the decay phases in Figure 32.

Table 14. Time constants of mechanical restitution of human myocardium in 0.5 μM ouabain. n=6

τ_1 (ms)	τ_2 (s)	τ_3 (s)
648.13 ± 149.40	8.63 ± 2.01	692.2 ± 148.6
(553.76 ± 114.72)	(5.20 ± 1.26)	(303.9 ± 85.3)
$p < 0.05$	ns	$p < 0.05$

(Mean ± standard error)
Significance tested using Wilcoxon test on paired samples. Paired control values are given in brackets.

Table 15. Intercepts of mechanical restitution of human myocardium in 0.5 μM ouabain. n=6

A	B	C
1.89 (1.30-2.24)	0.64 (0.41-1.09)	2.00 (1.45-2.22)
[1.98 (1.26-2.88)]	[0.55 (0.43-0.97)]	[1.53(1.27-1.96)]
ns	ns	$p < 0.05$

(Median and interquartile range)
Significance tested using Wilcoxon test on paired samples. Paired control values are given in brackets.

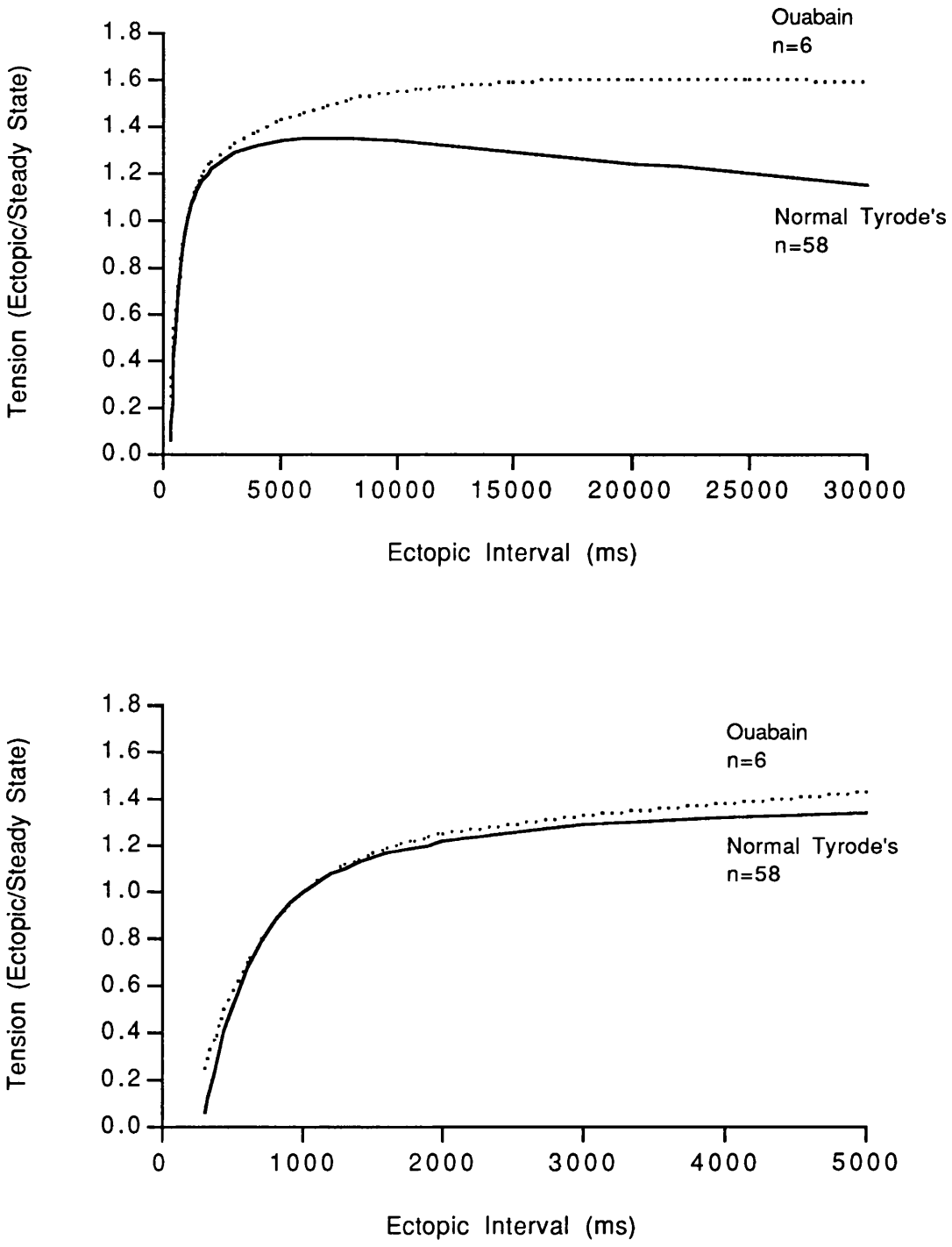

Figure 32. Mechanical restitution curves derived from the combined data of several experiments showing the effect of 0.5 μM ouabain.

iv. Verapamil

Six experiments were performed in the presence of 2.2 nM verapamil and the results are presented in Tables 16 and 17. Verapamil significantly prolonged both τ_1 and τ_2, and increased 'B' and 'C' (see Figure 33)

Table 16. Time constants of mechanical restitution of human myocardium in 2.2 nM verapamil. n=6

τ_1 (ms)	τ_2 (s)	τ_3 (s)
703.34 ± 172.40	8.41 ± 2.15	199.6 ± 23.3
(400.73 ± 59.06)	(3.88 ± 1.26)	(263.3 ± 87.7)
$p < 0.05$	$p < 0.05$	ns

(Mean ± standard error)
Significance tested using Wilcoxon test on paired samples. Paired control values are given in brackets.

Table 17. Intercepts of mechanical restitution of human myocardium in 2.2 nM verapamil. n=6

A	B	C
1.67 (1.42-1.93)	1.32 (0.98-1.82)	2.54 (1.72-3.20)
[2.06 (1.60-2.50)]	[0.62 (0.46-0.68)]	[1.48(1.27-1.57)]
ns	$p < 0.05$	$p < 0.05$

(Median and interquartile range)
Significance tested using Wilcoxon test on paired samples. Paired control values are given in brackets.

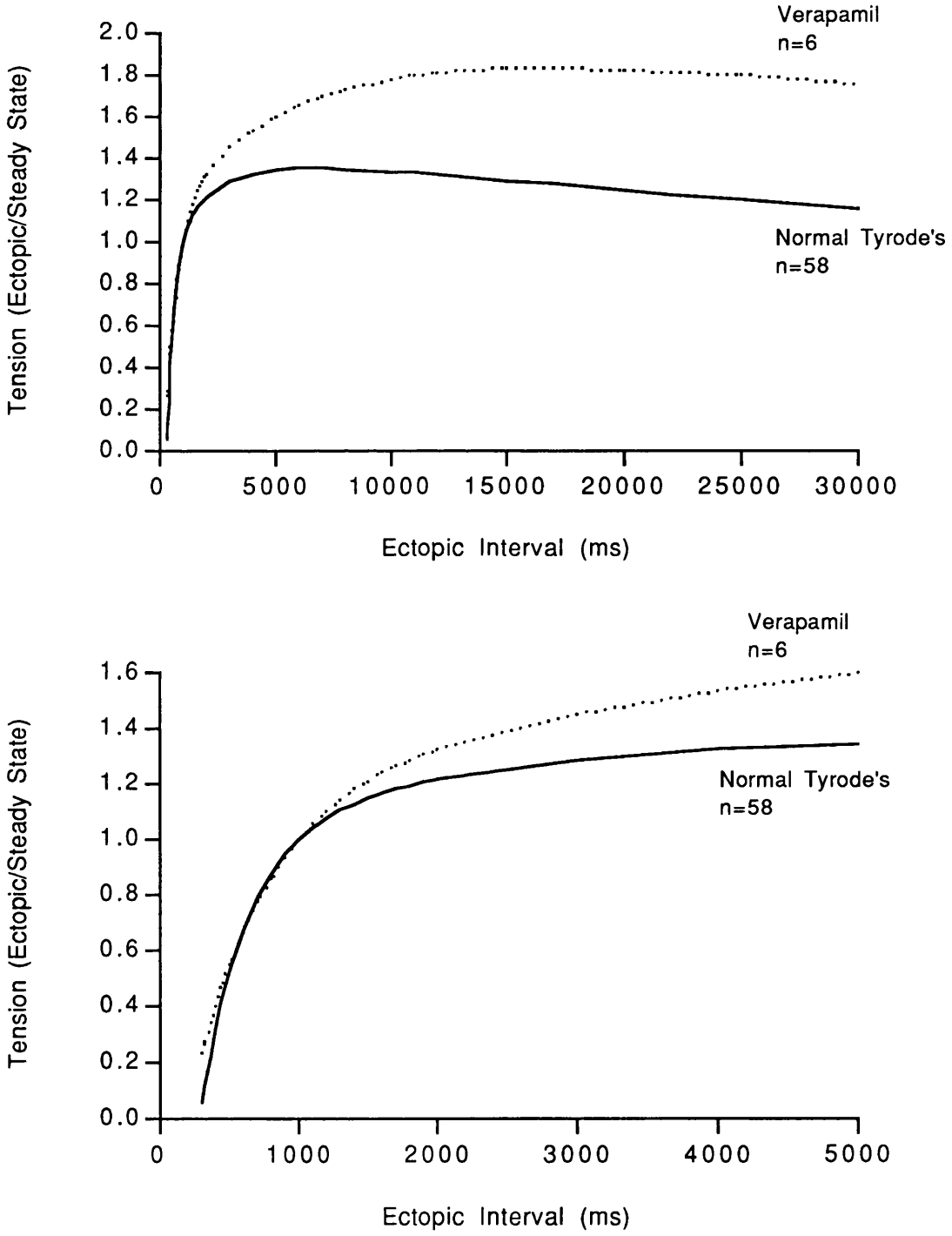

Figure 33. Mechanical restitution curves derived from the combined data of several experiments showing the effect of 2.2 nM verapamil.

v. Ryanodine

Six experiments were performed in the presence of 10μM Ryanodine and the results are presented in Tables 18 & 19. Ryanodine significantly abbreviated both τ_1 and τ_3. A slow rising exponential (τ_2) could not be identified in the presence of Ryanodine. The 'A' intercept is approximately six fold larger, in the presence of ryanodine, than in controls. 'C' is significantly reduced (Figure 34).

Table 18. Time constants of mechanical restitution of human myocardium in 10μM Ryanodine. n=6

τ_1 (ms)	τ_2 (s)	τ_3 (s)
119.62 ± 11.79		4.28 ± 1.05
(304.68 ± 35.24)	(5.90 ± 1.89)	(137.49 ± 25.58)
$p < 0.05$		$p < 0.05$

(Mean ± standard error)
Significance tested using Wilcoxon test on paired samples. Paired control values are given in brackets.

Table 19. Intercepts of mechanical restitution of human myocardium in 10μM Ryanodine. n=6

A	B	C
14.52 (5.51-49.9)		0.59 (0.42-0.70)
[2.33 (1.94-2.92)]	[0.37 (0.34-1.14)]	[1.40(1.25-1.98)]
$p < 0.05$		$p < 0.05$

(Median and interquartile range)
Significance tested using Wilcoxon test on paired samples. Paired control values are given in brackets.

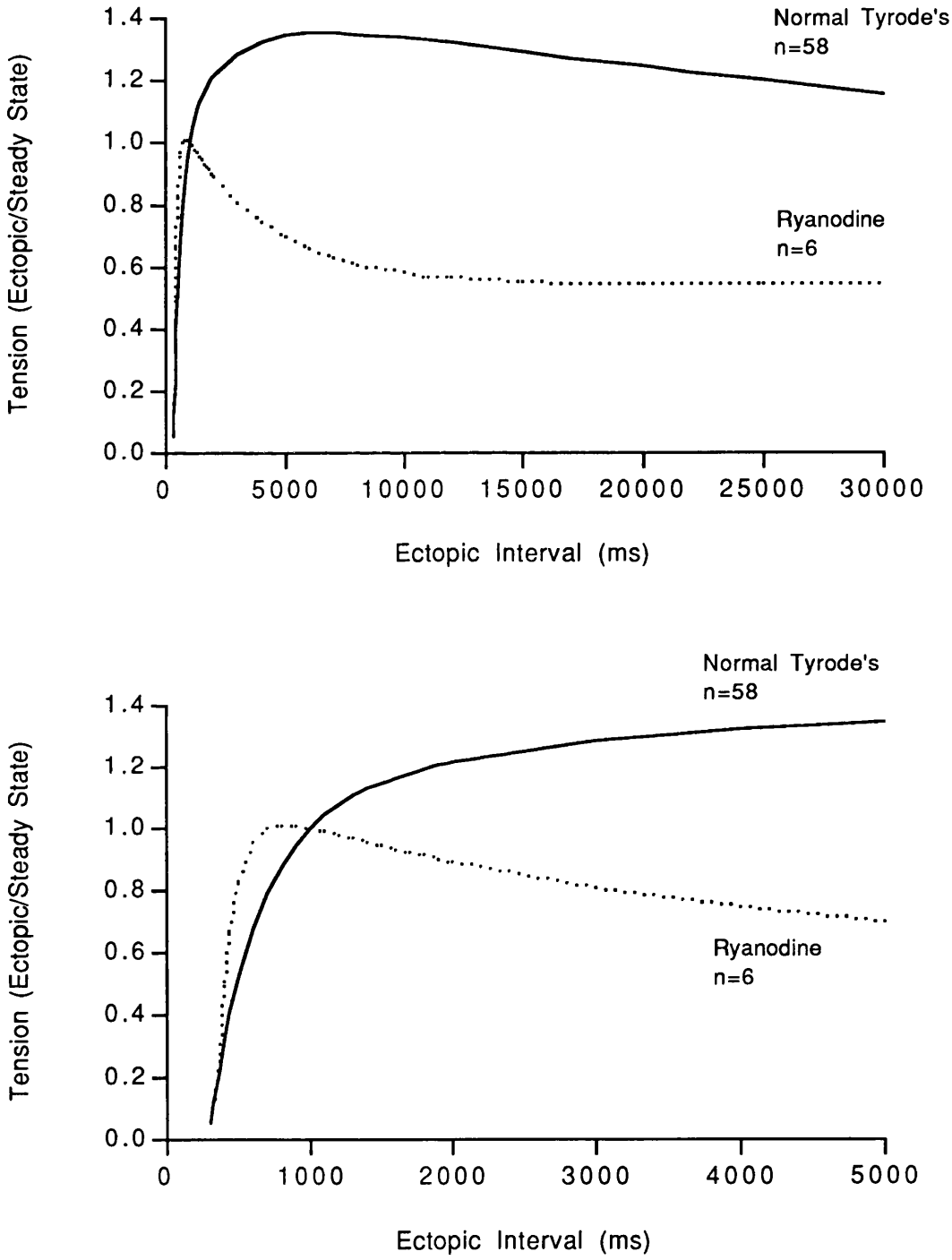

Figure 34. Mechanical restitution curves derived from the combined data of several experiments showing the effect of 10μM Ryanodine.

TRANS-MEMBRANE ACTION POTENTIALS

Stable micro-electrode penetration was successful in twenty preparations of human myocardium and was unsuccessful when attempted on a further ten occasions. Figure 35 is an original record of a human ventricular action-potential generated from the digital oscilloscope output. A summary of the parameters of human ventricular myocardial trans-membrane action potentials is presented in Table 20.

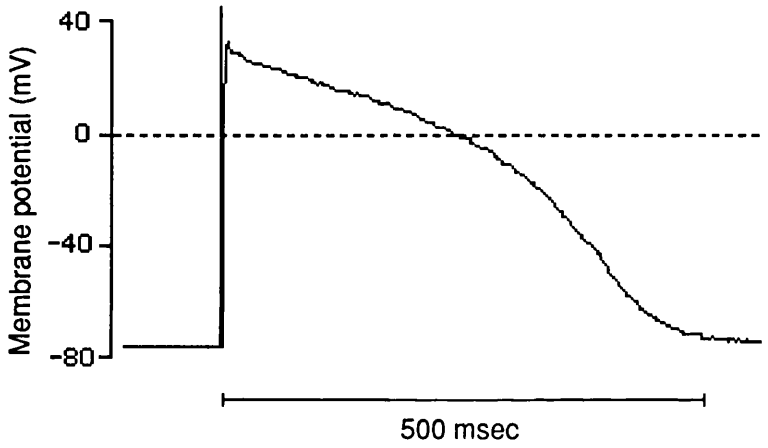

Figure 35. Digitised record of a human ventricular action potential.

Table 20. Characteristics of the human ventricular trans-membrane action potential in normal Tyrode's solution (n=20)

Resting Potent. (mV)	Overshoot (mV)	Amplitude (mV)	Duration 90% (ms)	dV/dt max Vs^{-1}
-81.8±2.5	18.7±3.4	100.5±2.9	433.5±17.5	134.7±19.2

(mean ± standard error)

'SLOW' ACTION POTENTIALS

As previously described, so-called 'Slow' action potentials were produced and recorded by raising the [K^+] in the superfusate. An effect of raising the external [K^+] was to make the muscle relatively unexcitable; and on occasions totally unexcitable. In practice the highest [K^+] at which the muscle could still be stimulated was chosen. This was 18mmol on five, 16mmol on eight, and 14mmol on three occasions. The effect of increased external [K^+] on the resting membrane potential is shown in Figure 36.

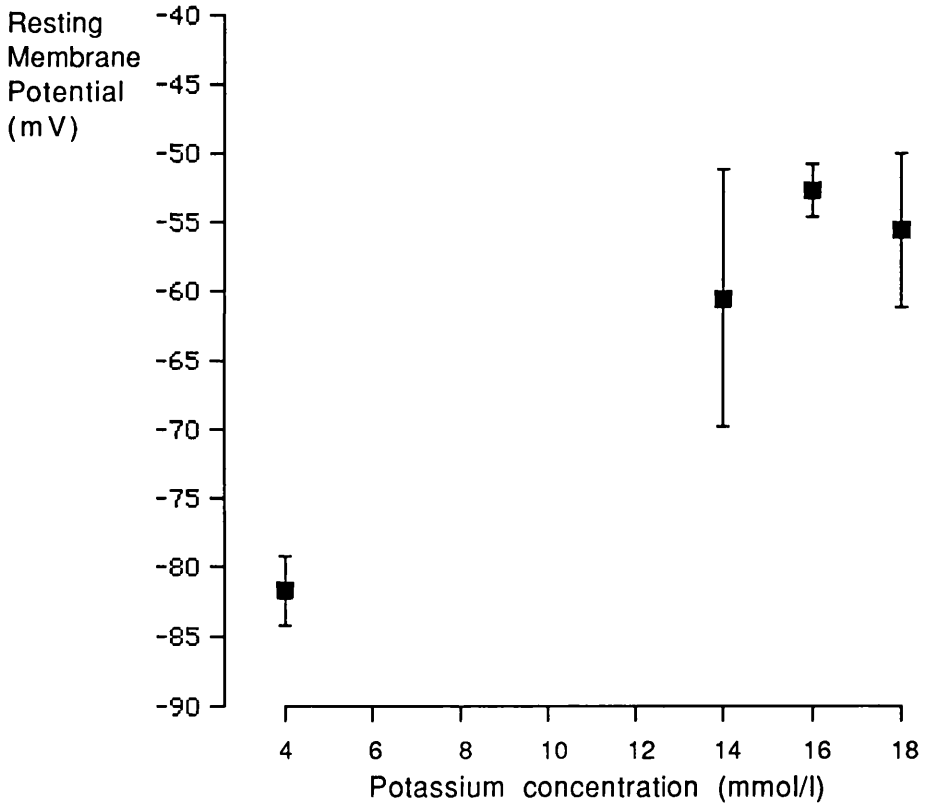

Figure 36. Resting membrane potentials at different external [K^+]

There was always a fall in peak twitch tension produced by the preparation in high external [K^+]. The amount of tension was dependent upon the size of the stimulus and therefore no attempt was made to quantify twitch tension in these circumstances. It is well documented that action potential duration is also dependent on stimulus strength (Tritthart *et al*, 1973a). Consequently supramaximal stimuli were required to produce

reproducible stable action potentials. Furthermore, the actual stimulus threshold was increased significantly in the presence of high external [K^+]. The threshold stimulus amplitude was increased from 5.2±1.1V (in normal Tyrode's soln.) to 29.8±6.6V (in high[K^+]), ($p < 0.01$). The threshold stimulus width was increased from 0.349±0.072ms (in normal Tyrode's soln.) to 0.55±0.117ms (in high[K^+]), ($p < 0.05$). The absolute stimulus threshold values are not important and will depend upon many factors including the geometry of the muscle bath and the relationship of the electrodes to the muscle strip. Notwithstanding, there were significant practical difficulties in reducing the influence of the stimulus artefact on the recording of the upstroke of the trans-membrane action potential at higher stimulus voltages (see Figure 37). This problem was found to be dealt with best by reducing the distance between the intracellular electrode and the reference electrode. This was achieved by constructing the reference electrode as a glass KCl filled microelectrode, clamping it to the same holder as the intracellular electrode and positioning its tip approximately 1mm higher, (see methods). With this arrangement the reference electrode is positioned in the solution just above the muscle preparation.

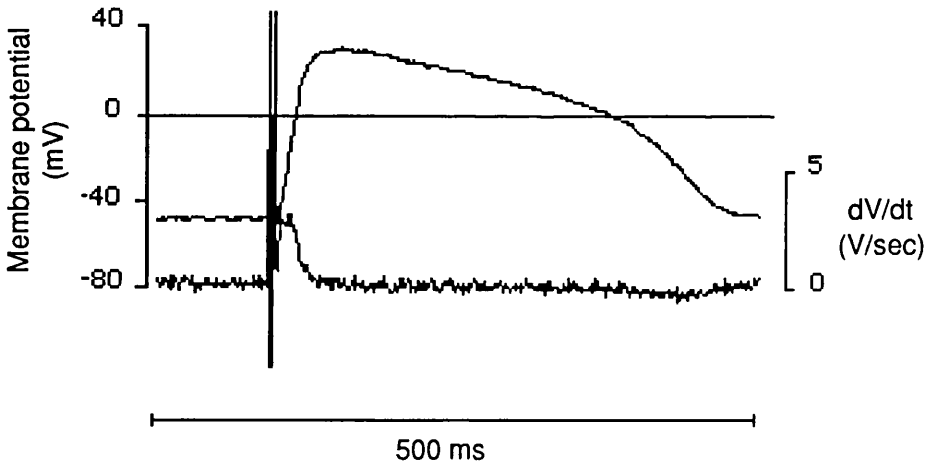

Figure 37. Human ventricular 'Slow' action potential recording. dV/dt is the lower trace and shows the large stimulus artefact which is very close to the peak maximun dV/dt.

Of the twenty experiments that electrode penetration was initially successful, this was only temporary in four. Therefore in sixteen preparations 'Slow' action potentials could be recorded. In order to obtain restitution curves for the upstroke velocity (dV/dt max) of the 'Slow' action potential two important requirements had to be met:

1. The stimulus artefact should be separate from the upstroke of the action potential. This was a particular problem with high stimulus thresholds, and was largely overcome by the use of twin microelectrode recordings.

2. In the twitching preparation the electrode penetration should be stable, so that beat-to-beat changes in dV/dt max could be obtained over periods of several minutes (or long enough to acquire sufficient data to construct a restitution curve).

Control

Table 21 shows the parameters of the 'Slow' action potential (n=16) and the time constant of recovery of dV/dt max (τ_{SAP}) (n=13). The 'Slow' action potential has a significantly lower amplitude, less negative resting membrane potential, shorter duration, and slower dV/dt max than the action potentials recorded under otherwise normal conditions (Figure 38).

Table 21. Characteristics of the human ventricular trans-membrane action potential in raised [K^+] solution('Slow' action potential) (n=16)

Resting Potent. (mV)	Overshoot (mV)	Amplitude (mV)	Duration 90% (ms)	dV/dt max (Vs^{-1})	τ_{SAP} (ms)
-55.0±2.5	16.5±4.0	71.6±3.5	260.5±17.4	4.40±0.35	72.2±13.1
(-83.1±3.0) $p < 0.001$	(17.9±4.2) ns	(101.0±3.5) $p < 0.001$	(435.9±21.2) $p < 0.001$	(126.59±19.10) $p < 0.001$	

Values are expressed as mean ± standard error, and are compared with values in normal Tyrode's solution (in brackets). Significance tested using Wilcoxon test on paired samples

The recovery of slow action potential dV/dt max (τ_{SAP}) was significantly faster than τ_1 of mechanical restitution (72±13ms and 463±32ms respectively) ($p < 0.0001$). This difference is illustrated in records from the same patient of both twitch tension and dV/dt max (Figure 39). In this example the slow action potential dV/dt max restitution

time constant (τ_{SAP}) was 58 ms and the mechanical restitution time constant (τ_1) was 372 ms. In other words, the recovery of dV/dt max is largely complete by the early stages of mechanical recovery.

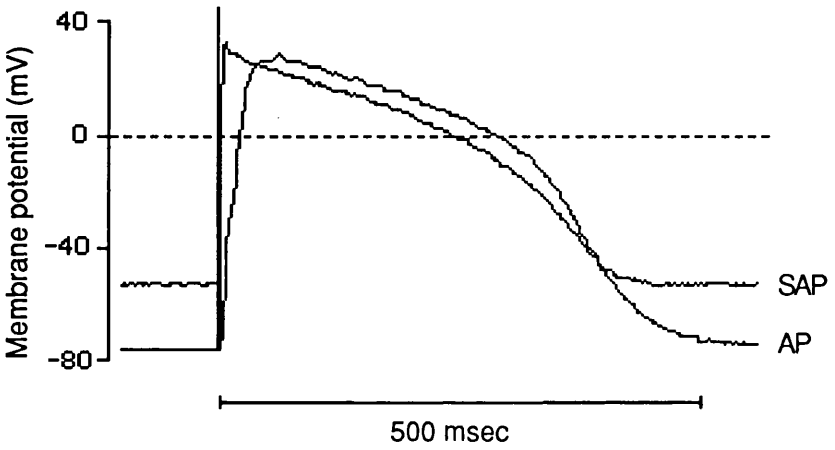

Figure 38. Human ventricular action potential recordings. AP = normal action potential. SAP = slow action potential.

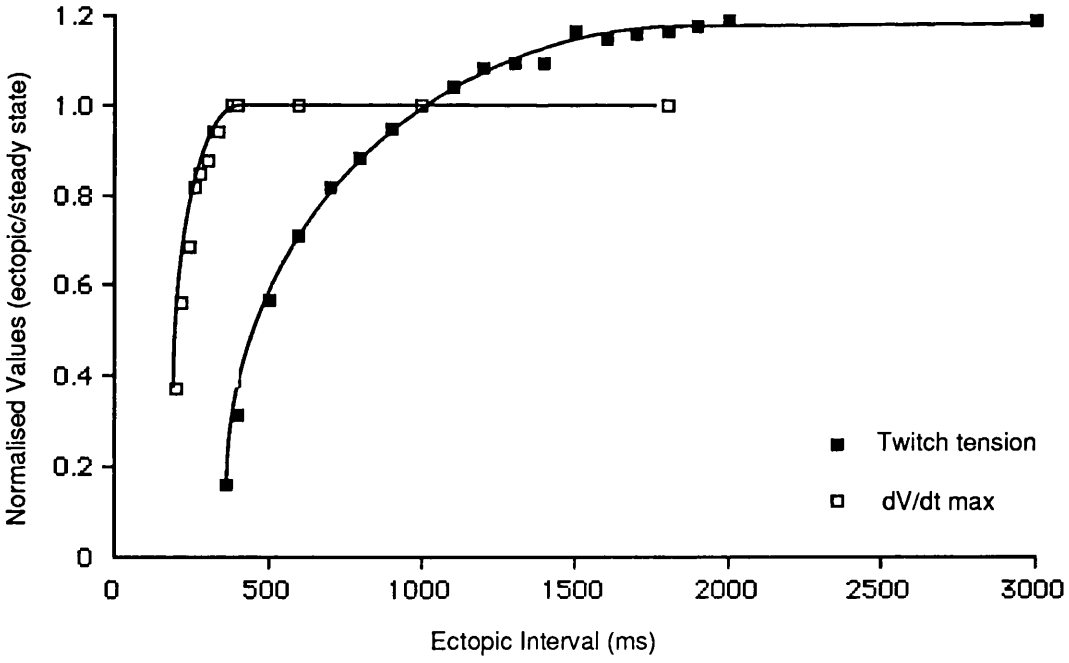

Figure 39. Restitution curves of twitch tension and 'slow' action potential dV/dt max from a strip of human papillary muscle (Patient No.32).

Interventions

i. Adrenalin

Nine experiments were performed in high [K^+] with the addition of 1μM adrenalin. While dV/dt max and τ_{SAP} tended to be faster with adrenalin, than matched controls, the differences did not reach significance at the 5% level (Table 22).

Table 22. Characteristics of the human ventricular 'slow' action potential in 1μM adrenalin (n=9)

Resting Potent. (mV)	Overshoot (mV)	Amplitude (mV)	Duration 90% (ms)	dV/dt max (Vs^{-1})	τ_{SAP} (ms)
-51.4±4.9	18.4±7.1	69.8±5.4	268.7±20.3	5.95±0.47	58.0±14.9
(-54.0±4.0)	(17.4±6.5)	(71.5±5.9)	(258.7±23.9)	(5.26±0.32)	(65.8±36.6)
ns	ns	ns	ns	ns	ns

Values are expressed as mean ± standard error. Paired values from control 'Slow' action potentials are given in brackets. Significance tested using Wilcoxon test on paired samples.

ii. High [Ca^{2+}]

In six experiments at high [K^+] in the presence of 3.6mmol [Ca^{2+}] again no significant difference was observed in parameters of the 'slow' action potential. However, τ_{SAP} tended to be slower in the presence of 3.6 mmol [Ca^{2+}] (Table 33).

Table 23. Characteristics of the human ventricular 'slow' action potential in 3.6mmol [Ca^{2+}] (n=6)

Resting Potent. (mV)	Overshoot (mV)	Amplitude (mV)	Duration 90% (ms)	dV/dt max (Vs^{-1})	τ_{SAP} (ms)
-51.9±7.3	14.3±7.2	66.25±7.1	233.5±17.0	4.20±0.72	87.1±33.71
(-52.5±5.6)	(17.8±9.0)	(70.3±7.9)	(243.8±30.1)	(5.24±0.48)	(73.3±17.8)
ns	ns	ns	ns	ns	ns

Values are expressed as mean ± standard error. Paired values from control 'Slow' action potentials are given in brackets. Significance tested using Wilcoxon test on paired samples.

iii. Verapamil

With the addition of 2.2 nM verapamil to high [K^+] Tyrode's solution the action potentials were shorter, had a smaller amplitude, slower dV/dt max and slower restitution time constant than in high [K^+] Tyrode's solution alone. While the direction of change was consistant in all three experiments the difference only reached a level of significance in the case of action potential duration.

Table 24. Characteristics of the human ventricular 'slow' action potential in 2.2 nM verapamil (n=3)

Resting Potent. (mV)	Overshoot (mV)	Amplitude (mV)	Duration 90% (ms)	dV/dt max (Vs^{-1})	τ_{SAP} (ms)
-48.2±2.2	8.0±10.4	62.2±7.5	209.7±17.0	2.97±0.32	70.2±11.7
(-54.0±4.0)	(39.5±1.8)	(87.7±0.4)	(294.9±38.4)	(4.78±0.54)	(35.3±10.2)
ns	ns	ns	$p < 0.01$	ns	ns

Values are expressed as mean ± standard error. Paired values from control 'Slow' action potentials are given in brackets. Significance tested using Student's paired t test.

iv. Caffeine

Two experiments were performed in the presence of 5mM caffeine. The resulting 'slow' action potentials were of larger amplitude (67.5mV mean vs 49.0mV) and similar duration (219.0ms mean vs 268.3ms). dV/dt max did not appear to be altered ($4.28Vs^{-1}$ mean vs $4.80Vs^{-1}$), but the time constant for recovery of dV/dt max (τ_{SAP}) was prolonged (192.9ms mean vs 83.5±1.6ms).

v. Ouabain

In one experiment 'slow' action potentials were recorded in the presence of 0.5 μM ouabain. These were of lower amplitude (45mV vs 80mV) and shorter duration (137ms vs 186ms) with a slower upstroke velocity ($2.38Vs^{-1}$ vs $6.16Vs^{-1}$)

COMPARISON OF *IN-VITRO* AND *IN-VIVO* FINDINGS

With one exception (coronary artery disease and left-ventricular aneurysm), all human myocardium was obtained from patients undergoing aortic or mitral valve replacement. The mean age of the patients at the time of surgery was 55 years (range 18 to 82 years). Twenty patients were male, and twenty-eight female. All had undergone prior cardiac catheterization (44 at St Thomas' Hospital; 14 elsewhere). The interval between cardiac catheterization and surgery was 6.26 ± 0.99 months. Tables 26 to 28 summarize the important *in-vivo* findings in the patients from whom biopsies were taken.

i. Symptoms

Symptom classification, according to the New York Heart Association class (NYHA, 1964), is shown in Figure 40. Forty (69%) patients were in class III or IV. Symptom class bore no significant correlation with twitch tension parameters, trans-membrane potential parameters or restitution time constants (Kendall's rank correlation).

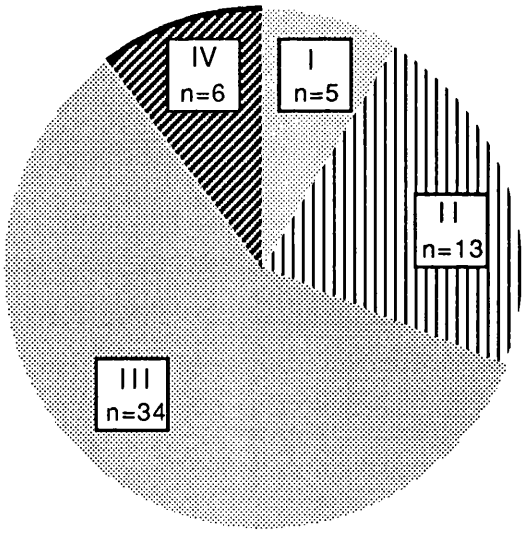

Figure 40. Distribution of NYHA symptom class

ii. Drug History

The patients in this study were taking an assortment of different drugs up to the time of surgery. It would be of no value to list and analyse the distribution of all medications. However, the most common categories, or groups of drugs, are listed in Table 25. Individual analysis of each of these groups, using the unpaired t-test, showed no difference in either any of the isometric twitch tension parameters or mechanical restitution time constants between those taking and those not taking a particular group of drugs.

Table 25. Drug history prior to surgery. (Number of patients)

β blockers	10	(17%)
Digoxin	20	(34%)
Calcium channel blockers	4	(7%)
Diuretics	39	(67%)
None	7	(12%)

Anaesthetic drugs were even more numerous and varied than regular medications. This information was therefore of little value in the identification of any influence a particular drug might have had on the performance of the tissue in the muscle bath. In general, the combination of drugs used by all anaesthetists for pre-medication, induction, maintainance and 'pump' drugs fell into similar distinct catagories. The gas mixture used prior to cardiopulmonary bypass did, however, vary between patients. In approximately two-thirds of cases a fluorinated hydrocarbon, such as halothane, was used in addition to nitrous oxide. The use of these compounds did not appear to influence the *invitro* findings (unpaired t-test).

Table 26. Preparation, patient age, diagnosis and symptomatic status

Patient No.	Preparation	Age (years)	Diagnosis	NYHA Class
1	LV wall	60	AS,CAD	I
2	Papillary	63	AS,AR,MS,MR	IV
3	LV wall	48	AR	I
4	LV wall	69	AR	III
5	LV wall	58	AS	II
6	LV wall	41	AR	I
7	LV wall	57	AR	III
8	LV wall	64	AS,AR,MR	III
9	LV wall	21	AR	III
10	LV wall	70	AS	IV
11	Papillary	66	MS,MR	III
12	Papillary	54	MR,MS	III
13	Papillary	42	MS	II
14	LV wall	69	AS	III
15	LV wall	64	AS,CAD	II
16	Papillary	63	AS, MS, MR, TR	III
17	LV wall	67	AS	III
18	LV wall	46	AS,AR	II
19	LV wall	73	AS	III
20	LV wall	26	AR	II
21	LV wall	57	CAD,LVAN	II
22	LV wall	35	AR,MS	II
23	LV wall	65	AS,AR	III
24	Papillary	60	MS,TR	III
25	LV wall	61	AR	I
26	LV wall	68	AR	III
27	LV wall	54	AS,AR,MS,MR	I
28	Papillary	55	AS,MS,MR	II
29	Papillary	57	MS,MR,TR	III
30	LV wall	54	MR	III
31	LV wall	69	AS	IV
32	Papillary	48	MR,TR	III
33	Papillary	50	MS	III
34	Papillary	30	MS,(AS,AR)	III
35	Papillary	67	MS	III
36	Papillary	31	AR,MS,MR	II
37	LV wall	42	AS,MR	II
38	Papillary	58	MS	III
39	LV wall	67	AS	III
40	LV wall	34	AR	II
41	LV wall	72	AS,CAD	III
42	LV wall	39	AR,CAD	III
43	LV wall	33	AR,MR	II
44	LV wall	61	AS	IV
45	Papillary	68	MS	III
46	LV wall	52	AR,CAD	III
47	Papillary	32	MS	III
48	Papillary	59	AS,MS,CAD	III
49	Papillary	61	MR	III
50	LV wall	61	AS,AR	II
51	Papillary	58	MS	III
52	Papillary	66	AS,AR,MR	III
53	Papillary	60	MR,MS,AR	III
54	LV wall	22	AR	IV
55	LV wall	75	AS	III
56	LV wall	18	AR	I
57	LV wall		AS	IV
58	Papillary	57	MS	III

AS = aortic stenosis.
AR = aortic regurgitation.
MS = mitral stenosis.
MR = mitral regurgitation.
CAD = coronary artery disease.
LVAN = left-ventricular aneurysm.

Table 27. Summary of Cardiac Catheterization Data

Patient No.	LVSP (mm Hg)	LVEDP (mm Hg)	AV area (cm^2)	SVR (units)	CI (l,min^{-1},m^{-2})	Mean Vcf ($circ,sec^{-1}$)	EF	EDVI (cm^3,m^{-2})
1	144	10	0.76	25.o	2.1	1.6	0.66	71.30
2	226	31	0.52	53.7	1.53	0.56	0.36	215.12
3	122	4		21.0	2.22	1.15	0.62	128.03
4	142	7		30.0	1.5	0.91	0.44	129.85
5	218	-2	0.28	17.0	2.42	1.22	0.66	53.68
6	155	6		13.5	3.43	0.6	0.45	127.61
7	146	24	0.6	25.4	1.77	0.63	0.54	259.69
8	209	13	0.33	28.8	1.69	0.89	0.63	65.08
9	140	0				1.64	0.48	
10	185	17	0.23	70.3	0.93	0.18	0.27	103.27
11	125	3		32.0	1.69	0.55	0.53	86.11
12	100	7		20.4	2.16			0.00
13	180	8	0.8		2.2		0.70	
14	243	3	0.4	24.5	1.97	0.64	0.42	105.65
15	239	9	0.3	20.5	1.9	0.27	0.39	50.11
16	172	9	0.31	56.7	1.15	0.34	0.44	138.90
17	133	7	0.33	21.0	2.53	2.06	0.73	43.29
18	171	13	0.8	13.3	3.1		0.53	
19	175	1	0.35	45.0	1.56	1.26	0.68	40.13
20	121	5		9.3	5.81	0.77	0.59	292.15
21	123	10				0.31	0.34	74.16
22	114	7		20.0	2.4	0.9	0.44	378.27
23				18.3	3.2			
24	240	15		22.4	2.78	3.3	0.69	96.72
25	138	2		11.2	4.68		0.69	0.00
26	165	4		23.0	2.49	0.69	0.48	160.05
27	152	8	0.62	15.7	2.89	3.03	0.79	175.29
28	161	3	0.32	42.0	1.49	0.69	0.43	236.15
29	120	0						
30	121	6		23.0	2.91	0.93	0.54	76.13
31				14.2	2.9			
32	120	8						
33	107	0		18.2	2.6	0.48	0.38	178.25
34	150	15			1.94			
35	133	3		35.0	1.62			
36	100	5		38.3	1.35	0.72	0.51	161.95
37							0.55	
38	144	6		32.0	2.1	1.29	0.67	83.62
39	265	-2	0.35	30.0	1.6			
40	180	6		10.6	4.35	1.33	0.62	165.93
41	194	-3	0.5	14.5	3.2	0.95	0.48	80.77
42	180	14		26.0	3.2	0.65	0.49	130.73
43	141	4		17.7	3.64	0.45	0.32	405.21
44	194	23	0.39	14.8	2.71	0.33	0.34	180.24
45	113	5		34.0	1.6	0.99	0.59	126.08
46	185	25		27.4	2	0.5	0.53	122.55
47	99	5		18.0	3.4	1.56	0.59	68.65
48	163	9	0.5	33.1	1.88	0.56	0.52	107.72
49	160	9			0.65	1.07	0.68	
50	209	26	0.37	26.0	1.79	0.57	0.51	72.24
51	124	6		25.9	2.16	0.97	0.67	154.70
52	220	32						
53								
54								
55	213	5	0.45	13.9	1.8			
56	160	15						
57	260	40						
58	120	16						

LVSP= peak left-ventricular pressure, LVEDP= left-ventricular end diastolic pressure
AV area= calculated aortic valve area, SVR= systemic vascular resistance
CI= cardiac index, mean Vcf= mean velocity of LV circumferential fibre shortening
EDVI= LV end-diastolic volume index, EF= LV ejection fraction

Table 28. Electrocardiographic, echocardiographic and radiological findings.

Patient No.	Rate (min^{-1})	Rhythm	QRS axis (degrees)	LV voltage (mV)	Strain	LV wall (mm)	CTR
1	80	S	-30	LBBB			.55
2	72	S	-80	21	-	30	.6
3	71	S	40	56	+	22	.49
4		S	30	39	+	22	
5	80	S	20	29	+		.45
6	45	S	60	52	-		
7	68	S	0	61	+	26	.56
8	60	AF	30	33	+	26	.62
9	80	S			-		
10	80	S		45	+		
11	80	AF	-10	27	-	23	
12		AF	90	38	+	25	.61
13		S	40				.5
14	78	S	30	61	+	32	.56
15	75	S	60	67	+	31	.55
16	77	AF	60	28	+		.75
17	80	S	-30	25	-		.5
18	65	S	60	46	+	25	.53
19	76	S	-10	34	-	25	.52
20		S	0	60	+		
21	52	S	0	20	-		.47
22	90	S	-10	68	+	18	.73
23	65	S	-30	37	+	29	
24	90	AF	60	32			
25	81	S	0	39	-	22	.53
26	73	AF	30	42	-	22	.58
27	60	S	-10	37	-	26	.47
28	68	AF	-45	99	+		.71
29		S					
30	85	AF	120	RBBB		25	
31	107	S	-60	49	+	25	.61
32	100	AF	60	22		21	.6
33	75	S	80	20	-	19	.54
34		S	60	43			
35	105	AF	0	29	+	22	.52
36	70	S	110	38	-	19	.5
37		S	0	33			
38	103	AF	90	37	+		.69
39	100	S	-15	34		26	
40	90	S	30	47	+	22	
41	87	S	0	40	+		
42		S	0	35	+	19	.43
43	120	S	0	80	+	21	.67
44	86	S	-15	82	+	26	.52
45	60	S	60	21	-	20	.42
46	75	S	-15	28	-	27	.5
47	72	S	60	23	-	17	.39
48	103	AF	0	21	-	22	.71
49	80	AF	60	29	+		
50	60	S	-10	43	+	25	.5
51	90	AF	75	29			.54
52	80	S	15	40	-	22	
53	100	S	30	15	-		
54	80	S		39	-		
55	70	S		52	+		
56	90	S	-30		+		
57	72	S		42	+		
58	90	AF		25	-		

S = sinus rhythm
AF = atrial fibrillation.
"+" &"-" indicate presence and absence of strain pattern in those patients not taking digoxin.
"LV wall" = sum of posterior wall and septum measurements from M-mode echocardiographs.
CTR = cardiothoracic ratio.

iii. Catheter derived indices of contractility

Listed in Table 29 are indices of left-ventricular performance derived from *in-vivo* catheterization data (on the left) and *in-vitro* measurements made in the muscle bath (on the right). Each of the *in–vivo* indices was compared with each of the *in-vitro* measurements. In no comparison performed was there a significant correlation (Kendall's rank correlation).

Table 29. Correlation of *in-vivo* (patient) and *in-vitro* (isolated muscle) findings.

IN-VIVO (Catheter derived)	*IN-VITRO* (Muscle bath)
Cardiac Index	Peak Tension
Ejection Fraction	Time to peak tension
Mean Vcf	dT/dt max
Ejection Time	dT/dt min
End-diastolic Volume Index	Mechanical restitution time constants
LV Systolic Pressure	
LV End-diastolic Pressure	**Trans-membrane action potential:**
	Resting membrane potential
	Overshoot
	Time to 90% repolarisation
	dV/dt max
	'Slow' action potential:
	Resting membrane potential
	Overshoot
	Time to 90% repolarisation
	dV/dt max
	dV/dt max restitution time constant

Vcf = velocity of circumferential shortening.
LV = left ventricular.

iv. Disease Classification.

Biopsy material obtained from this group of human subjects undergoing cardiac surgery forms a heterogeneous group and by definition does not provide a group of normal controls. In an attempt to classify the myocardium studied according to underlying pathology the results of *in-vitro* investigations have been analysed according to the diagnosis of each patient.

Ischaemic Heart Disease

Eight of the fifty-eight patients were found to have coronary artery disease at cardiac catheterization. Since the effect of occlusive coronary artery disease on the myocardium would be patchy, one would expect the function of viable myocardium to be unimpaired. This assumption is borne out by the fact that there was no difference between the *in-vitro* performance of myocardium from those with and those without coronary artery disease (Unpaired t-test: twitch tension parameters and mechanical restitution time constants). With the exception of one patient, the primary indication for cardiac surgery was significant valvular heart disease. Since the presence of ischaemic heart disease did not affect *in-vitro* measurements, the ensuing analysis will ignore this as a parameter.

Valvular heart disease

Central to this study is an examination of the influence of different chronic valve lesions on the myocardium. Tables 30 and 31 summarize the *in-vitro* measurements in patients with different valve lesions. The patients are classified according to the predominant valve lesion, and patients are assigned to the mixed valve group if more than one valve lesion was of haemodynamic significance (see Figure 41).

Analysis of variance and its non-parametric equivalent, the Kruskal and Wallis rank-sum test, both produced identical results when comparing data from all groups of patients. The only significant difference observed is in the value of the mechanical restitution time constant (τ_1). This is prolonged in myocardium from patients with pure aortic stenosis (602.9±80.3ms, $p < 0.025$). In all other respects there was no difference between myocardium from patients in each group.

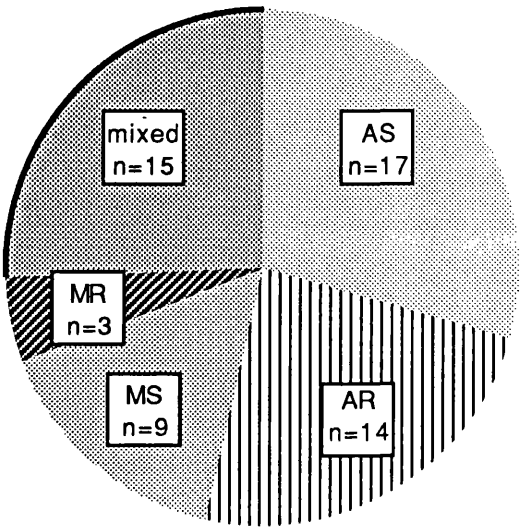

Figure 41. Distribution of diagnosis
'Mixed' = mixed valve lesions or coronary artery disease alone (in one case)

Table 30. In-vitro measurements (isolated muscles) of action potential parameters in relation to disease classification.

	Aortic Stenosis	Aortic Regurg.	Mitral Stenosis	Mitral Regurg.	Mixed Valve.
	n=6	n=7	n=3	n=1	n=3
Resting potential (mV)	-81.8±5.9	-85.5±4.6	-80.0±5.3	-85.0	-73.9±1.5
Overshoot (mV)	22.3±6.2	9.5±5.3	24.8±4.0	37.0	20.65±11.96
Time to 90% rep. (ms)	462.0±42.8	462.8±25.9	391.2±7.7	349.0	378.9±10.9
dV/dt max (Vs^{-1})	90.0±14.5	132.5±37.4	159.7±82.2	254.6	163.4±33.5
	n=4	n=4	n=1	n=1	n=3
τ_{SAP} (ms)	114.3±33.9	64.1±7.1	39.0	58.4	42.2±13.1

Values are expressed as mean ± standard error.
Significance is tested by Kruskal and Wallis rank-sum test. No significant difference was found between each of the groups.

Table 31. In-vitro measurements (isolated muscles) of twitch tension and mechanical restitution in relation to disease classification.

	Aortic Stenosis n=17	Aortic Regurg. n=14	Mitral Stenosis n=9	Mitral Regurg. n=3	Mixed Valve n=15
Peak Tension ($kNkg^{-1}$)	0.62±0.15	0.47±0.14	0.61±0.24	0.80±0.52	1.52±0.65
Time to peak tens. (ms)	319.1±10.2	283.9±12.0	303.9±10.9	273.3±8.8	295.83±14.35
dT/dt max ($kN\ kg^{-1}\ s^{-1}$)	2.52±0.63	2.75±0.83	4.02±1.94	4.78±2.86	7.01±3.05
dT/dt min ($kN\ kg^{-1}\ s^{-1}$)	-1.66±0.50	-2.09±0.77	-2.08±0.71	-5.19±3.05	-5.05±2.34
τ_1 (ms) $p < 0.025$	602.9 ±80.3	367.4 ±52.9	259.7 ±45.2	408.1 ±18.2	500.1 ±34.4
τ_2 (s)	4.13 ±0.79	2.62 ±0.58	3.01 ±0.97	7.01 ±2.81	5.32 ±0.92
τ_3 (s)	199.0 ±16.6	131.4 ±26.6	177.2 ±70.2	300.2 ±97.7	237.6 ±67.0
A	1.66 (1.26-2.18)	2.45 (1.51-6.96)	2.65 (2.42-199.7)	1.72 (1.35-2.26)	1.90 (1.47-2.27)
B	0.60 (0.40-0.78)	0.52 (0.37-0.67)	0.58 (0.24-1.26)	0.46 (0.26-0.50)	0.67 (0.45-1.03)
C	1.52 (1.41-1.73)	1.35 (1.25-1.55)	1.26 (1.18-1.39)	1.57 (1.33-1.60)	1.76 1.45-1.98)

Values are expressed as mean ± standard error except for intercepts which are medians (interquartile range).
Significance is tested by Kruskal and Wallis rank-sum test.

The analytical approach in Table 31 may not be satisfactory as the 'mixed' group is relatively large and might conceal any real differences. For example, a patient with both aortic and mitral stenosis would have been classified as mixed, even though the mitral stenosis may not contribute to left-ventricular dysfunction. It would be more important to examine these patients in terms of the pathogenesis of ventricular dysfunction, and, as such, they may be conveniently divided into three groups 1. pressure over-load, 2. volume over-load, and 3. neither pressure nor volume over-load (i.e. a group which should have relatively normal myocardium). One approach to such a classification would be to use the diagnosis as a form of classification of abnormalities of loading.

The following scheme was used:

1. Aortic Stenosis (or pressure over-load)
Defined as an aortic valve area less than $1cm^2$ in the absence of significant valvular regurgitation.

2. Aortic Regurgitation (or volume over-load)
Defined as grade 3 or 4 regurgitation. (Sellers *et al* 1964), in the absence of significant aortic stenosis.

3. Control (neither volume nor pressure over-load)
Defined as the absence of aortic stenosis or significant aortic or mitral regurgitation.

In order to justify this approach, indices of left-ventricular size and performance are compared in each of the three groups in Table 32. As expected, patients with aortic stenosis (AS) have significantly higher left-ventricular pressures, thicker left-ventricular walls, have an electrocardiographic QRS axis inclined towards the left and larger left ventricular voltages than 'Others'. On the other hand, patients with aortic regurgitation (AR) have increased left-ventricular volume and cardiac index with a similar tendency to abnormal ECGs.

The *in-vitro* mechanical data in these three groups is shown in Table 33. Significant differences were observed in the *in-vitro* mechanical properties of the 'AS' group when compared to both the 'AR' and 'Other' groups. However, despite significant differences of the *in-vivo* ventricular performance of the 'AR' and 'Other' groups (Table 32), the mechanical properties of the isolated myocardium from these patients appeared to be similar. Further analysis was therefore performed on the 'AS' group in

comparison with *all* patients without evidence of left-ventricular outflow obstruction (noAS), and the results are presented in Table 33.

Table 32. Comparison of left-ventricular volume, size and performance in patients classified according to diagnosis.

	AS n=24	AR n=14	Other n=14
EDVI (cm^3m^{-2})	96.6±16.2 ns	197.2±36.9 $p < 0.05$	114.5±13.9
Cardiac Index ($l\ min^{-1}m^{-2}$)	2.1±0.15 ns	3.1±0.42 $p < 0.05$	2.0±0.23
LVEDP (mm Hg)	12.0±2.6 ns	8.4±2.2 ns	6.5±1.3
LVSP (mm Hg)	197.4±8.2 $p < 0.0001$	146.8±6.0 ns	134.9±10.05
Ejection Fraction	0.52±0.03 ns	0.52±0.03 ns	0.58±0.04
Mean Vcf (circ. s^{-1})	0.95±0.19 ns	0.89±0.11 ns	1.12±0.27 ns
LV wall thickness (mm)	26.4±0.81 $p < 0.001$	21.9±0.96 ns	20.0±0.89
QRS frontal axis (°)	-3.9±7.6 $p < 0.001$	15±7.2 $p < 0.01$	52.1±10.9
LV voltage (mm)	43.4±3.9 $p < 0.01$	50.9±4.3 $p < 0.0001$	27.5±1.76

EDVI = left-ventricular end-diastolic volume index.
LVEDP = left-ventricular end-diastolic pressure.
LVSP = left-ventricular peak systolic pressure.
Mean Vcf = mean left-ventricular velocity of circumferential fibre shortening (angiographic)
LV wall thickness = sum of posterior wall and septum thickness derived from M-mode echocardiograph.
QRS frontal axis = mean frontal QRS axis taken from the 12 lead ECG
LV voltage = sum of deepest S wave in V1 or V2 and tallest R wave in V5 or V6 (1mV per cm)

p-values refer to an unpaired t-test between the column and 'Other'

There is a significant increase in the mechanical restitution time constant (τ_1) ($p < 0.001$) in myocardium from patients with aortic stenosis (Figures 42 and 43), and a small but significant increase in time to peak tension in this group ($p < 0.025$).

Table 33. Mechanical properties of isolated myocardium from patients with aortic stenosis (AS), aortic regurgitation (AR) and those without evidence of pressure or volume overload (Other)

	AS n=24	AR n=14	Other n=14	no AS n=34
Peak Tension ($kN\ kg^{-1}$)	1.07±0.41	0.48±0.14 ns	0.69±0.18 ns	0.65±0.12 ns
Time to peak tens. (ms)	317.3±10.5	278.2±11.1 $p < 0.025$	298.8±7.8 ns	287.6±6.4 $p < 0.025$
dT/dt max ($kN\ kg^{-1}\ s^{-1}$)	4.91±1.98	2.85±0.82 ns	4.25±1.30 ns	3.58±0.74 ns
dT/dt min ($kN\ kg^{-1}\ s^{-1}$)	-3.45±1.53	-2.19±0.75 ns	-2.72±0.70 ns	-2.49±0.50 ns
τ_1 (ms)	585.9±57.6	383.0±51.8 $p < 0.025$	377.8±40.1 $p < 0.025$	364.5±29.9 $p < 0.001$
τ_2 (s)	4.89±0.65	2.71±0.56 $p < 0.05$	3.50±0.75 ns	3.64±0.59 ns
τ_3 (s)	224.9±37.7	132.9±26.5 ns	202.0±47.2 ns	171.8±24.9 ns
A	1.73 (1.31-2.28)	2.38 (1.51-4.10) ns	2.17 (1.60-2.65) ns	2.38 (1.61-2.92) ns
B	0.68 (0.47-0.85)	0.44 (0.33-0.65) ns	0.57 (0.28-0.86) ns	0.52 (0.29-0.68) ns
C	1.53 (1.42-1.77)	1.37 (1.25-1.55) $p < 0.025$	1.39 (1.25-1.58) ns	1.39 (1.25-1.59) $p < 0.025$

Values are expressed as mean ± standard error except for intercepts which are medians (interquartile range). p values refer to comparison with 'AS' group. (unpaired t test, or Mann-Whitney test)

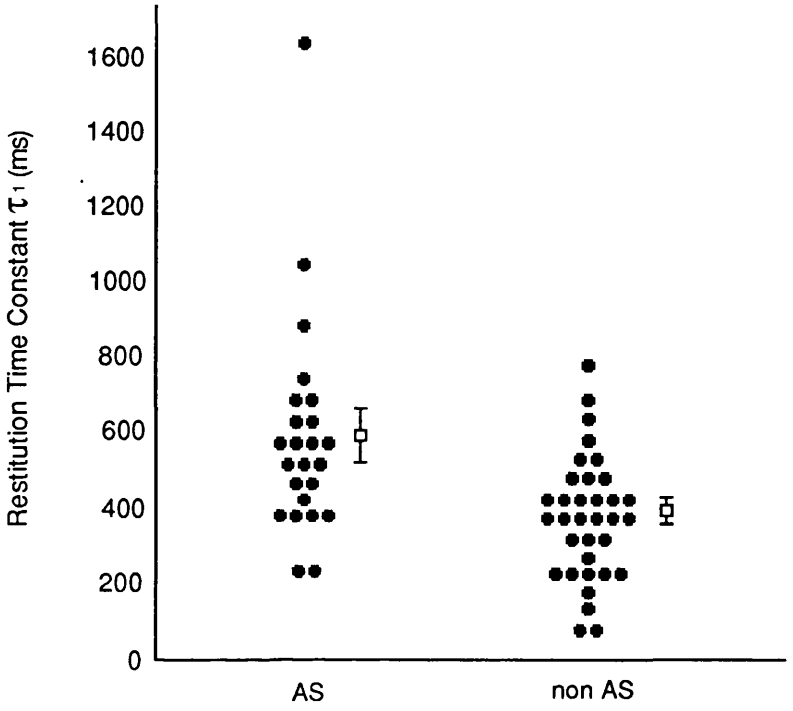

Figure 42. Mechanical restitution time constant τ_1 in individual muscles from patients with and without aortic stenosis.
Bars represent mean ± standard error.

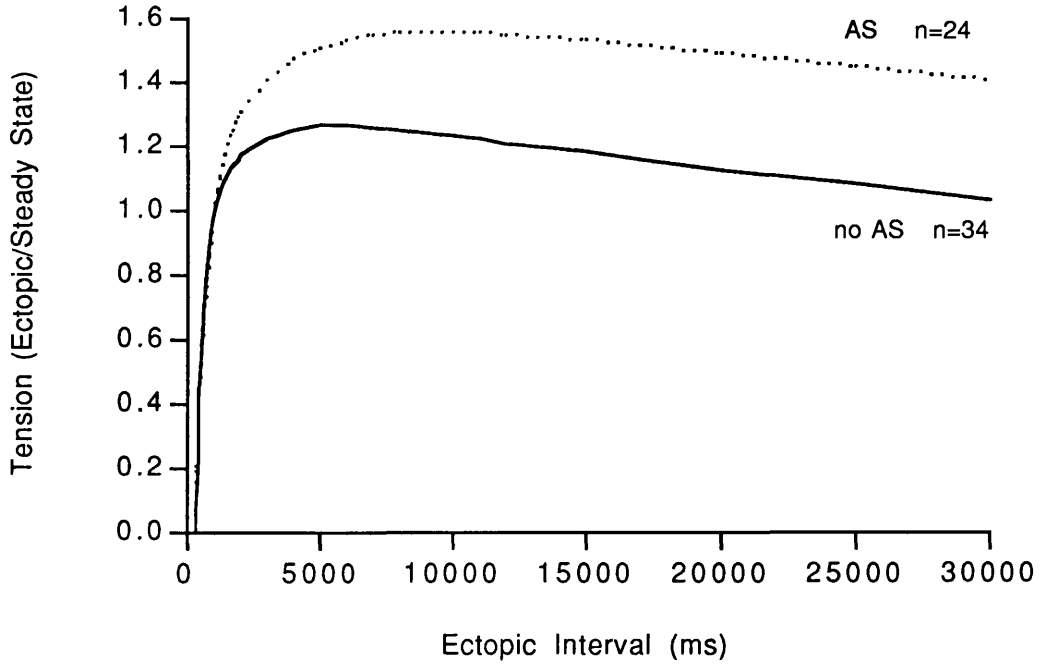

Figure 43. Combined mechanical restitution curves derived from tissue obtained from patients with aortic stenosis (AS) and no aortic stenosis (no AS)

iv. Aortic stenosis

The relationship between aortic stenosis and mechanical restitution was investigated further by examining the relationship of the degree of stenosis and τ_1 .

The aortic valve areas of individual patients with aortic stenosis were correlated with τ_1 using both least squares linear regression and Kendall's rank correlation. Figure 44 demonstrates a poor but significant correlation between the aortic valve area and τ_1. It is notable that the patient (No.10) with the highest value of τ_1 also had the most severe degree of stenosis (0.23 cm^2). It should also be pointed out that the significant relationship between τ_1 and aortic valve area persists even if this patient is removed from the analysis. This patient was severely ill at the time of cardiac catheterization and operation. He had symptoms at rest and a cardiac index of 0.93 $lmin^{-1}m^{-2}$ with a left-ventricular ejection fraction of 27%.

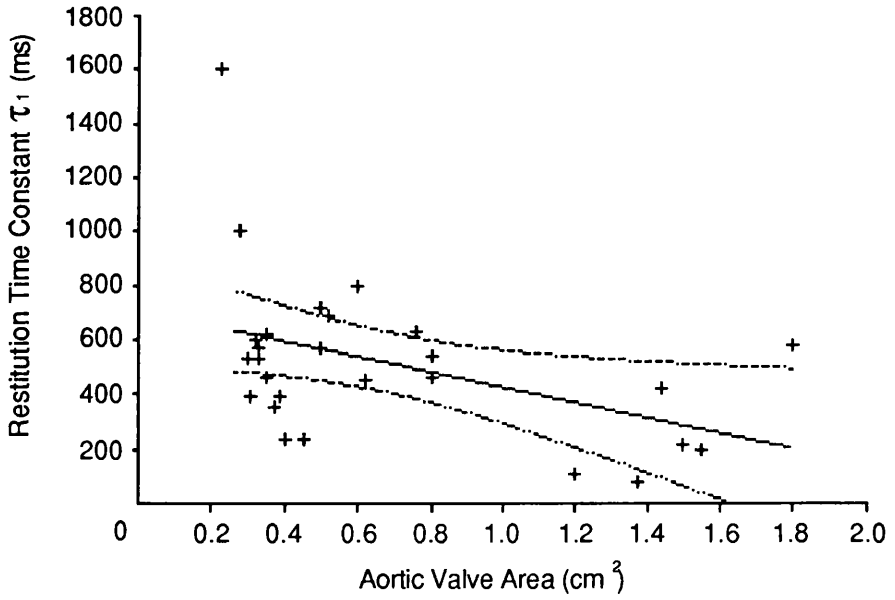

Figure 44. Scatter plot of τ_1 / Aortic valve area showing least squares linear regression and 95% confidence limits of the means of τ_1
y = -281x +710 r = 0.43 p<0.025

In order to examine the relationship between afterload and τ_1 in patients with and without aortic stenosis, systemic vascular resistance and the resistance to left-ventricular outflow from aortic stenosis were combined as an index which I have called 'Systemic Resistance'. This index shows a significant positive correlation with τ_1 (Figure 45) .

$$\text{Systemic Resistance} = \text{SVR} + \left[\frac{\text{mean AVG} \times \frac{\text{SEP}}{60}}{\text{CO}} \right]$$

Where:

$$\text{SVR} = \frac{\text{mean aortic pressure - mean right atrial pressure}}{\text{cardiac output}}$$

mean AVG = mean aortic valve gradient (in mm Hg)

SEP = systolic ejection period (in sec per minute)

CO = cardiac output (in litres per minute)

(All pressures in mm Hg)

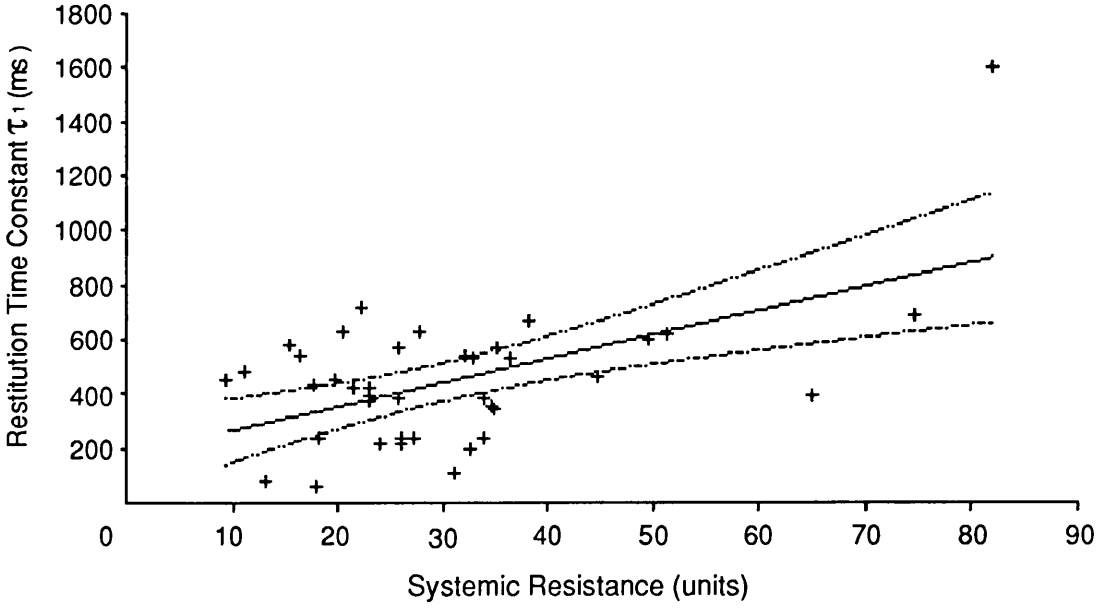

Figure 45. Scatter plot of τ_1 against systemic resistance (calculated from the sum of the systemic vascular resistance and the resistance across the aortic valve).
$y = 8.9x + 179$, $r = 0.55$, $p < 0.0005$

v. Hypertrophy

There was an inverse correlation between aortic valve area and the degree of left ventricular hypertrophy as assessed by wall thickness ($r = 0.73$, $p<0.002$) (Figure 46). The sum of left ventricular free wall and inter-ventricular septal thickness (as measured from the M-mode echocardiograph at end diastole) was used as a measure of wall thickness. This measurement was the best available estimate as the exposure quality of the left-ventricular ciné angiograms was generally not suitable for this purpose.

Using the same method to assess the degree of hypertrophy, there was a significant, but poor, positive correlation with the mechanical restitution time constant, τ_1 (Figure 47).

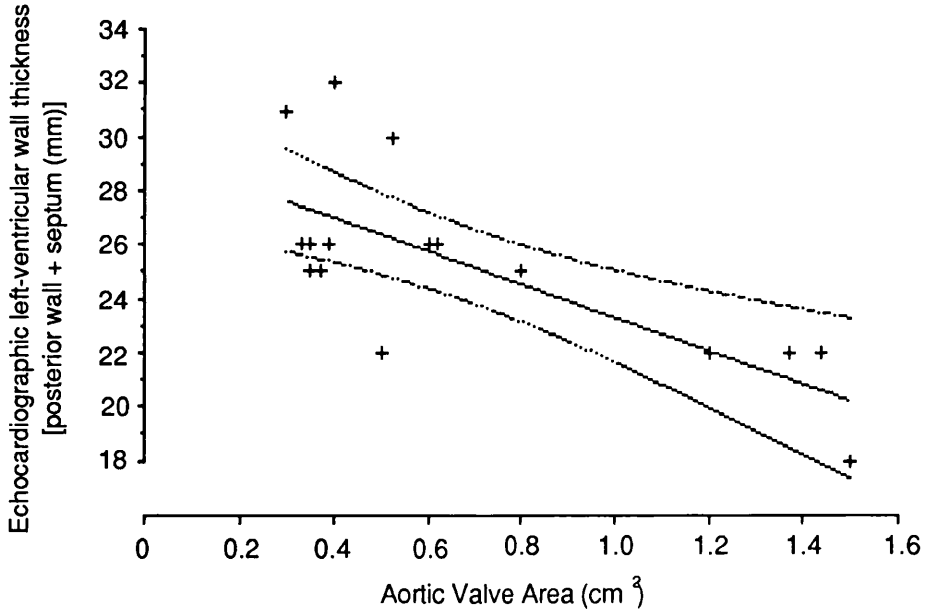

Figure 46. Scatter plot of left-ventricular wall thickness (posterior wall plus septum) against aortic valve area showing least squares linear regression and 95% confidence limits of the means of LV wall thickness.
$y = -6.13x + 29.5$, $r = 0.73$, $p = 0.0013$

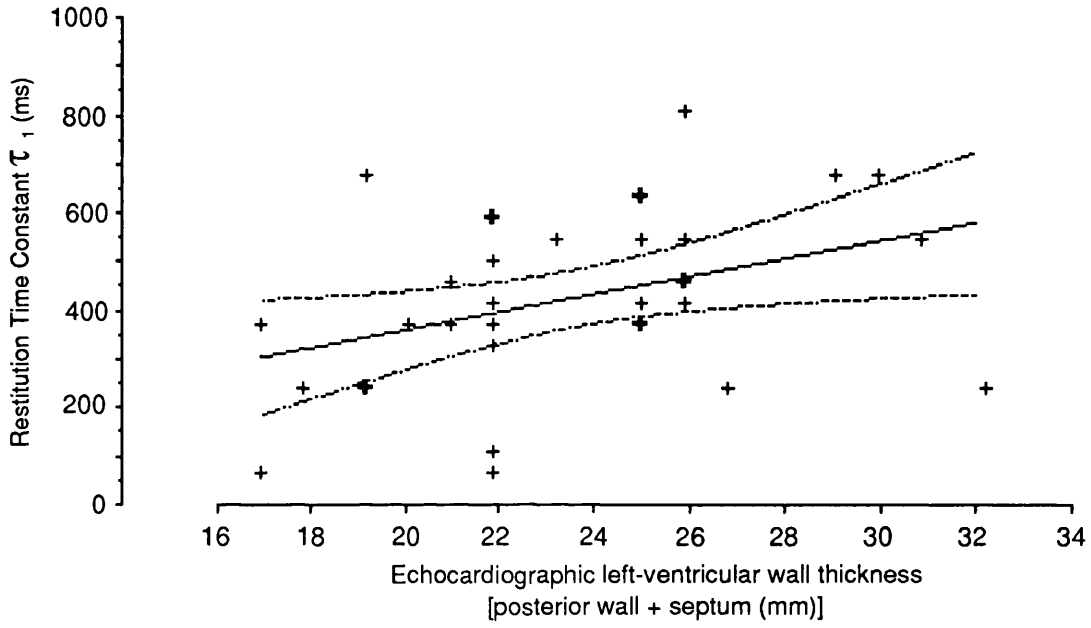

Figure 47. Plot of τ_1 against left-ventricular wall thickness showing least squares linear regression and 95% confidence limits of the means of τ_1. Large points indicate an overlay of more than one point.

$y = 18.4x - 8.1$, $r = 0.39$, $p<0.025$

Kendall's rank correlation coefficient (Tau) = 0.273, $p<0.025$

COMPARISON OF HUMAN AND OTHER MAMMALIAN MYOCARDIUM

Muscle Preparations

Experiments were performed on tissue from thirty-seven guinea-pigs and six ferrets. All guinea-pig preparations were obtained from right-ventricular papillary muscles. In the ferret, three preparations were obtained from right-ventricular papillary muscles and three from right ventricular trabeculae. The relative size and weight of preparations from the two species are shown in Table 34. The two types of ferret preparation are not distinguished here because of the small numbers involved. Human preparations were significantly heavier than those of both guinea-pig and ferret ($p < 0.001$, and $p < 0.05$ respectively). Both human and ferret preparations were longer than those of guinea-pig ($p < 0.001$, and $p < 0.05$ respectively). The diameter of human and ferret preparations was greater than in the guinea-pig ($p < 0.001$, and $p < 0.05$ respectively).

Table 34. Size and weight of human and animal tissue preparations.

	HUMAN n=58	GUINEA-PIG n=37	FERRET n=6
Weight (mg)	7.60±0.80	2.67±0.53	2.60±0.90
Length (mm)	4.46±0.19	2.82±0.12	3.93±0.87
Diameter (mm)	1.33±0.06	0.81±0.03	1.04±0.13

(mean ± standard error)

Isometric Twitch Parameters

Since two separate groups of human subjects may be distinguished by the performance of isolated strips of myocardium (in terms of the restitution time constants), these two groups have been separated for further comparison with different mammalian species. There is therefore a group of patients with aortic stenosis, and a mixed group of

subjects mostly with valvular heart disease, but no evidence of significant left ventricular out-flow obstruction. Parameters of isometric twitch tension is made between guinea-pig, ferret and the two groups of human myocardium in Table 35. This shows significant differences between both animal species and each type of human preparation; the human preparations producing less tension, having a longer time to peak tension and slower peak rates of contraction and relaxation than either animal species. There were no significant differences between each of the animal species.

Table 35. Comparison of isometric twitch tension parameters in different mammalian preparations.

	GUINEA-PIG n=37	FERRET n=6	HUMAN (noAS) n=34	HUMAN (AS) n=24
Peak Tension ($kN\ kg^{-1}$)	1.22±0.16	1.82±0.40 ns	0.65±0.12 $p < 0.01$ $p < 0.01$	1.08±0.41 $p < 0.001$ ns
Time to peak tension (ms)	172.4±6.3	156.7±6.7 ns	292.4±6.6 $p < 0.001$ $p < 0.001$	317.3±10.5 $p < 0.001$ $p < 0.001$
dT/dt max ($kN\ kg^{-1}\ s^{-1}$)	10.57±1.46	17.10±2.52 ns	3.58±0.74 $p < 0.001$ $p < 0.001$	4.91±1.98 $p < 0.025$ $p < 0.025$
dT/dt min ($kN\ kg^{-1}\ s^{-1}$)	-8.93±1.35	-14.06±2.20 ns	-2.49±0.50 $p < 0.001$ $p < 0.001$	-3.45±1.53 $p < 0.001$ $p < 0.001$

Values are expressed as mean ± standard error.
'p' values are given for unpaired t tests with guinea-pigs (upper value) and ferrets (lower value).

Mechanical Restitution

Figure 48 shows the superimposed restitution curves from the combined results in the different mammalian species. As before, the results from human muscles have been divided into two groups. Each curve represents mean values for the group. It is immediately clear that there are marked differences in the mechanical restitution curves of guinea-pig, ferret and human isolated myocardium. These differences have important practical implications in terms of deriving the values of the time constants of restitution. While evidence has been provided for the recognition of two recovery phases in the human, each with identifiable time constants, the decay phase of the guinea-pig curve tends to be much more rapid than in the human and a 'slow' recovery phase could not be distinguished. In guinea-pig control experiments only two time constants are used to describe the restitution curve.

Three important observations are apparent from the curves in Figure 48. First is the entirely different shaped curve of the guinea-pig compared to the other species. Whereas in man the decay part of the curve forms a virtual 'plateau', in the guinea-pig the decay is much more rapid. The value of the decay constant (τ_3) is in the region of 30 seconds in guinea-pig and is 200-300 seconds in both man and the ferret. (The differences being significant at the 0.1% level when both types of human preparation were compared to the guinea-pig, and at the 1% level when ferret is compared to guinea-pig). A second observation is the similarity of the ferret data to that of human subjects without aortic stenosis as distinct from those with aortic stenosis. Thirdly, in the presence of a relatively rapid decay phase in the guinea-pig, there is no discernible phase 2 and consequently τ_2 (if present) could not be quantified.

Values of τ_1 are of the same order of magnitude in each of the four groups (Table 36). τ_1 in guinea-pig and ferret is similar at around 200ms. Human preparations, however, exhibit significantly longer τ_1 ($p < 0.001$), both in those from patients without (377.9±28.4ms) and those with aortic stenosis (585.9±57.6ms) when compared to the guinea-pig. τ_1 in non-AS subjects was only significantly different from the ferret at the 2.5% level as opposed to the 0.1% level for the AS group, further emphasizing the similarity of non-hypertrophied human tissue and ferret myocardium. As already described, there are significant differences between the two groups of human preparations.

Table 36. Comparison of the time constants and intercepts of mechanical restitution in different mammalian preparations.

	GUINEA-PIG n=37	FERRET n=6	HUMAN (noAS) n=34	HUMAN (AS) n=24
τ_1 (ms)	220.0±22.7	192.5±43.2	364.5±29.9	585.9±57.6
		ns	p < 0.001	p < 0.001
			p < 0.025	p < 0.001
τ_2 (s)		4.45±1.47	3.64±0.59	4.89±0.65
		-	-	-
		ns	ns	
τ_3 (s)	28.5±8.4	221.0±156.3	171.8±24.9	224.9±37.7
		p < 0.01	p < 0.001	p < 0.001
			ns	p < 0.05
A	2.31(1.52-3.88)	3.34(2.18-7.90)	2.38(1.61-2.92)	1.73(1.31-2.28)
		ns	ns	p < 0.05
		ns	p < 0.025	
B		1.01(0.64-1.39)	0.52(0.30-0.69)	0.68(0.47-0.85)
		-	-	-
		ns	ns	
C	0.74(0.53-0.98)	1.66(1.18-2.00)	1.01(0.64-1.39)	1.53(1.42-1.77)
		p < 0.001	p < 0.001	p < 0.001
			ns	ns

Time constants are expressed as mean ± standard error, and p values are derived from an unpaired t test with guinea-pigs (on the top line), and ferrets (on the lower line). Intercepts are expressed as medians (interquartile range) and significance is tested with the Mann-Whitney test.

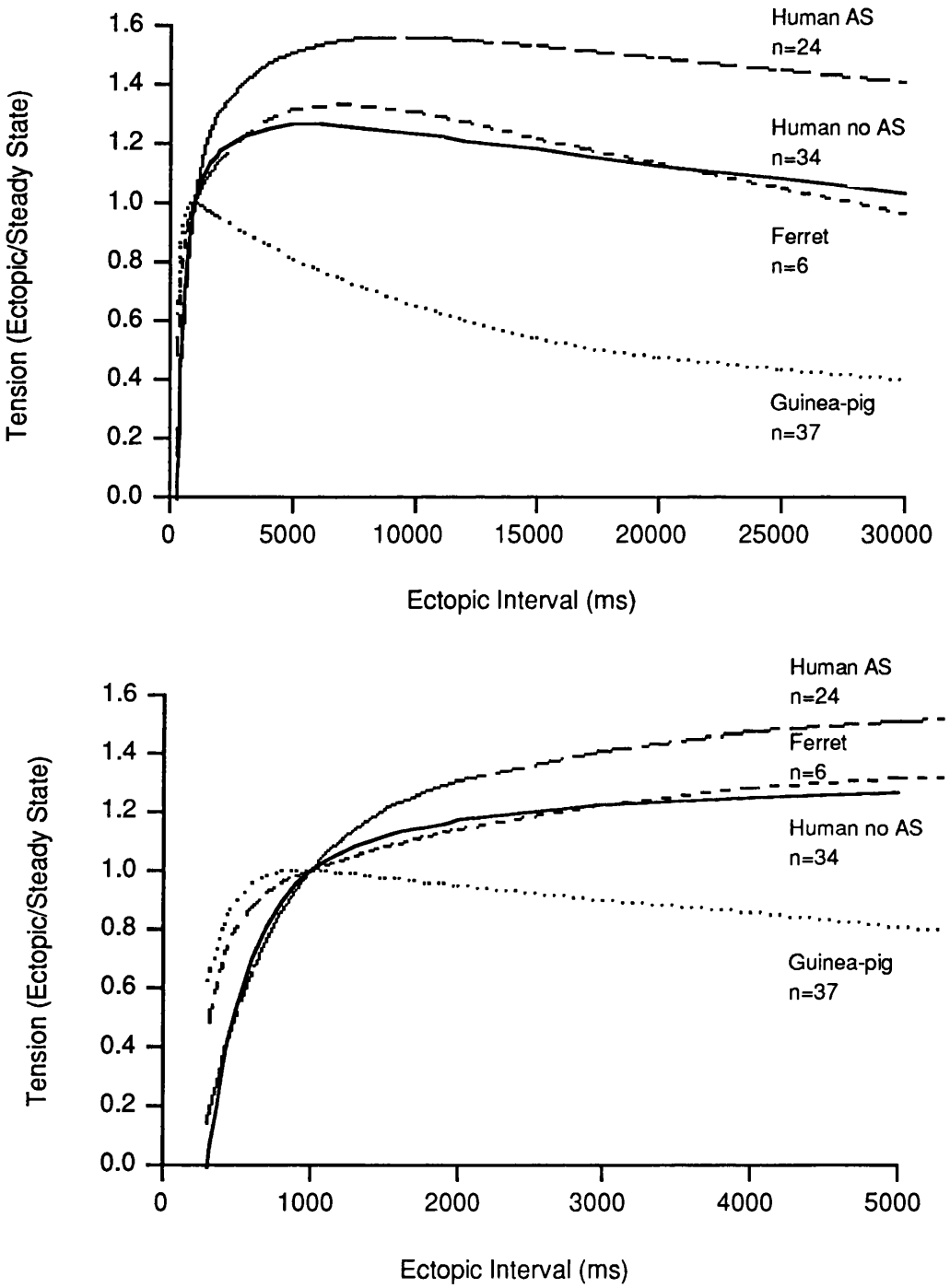

Figure 48. Mechanical Restitution Curves formed from the mean time constants found in different species.

The lower panel shows the same data as the upper on an expanded time scale.

'Normal' human vs. guinea-pig and ferret myocardium

It may be more appropriate to compare myocardium from patients believed to have relatively normal myocardium with that of other mammals. The sub-group of patients most likely to have unimpaired left-ventricular function are those with pure mitral stenosis. All patients were female, aged 55±3.9 years. Eight patients were in the New York Heart Association (NYHA) symptom class 3, and one was in class 2. The cardiac index was $2.31\pm0.21 \cdot l \cdot min^{-1} \cdot m^{-2}$; left ventricular cinéangiographic ejection fraction 61±4%; left ventricular peak systolic pressure 140±15 mm Hg; left ventricular end diastolic pressure 7.1±1.8 mm Hg.

The *in-vitro* data from the myocardium of these patients is shown in Table 31. Comparison of twitch tension parameters show differences between human and animal tissue in a similar manner and to a similar degree to the differences observed in the non-AS group in Table 35. The rapid recovery phase time constant (τ_1) was 259.7±45.2ms in tissue from patients with mitral stenosis. This was not significantly different from either the guinea-pig or ferret. Futhermore there was no significant difference between any of the three time constants of restitution in human and in ferret tissue. When this comparison is made between so-called 'relatively normal' human myocardium the only species difference in the MRC is that the guinea-pig does not display a second slow recovery phase and decay is more rapid than in both human and ferret myocardium (see Figure 49).

In summary, the human mechanical restitution curve appears to be more similar to that of the ferret than the guinea-pig, particularly in myocardium from patients without left-ventricular out-flow obstruction and in patients with no evidence of impaired left-ventricular function. Man and the ferret are distinguished from the guinea-pig largely by the difference in the decay of twitch tension which is very much slower and appears to form a 'plateau' at intervals up to 30 seconds.

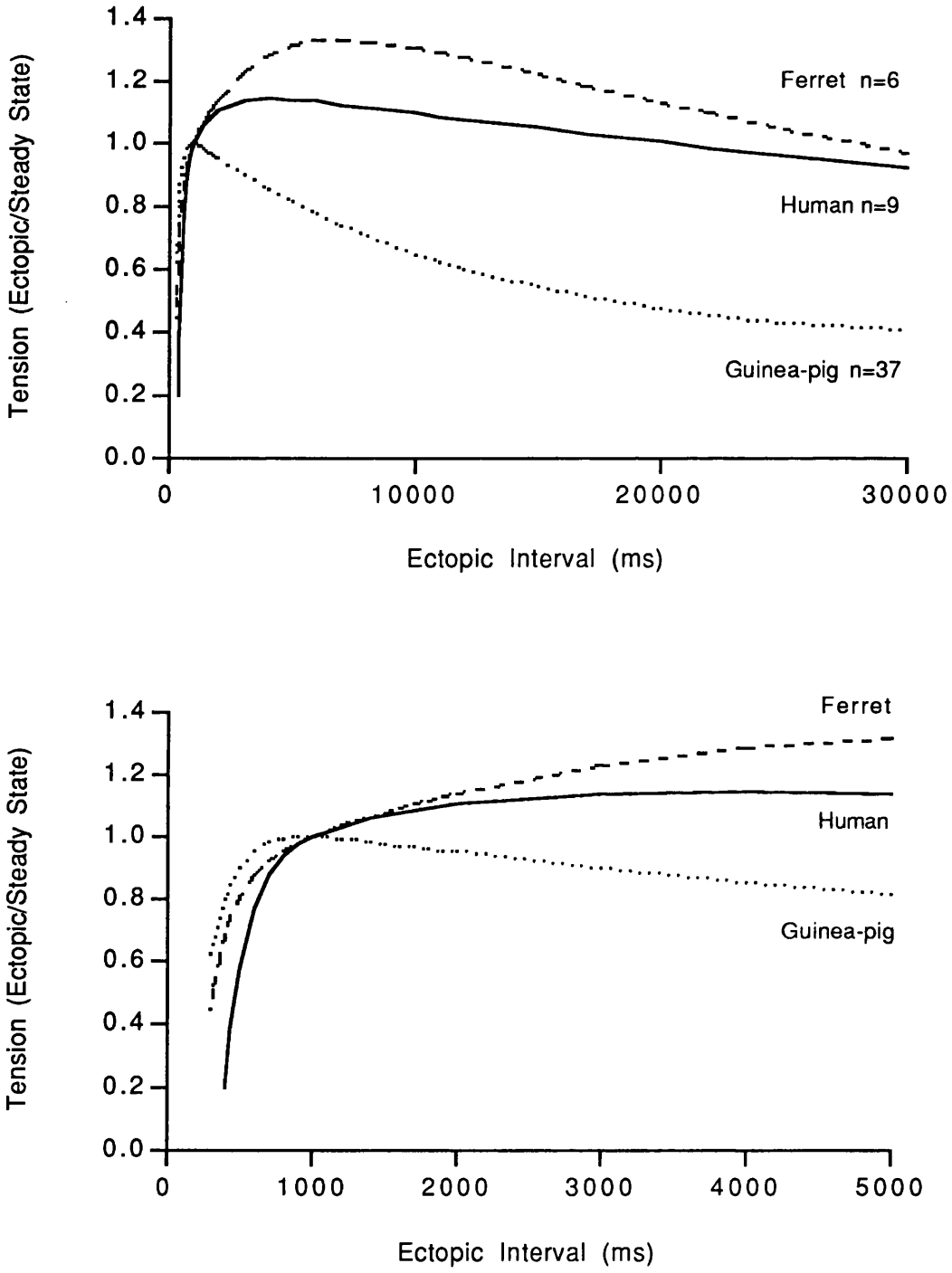

Figure 49. Mechanical restitution in different species.

Human myocardium was obtained from patients with pure mitral stenosis. The lower panel shows the same data as the upper on an expanded time scale.

ANIMAL TISSUE - INTERVENTIONS

i. Alterations in $[Ca^{2+}]$.

Six experiments were performed on guinea-pig papillary muscles at 0.9 mmol/l $[Ca^{2+}]$ and eight at 3.6 mmol/l $[Ca^{2+}]$. The results are shown in Tables 37, 38 and 39 and Figures 50 to 53. There was an expected dose-response effect of increasing $[Ca^{2+}]$ on twitch tension, but little consistent effect on mechanical restitution time constants. τ_1 in 0.9 mmol/l $[Ca^{2+}]$ was faster than in 1.8 and 3.6 mmol/l $[Ca^{2+}]$ ($p < 0.05$). 'A' was larger in 0.9mmol/l $[Ca^{2+}]$ than in 1.8 or 3.6 mmol/l ($p < 0.05$).

Table 37. Guinea-pig papillary muscle: The effect of changes of $[Ca^{2+}]$ on isometric twitch parameters.

$[Ca^{2+}]$ (mmol/l)	Tension (kN kg^{-1})	Time to peak Tens. (ms)	dT/dt max (kN kg^{-1} s^{-1})	dT/dt min (kN kg^{-1} s^{-1})
0.9 (n=6)	0.40±0.19 $p < 0.05$	164.17±4.55 ns	4.24±2.21 $p < 0.05$	-2.32±1.18 $p < 0.05$
1.8 (n=8)	0.81±0.28	165.63±7.59	8.30±3.01	-7.25±2.73
3.6 (n=8)	2.01±0.60 $p < 0.05$	165.00±6.12 ns	19.02±7.08 $p < 0.025$	-18.27±6.86 $p < 0.025$

Values are expressed as mean ± standard error

Significance tested (for comparison with 1.8 mmol/l $[Ca^{2+}]$) using Wilcoxon test on paired samples

Table 38. The effect of changes of $[Ca^{2+}]$ on the mechanical restitution time constants of guinea-pig papillary muscle

$[Ca^{2+}]$ (mmol/l)	τ_1 (ms)	τ_2 (s)	τ_3 (s)
0.9 (n=6)	156.34 ± 21.07 $p < 0.05$		46.04 ± 22.65 ns
1.8 (n=8)	211.64 ± 26.24		21.28 ± 8.03
3.6 (n=8)	198.73 ± 9.84 ns	1640.89	17.84 ± 5.49 ns

(Mean ± standard error)

Significance tested (for comparison with 1.8 mmol/l $[Ca^{2+}]$) using Wilcoxon test on paired samples

Table 39. The effect of changes in $[Ca^{2+}]$ on the intercepts of mechanical restitution of guinea-pig papillary muscle

$[Ca^{2+}]$ (mmol/l)	A	B	C
0.9 (n=6)	2.81 (2.47-9.38) $p < 0.05$		0.69 (0.35-0.82) ns
1.8 (n=8)	2.24 (1.61-2.94)		0.75 (0.59-0.85)
3.6 (n=8)	1.73 (1.47-3.12) ns	0.33	1.05 (0.76-1.19) ns

(Median and interquartile range)

Significance tested (for comparison with 1.8 mmol/l $[Ca^{2+}]$) using Wilcoxon test on paired samples

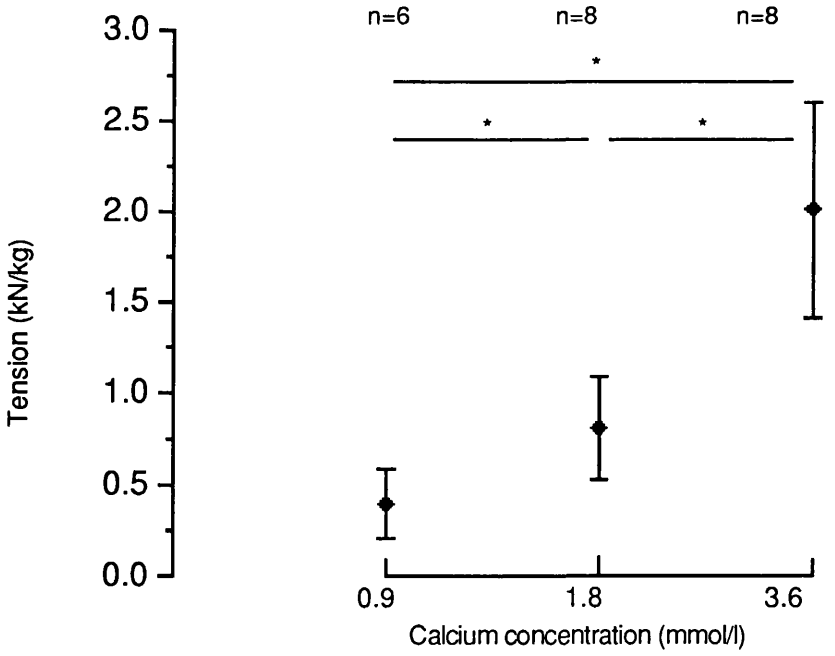

Figure 50. Calcium dose-response for twitch tension in guinea-pig papillary muscle.

* = $p < 0.05$

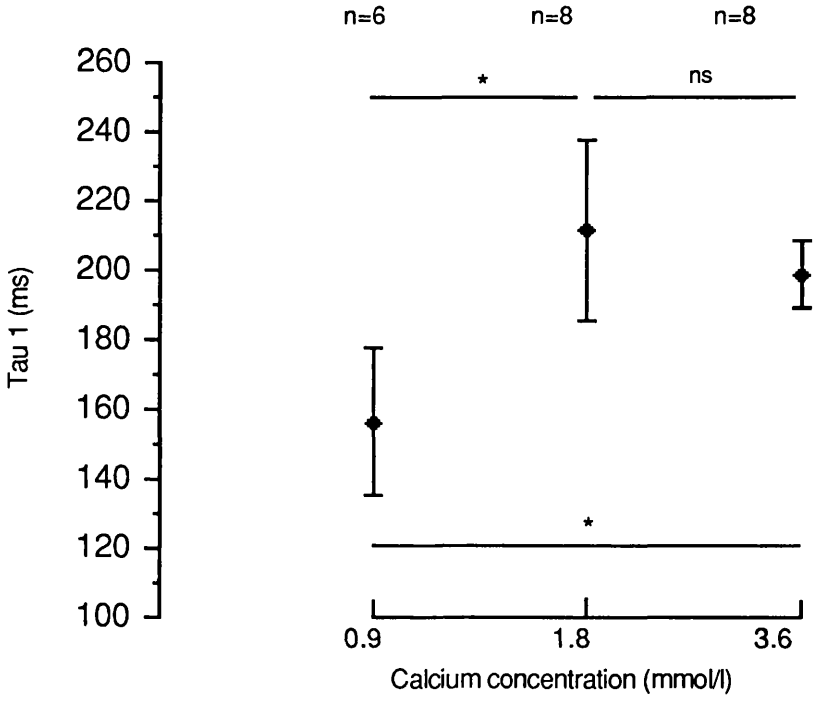

Figure 51. Calcium dose-response for τ_1 in guinea-pig papillary muscle.
* = $p < 0.05$

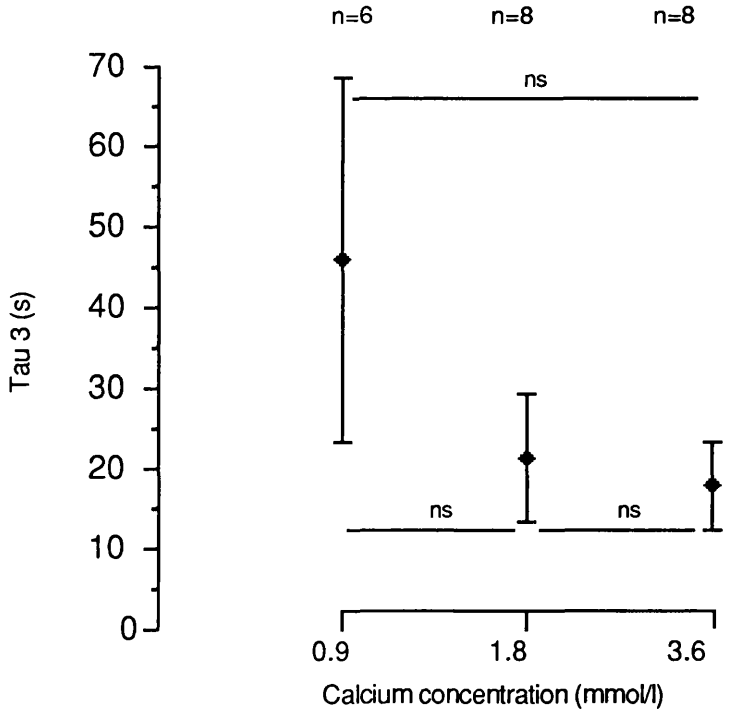

Figure 52. Calcium dose-response for τ_3 in guinea-pig papillary muscle.

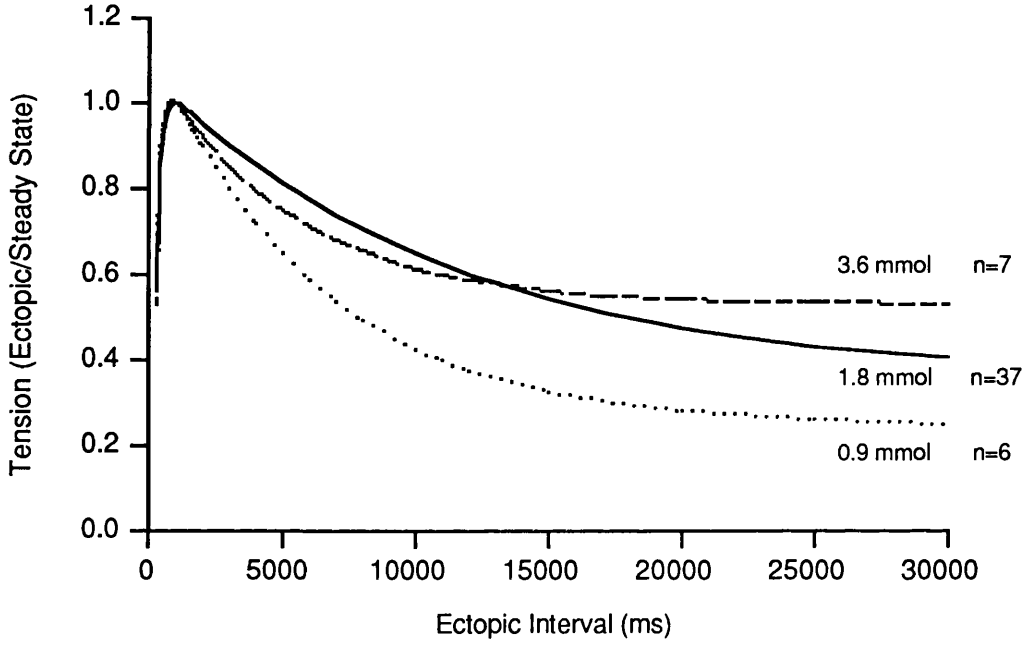

Figure 53. Mechanical restitution curves in the guinea-pig derived from the combined data of several experiments at different [Ca2+].

ii. Adrenalin

Nine experiments were performed on guinea-pig papillary muscles with 1μM Adrenalin. The results are shown in Tables 40–42 and Figure 54. Adrenalin significantly increased twitch tension and the maximum rates of change of tension. Neither τ_1 and τ_3 were modified by the addition of adrenalin to the superfusate.

Table 40. Guinea-pig papillary muscle: Isometric twitch parameters in Tyrode's solution containing 1μM Adrenalin. n=9

Tension (kN kg^{-1})	Time to peak tension (ms)	dT/dt max (kN kg^{-1} s^{-1})	dT/dt min (kN kg^{-1} s^{-1})
1.83±0.36	151.25±18.85	13.45±8.31	-12.24±3.2
(1.41±0.28)	(162.22±18.11)	(9.39±1.86)	(-7.40±1.58)
$p < 0.025$	ns	$p < 0.025$	$p < 0.025$

Values are expressed as mean ± standard error. Paired values (normal Tyrode's solution) are in brackets.
Significance tested using Wilcoxon test on paired samples

Table 41. Time constants of mechanical restitution of guinea-pig papillary muscle in 1μM adrenalin. n = 9

τ_1 (ms)	τ_2 (s)	τ_3 (s)
194.81 ± 28.97		18.86 ± 3.13
(209.12 ± 20.10)		(18.59 ± 2.75)
ns		ns

(Mean ± standard error)
Significance tested using Wilcoxon test on paired samples. Paired control values are given in brackets.

Table 42. Intercepts of mechanical restitution of guinea-pig papillary muscle in 1μM adrenalin. n = 9

A	B	C
1.65 (1.35-12.37)		0.59 (0.56-0.70)
[2.10 (1.66-2.52)]		[0.69 (0.57-0.83)]
ns		ns

(Median and interquartile range)
Significance tested using Wilcoxon test on paired samples. Paired control values are given in brackets.

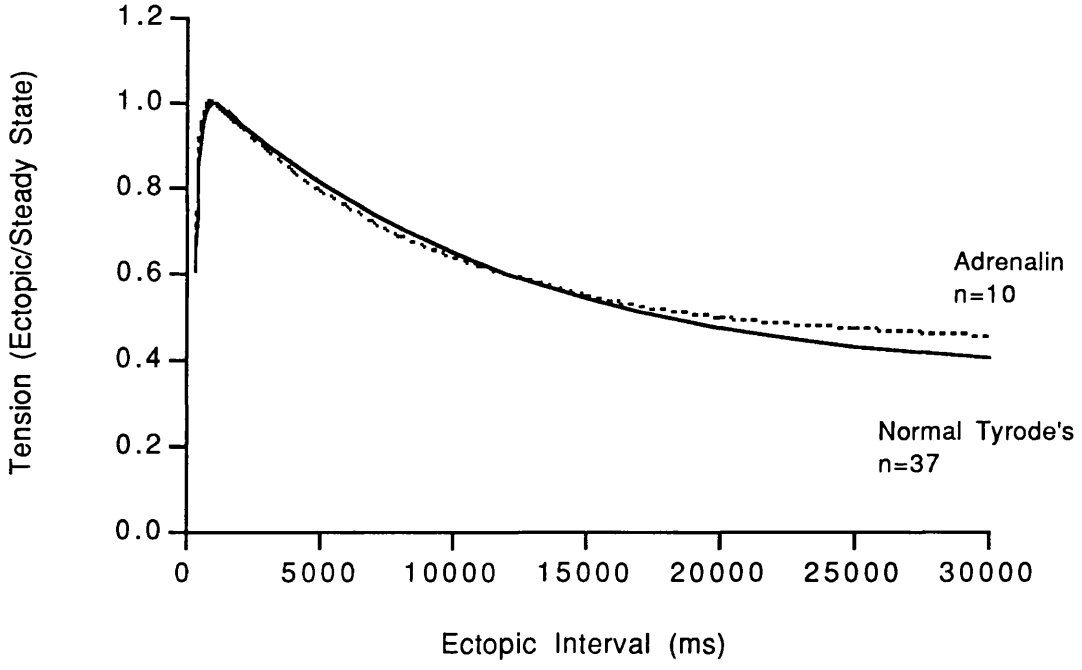

Figure 54. Mechanical restitution curves in the guinea-pig derived from the combined data of several experiments in the presence of 1μM Adrenalin.

iii. Ouabain

Five experiments were performed on guinea-pig papillary muscles with 0.5μM Ouabain. The results are shown in Tables 43–45 and Figure 55. Ouabain increased twich tension, time to peak tension, max dT/dt and min dT/dt ($p < 0.05$). τ_3 was slower than controls ($p < 0.05$) and an identifiable τ_2 was present. No consistent effect was observed on τ_1.

Table 43. Guinea-pig papillary muscle: Isometric twitch parameters in Tyrode's solution containing 0.5μM Ouabain. n=5

Tension ($kN\ kg^{-1}$)	Time to peak tension (ms)	dT/dt max ($kN\ kg^{-1}\ s^{-1}$)	dT/dt min ($kN\ kg^{-1}\ s^{-1}$)
2.43±0.50	176.00±13.55	26.90±5.79	-23.18±5.69
(1.05±0.16)	(154.00±4.30)	(11.58±1.58)	(-9.13±1.47)
$p < 0.05$	$p < 0.05$	$p < 0.05$	$p < 0.05$

Values are expressed as mean ± standard error. Paired values (normal Tyrode's solution) are in brackets.
Significance tested using Wilcoxon test on paired samples

Table 44. Time constants of mechanical restitution of guinea-pig papillary muscle in 0.5μM Ouabain. n=5

τ_1 (ms)	τ_2 (s)	τ_3 (s)
267.96±48.75	7.86±2.48	282.58±155.99
(169.00 ± 12.22)		(13.71 ± 2.22)
ns		$p < 0.05$

(Mean ± standard error)
Significance tested using Wilcoxon test on paired samples. Paired control values are given in brackets.

Table 45. Intercepts of mechanical restitution of guinea-pig papillary muscle in 0.5μM Ouabain. n=5

A	B	C
1.03 (0.66-1.56)	0.28 (0.15-0.35)	1.26 (0.95-1.33)
[2.44 (2.25-3.11)]		[0.60 (0.57-0.70)]
$p < 0.05$		ns

(Median and interquartile range)
Significance tested using Wilcoxon test on paired samples. Paired control values are given in brackets.

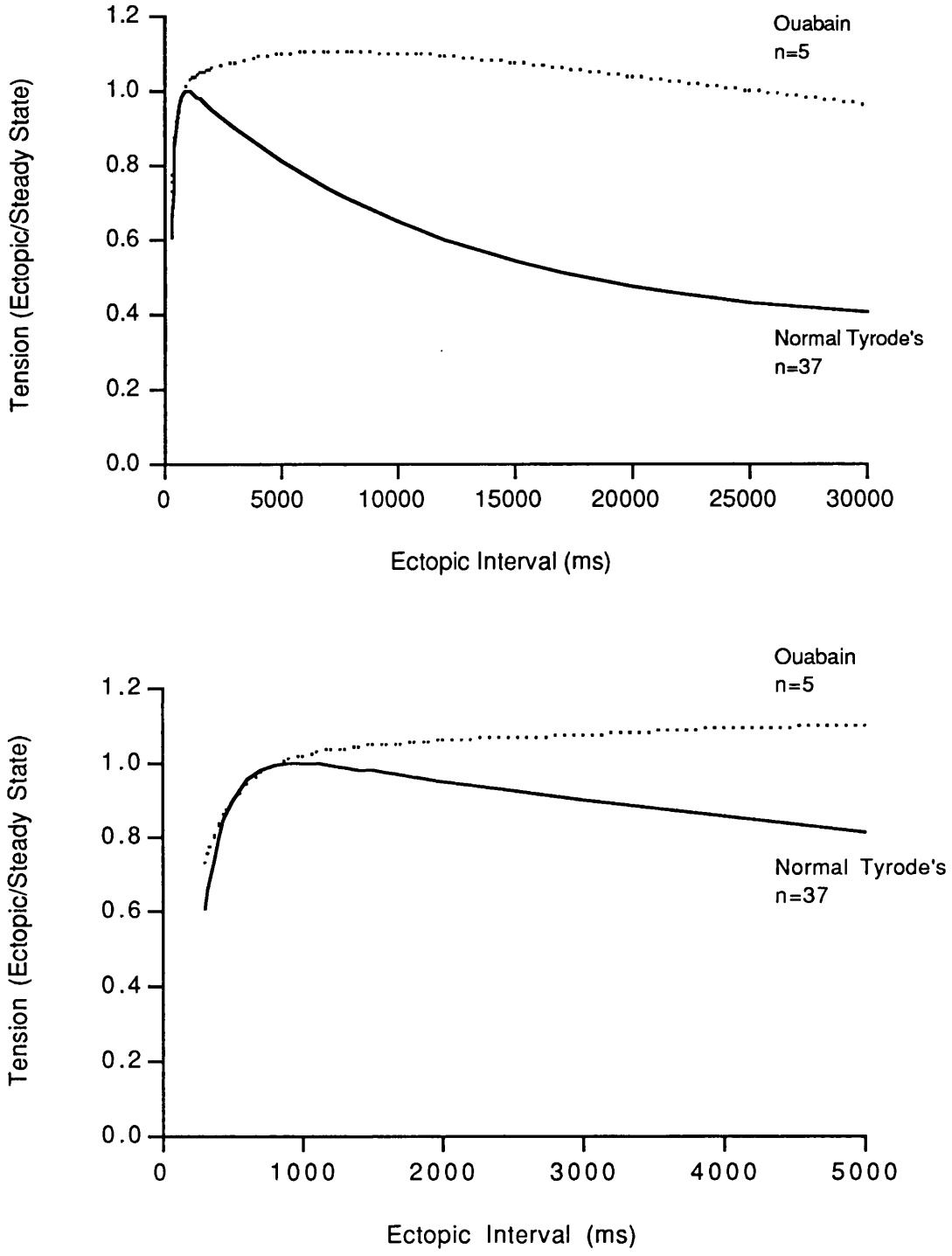

Figure 55. Mechanical restitution curves derived from the combined data of several experiments in the presence of 0.5μM Ouabain.

iv. Verapamil

Six experiments were performed on guinea-pig papillary muscles with 2.2 nM Verapamil. The results are shown in Tables 46–48 and Figure 56. Verapamil reduces isometric twitch tension ($p < 0.05$). τ_1 and τ_3 are both slowed ($p < 0.05$). In five out of six experiments the decay part of the mechanical restitution curve was virtually flat and an accurate figure for τ_3 could not be obtained. In the presence of verapamil a slow recovery phase is apparent and τ_2 could be measured.

Table 46. Guinea-pig papillary muscle: Isometric twitch parameters in Tyrode's solution containing 2.2 nM Verapamil. n=6

Tension (kN kg^{-1})	Time to peak tension (ms)	dT/dt max (kN kg^{-1} s^{-1})	dT/dt min (kN kg^{-1} s^{-1})
0.30±0.13	149.00±3.32	0.53 (n=2)	-0.51 (n=2)
(0.55±0.13) $p < 0.05$	(158.00±8.60) ns	(1.43)	(-1.08)

Values are expressed as mean ± standard error. Mean values only are given for dT/dt max and dt/dt min.
Paired values (normal Tyrode's solution) are in brackets.
Significance tested using Wilcoxon test on paired samples

Table 47. Time constants of mechanical restitution of guinea-pig papillary muscle in 2.2 nM Verapamil. n=6

τ_1 (ms)	τ_2 (s)	τ_3 (s)
348.62 ± 141.26	8.82±2.24	Unmeasurably slow
(164.35 ± 47.33) $p < 0.05$		(15.25 ± 3.70) $p < 0.05$

(Mean ± standard error)
Significance tested using Wilcoxon test on paired samples. Paired control values are given in brackets.

Table 48. Intercepts of mechanical restitution of guinea-pig papillary muscle in 2.2 nM Verapamil. n=6

A	B	C
1.06 (0.84-1.93)	0.52 (0.51-0.92)	1.49 (1.39-1.72)
[1.72 (1.27-6.89)] ns		[0.53 (0.31-0.55)] $p < 0.05$

(Median and interquartile range)
Significance tested using Wilcoxon test on paired samples. Paired control values are given in brackets.

v. Diltiazem

Five experiments were pereformed on guinea-pig papillary muscles with 4μM Diltiazem. The results are shown in Tables 49–51 and in Figure 56. As with verapamil, twitch tension was reduced and τ_1 and τ_3 were slowed. A separate τ_2 could not be measured with diltiazem.

Table 49. Guinea-pig papillary muscle: Isometric twitch parameters in Tyrode's solution containing 4μM Diltiazem. n=5

Tension (kN kg^{-1})	Time to peak tension (ms)	dT/dt max (kN kg^{-1} s^{-1})	dT/dt min (kN kg^{-1} s^{-1})
0.44±0.12	170.00±10.00	2.62±1.19	-2.22±1.01
(1.10±0.31)	(171.00±18.60)	(6.48±3.32)	(-6.20±3.14)
p < 0.05	ns	ns	ns

Values are expressed as mean ± standard error. Paired values (normal Tyrode's solution) are in brackets.
Significance tested using Wilcoxon test on paired samples

Table 50. Time constants of mechanical restitution of guinea-pig papillary muscle in 4μM Diltiazem. n=5

τ_1 (ms)	τ_2 (s)	τ_3 (s)
397.89 ± 84.58		233.26 ± 96.16
(194.68 ± 33.96)		(10.66 ± 2.06)
p < 0.05		p < 0.05

(Mean ± standard error)
Significance tested using Wilcoxon test on paired samples. Paired control values are given in brackets.

Table 51. Intercepts of mechanical restitution of guinea-pig papillary muscle in 4μM Diltiazem. n=5

A	B	C
1.06 (0.94-1.52)	.311	0.99 (0.43-1.14)
[2.10 (1.89-4.29)]		[0.66 (0.54-0.72)]
p < 0.05		ns

(Median and interquartile range)
Significance tested using Wilcoxon test on paired samples. Paired control values are given in brackets.

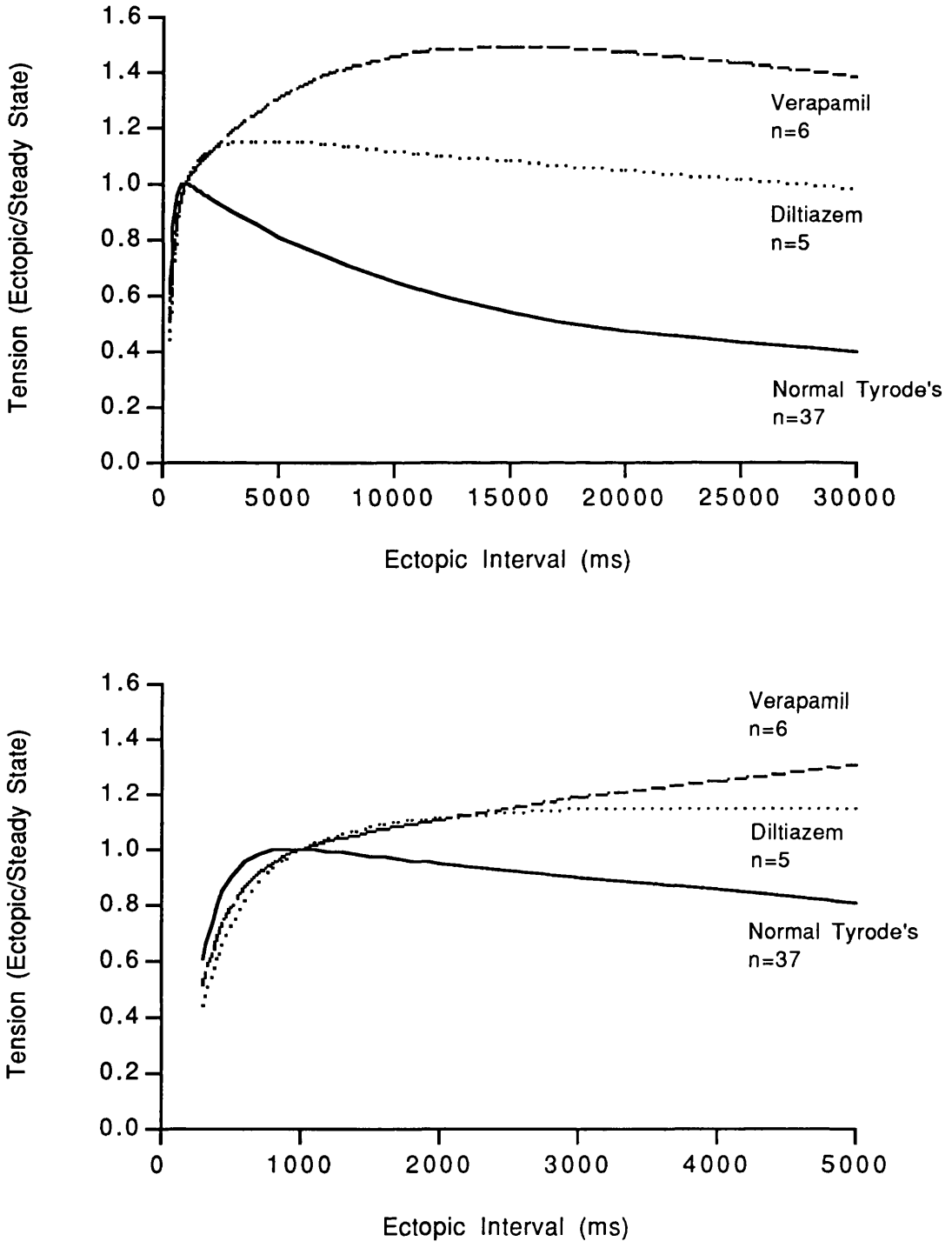

Figure 56. Mechanical restitution curves derived from the combined data of several experiments in the presence of 2.2 nM Verapamil and 4μM Diltiazem.

vi. Ryanodine

Six experiments were performed on guinea-pig papillary muscles with 10μM Ryanodine. The results are shown in Tables 52–54 and Figure 57. Ryanodine reduced twitch tension ($p < 0.05$) and abbreviated both τ_1 and τ_2.

Table 52. Guinea-pig papillary muscle: Isometric twitch parameters in Tyrode's solution containing 10μM Ryanodine. n = 6

Tension (kN kg^{-1})	Time to peak tension (ms)	dT/dt max (kN kg^{-1} s^{-1})	dT/dt min (kN kg^{-1} s^{-1})
0.38±0.13	180.83±0.12	1.05 (n=2)	-1.02 (n=2)
(1.26±0.64) $p < 0.05$	(164.17±10.04) ns	(2.94)	(-2.22)

Values are expressed as mean ± standard error. Mean values only are given for dT/dt max and dt/dt min.
Paired values (normal Tyrode's solution) are in brackets.
Significance tested using Wilcoxon test on paired samples

Table 53. Time constants of mechanical restitution of guinea-pig papillary muscle in 10μM Ryanodine. n = 6

τ_1 (ms)	τ_2 (s)	τ_3 (s)
47.08 ± 6.88		2.48 ± 0.39
(161.49 ± 33.14) $p < 0.05$		(97.05 ± 54.86) $p < 0.05$

(Mean ± standard error)
Significance tested using Wilcoxon test on paired samples. Paired control values are given in brackets.

Table 54. Intercepts of mechanical restitution of guinea-pig papillary muscle in 10μM Ryanodine. n = 6

A	B	C
34.72 (29.77-73948.1)		0.43 (0.31-0.82)
[3.53 (2.74-9.24)] $p < 0.05$		[0.88 (0.45-1.11)] ns

(Median and interquartile range)
Significance tested using Wilcoxon test on paired samples. Paired control values are given in brackets.

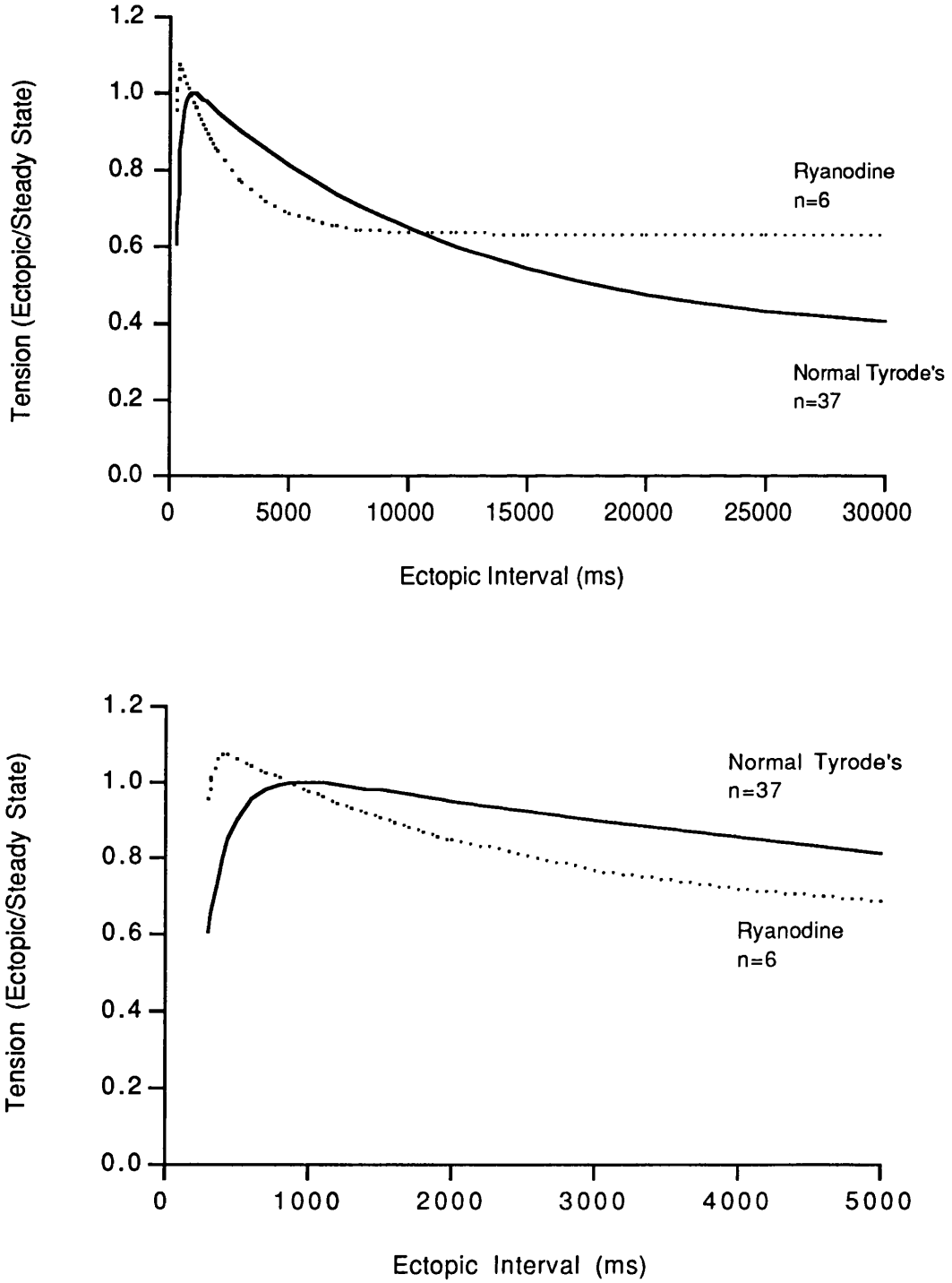

Figure 57. Mechanical restitution curves derived from the combined data of several experiments in the presence of 10μM Ryanodine.

SUMMARY OF RESULTS

In this study of contractility in the isolated mammalian ventricular myocardium several important species differences are described. Human myocardium produces less tension, has a prolonged time to peak tension, a reduced rate of tension development and a reduced rate of relaxation than either guinea-pig or ferret myocardium.

Mechanical restitution also appeared to differ in the three species. All three species have a rapid recovery phase with a time constant (τ_1) between 190-260ms. The guinea-pig MRC is then characterized by a rapid decay time constant (τ_3) of approximately 29 seconds. Ferret and human myocardium, however, display a second, slower, recovery phase time constant (τ_2) of 3.0-4.5 seconds followed by a very slow decay (τ_3) of approximately 200 seconds.

Twitch tension parameters and mechanical restitution time constants are not affected by the clinical status (cardiac output, ventricular function or drug history) of the patient.

Patients with aortic stenosis are shown to have significantly higher left-ventricular systolic pressures and increased left-ventricular wall thickness. The myocardium from this group of patients demonstrates normal twitch tension and rate of development of tension, but has significantly prolonged time to peak tension, when compared to controls. Furthermore, mechanical restitution differs in this group. The rapid recovery phase of mechanical restitution is slowed in comparison to myocardium from patients without aortic stenosis (τ_1 : 586±58ms and 377±28ms respectively). There is a significant correlation between this time constant and both the degree of aortic stenosis and left-ventricular wall thickness.

No difference is observed between the trans-membrane action potentials recorded from patients with and those without aortic stenosis. Likewise, slow action potentials are no different in the two groups. Neither does clinical status and ventricular function appear to affect the configuration of both normal and slow action potentials. The time constant of restitution of dV/dt max of slow action potentials (τ_{SAP}) is much faster than mechanical recovery (τ_1) (time constants: 72±13ms and 482±34ms respectivly).

The effects of pharmacological interventions on twitch tension parameters and the time constants of mechanical restitution in both human and guinea-pig myocardium, are summarized in Tables 55 and 56.

Modification of isometric tension

Changes of peak isometric tension were always mirrored by alteration of the maximum rate of tension development (max dT/dt) and the maximum rate of relaxation (min dT/dt). The time to peak tension was unaltered in all of the interventions with the exception of a significant reduction shown by human myocardium in the presence of 1μM adrenalin.

τ_1

The rapid recovery phase time constant, τ_1, was significantly shortened in human myocardium by adrenalin, ouabain and ryanodine, whilst in the guinea-pig, ryanodine, alone of these three agents, shortened τ_1. In addition the calcium antagonist verapamil prolonged τ_1 in both species by a similar degree.

Alteration of the ionic environment had no consistent effect on τ_1. Change in extracellular [Ca^{2+}] had no significant effect on human myocardium, but a reduction of extracellular [Ca^{2+}] to 0.9mM reduced τ_1 in guinea-pig myocardium.

τ_3

The reduction of force after a rest interval was also influenced by alteration of the extracellular environment. Again, the magnitude of the effect was different in guinea-pig and human myocardium which may in part reflect the fact that the control value was significantly shorter in guinea-pig.

The most dramatic effects were noted in guinea-pig where ouabain and verapamil produced a large increase in the value of τ_3. In fact when verapamil was added to the superfusate the decline of tension after a rest interval was virtually negligible so that no value could be attributed to τ_3. Ouabain and verapamil also prolonged τ_3 in human myocardium although the proportional increase was much less. Adrenalin however exerted no effect on the value of τ_3.

The effects of ryanodine were equally pronounced, but in this case a profound reduction of the time constant was observed. In both tissues the decay of force after a rest interval was considerably accelerated.

In contrast to the effect on τ_1, alteration of the extracellular ionic environment changed the decay time constant, τ_3. In human myocardium an increase of extracellular [Ca^{2+}] increased τ_3. Changes to the extracellular [Ca^{2+}] were without significant effect on the decay time constant in guinea-pig myocardium and this may reflect the large variability

in the data with this intervention (coefficient of variation 120% in 0.9mM Ca and 87% in 3.6mM Ca). The reason for this increased variance in the data could not be ascertained.

τ_2

This component of the rising phase of the restitution curve was only normally distinguishable in human myocardium and was not consistently altered by the interventions shown in Table 5, again partly a reflection of substantial variability in the data. Only addition of verapamil and increase in the $[Ca^{2+}]$ to 5.4mM produced an increase in the value of τ_2 .

Table 55.
Summary of the effects of interventions on isometric tension variables of isolated human and guinea-pig myocardium

	GUINEA-PIG					HUMAN				
INTERVENTION	n	Tension	TPT	max dT/dt	min dT/dt	n	Tension	TPT	max dT/dt	min dT/dt
0.9mM Ca	6	47±6*	100±5	47±5*	37±6*	5	64±5*	108±4	60±8*	80±13
3.6mM Ca	8	480±263*	100±3	218±36**	250±39**	9	142±11***	98±3	140±11*	170±16***
5.4mM Ca						9	192±22***	98±2	318±140***	232±36***
1μM Adrenalin	9	141±17**	105±3	150±20**	179±26**	15	167±20***	84±2***	188±31***	216±38***
0.5μM Ouabain	5	229±32*	114±6*	230±40*	247±40*	11	171±23*	102±3	164±21*	219±40*
2.2nM Verapamil	6	50±10*	92±2	36 (n=2)	47 (n=2)	6	47±8*	99±4	40±7	45±2*
10μM Ryanodine	6	37±4*	111±5	34 (n=2)	45 (n=2)	5	55±5*	110±4	NM	NM

Values are expressed as percentage change from controls (mean±SE).

Significance was tested using the Wilcoxon test for paired samples on the absolute values.
* = $p< 0.05$, ** = $p< 0.025$, *** = $p< 0.01$.

NM = not measured.

Table 56.
Summary of the effects of interventions on mechanical restitution time constants of isolated human and guinea-pig myocardium

	GUINEA-PIG				HUMAN			
INTERVENTION	n	τ_1	τ_2	τ_3	n	τ_1	τ_2	τ_3
0.9mM Ca	6	74±7*		502±275	5	340±210	210±108	103±26
3.6mM Ca	8	102±11		144±38	8	140±43	185±59	152±11***
5.4mM Ca					9	150±36	338±83*	362±138***
1μM Adrenalin	9	100±19		115±24	8	70±10*	198±11	102±18
0.5μM Ouabain	5	168±38		393±30 *	6	70±10*	182±36	402±129*
2.2nM Verapamil	6	216±35*		unmeasurably slow*	6	171±32*	409±179*	88±42
10μM Ryanodine	6	36±10*		36±21*	6	43±8*		5±2*

Values are expressed as percentage change from controls (mean±SE). Significance was tested using the Wilcoxon test for paired samples on the absolute values.

* = $p < 0.05$.

CHAPTER 4: DISCUSSION

VALIDITY OF RESULTS

A study of isolated strips of human ventricle presents a number of practical problems not encountered with similar preparations from other mammals. The size of preparation required was larger than could be obtained by endomyocardial biopsy at cardiac catheterization; open biopsy at the time of cardiac surgery was therefore necessary. Since ventricular myocardium was required, samples could only be obtained from those cases where the ventricular cavity was exposed. Thus, the number of patients available for study were restricted. Animal muscle preparations were obtained from either papillary muscles or trabeculae carneae, each of which tended to be of a size conveniently suited to *in-vitro* studies of this type. Human myocardium, however, was obtained either as a small strip excised by the surgeon from the subendocardial region of the left-ventricular outflow tract, or from a papillary muscle excised before replacing the mitral valve. In the former situation, the samples were small and by necessity were subject to instrumentation rather more than were the papillary muscles. On a small number of occasions mechanical injury to the tissue was severe and no viable tissue remained. These were technical problems which were largely overcome with practice and experience.

The fibre alignment in human myocardial biopsies was not always conveniently arranged in parallel formation as it was in animal papillary muscles and trabeculae. This presented technical difficulties in the dissection of a muscle strip suitable for mounting in the tissue bath. Thus increasing the amount of tissue handling; the development of a certain technical expertise was therefore important. Furthermore, there was an inevitable delay in transferring human tissue from the operating theatre to the laboratory. This delay was always kept to a minimum, but in practice it was evident that the tissue remained viable for several hours if kept in physiological saline at room temperature. The technical difficulties associated with excision, transport and dissection

of human specimens were largely overcome and ultimately did not present a significant problem.

The viability of isolated myocardial preparations such as used in this study depends on the diffusion of oxygen to the centre of the muscle (Koch-Weser, 1963). If a certain critical diameter is exceeded, the innermost fibres become hypoxic and the developed tension will fall off rapidly (Hill, 1928, Koch-Weser, 1963 and Shattock *et al*, 1983). This critical diameter varies in relation to the oxygen consumption and is smaller at higher rates of stimulation and would appear to be in the region of $1mm^2$. The cross-sectional area of the preparations in this study were $0.97\pm0.1mm^2$ in human tissue, $0.91\pm0.22mm^2$ in ferrets, and $0.51\pm0.1mm^2$ in guinea-pigs. The human and ferret preparations were therefore larger than those of guinea-pig and their cross-sectional area approached the upper limits (in terms of tissue viability) proposed both by Hill (1928) and Koch-Weser (1963). In all preparations there was a gradual decline in twitch tension throughout the experiment; this tended to be more marked in the human preparation. A likely explanation for this may have been related to the fact that the human preparations consist of fibres of different orientation allowing slippage and reduction in resting tension to occur more rapidly than in the intact unit of, say, a guinea-pig papillary muscle. It is likely, also, that this phenomenon explains the observation that human muscles generally took longer to establish both L_{max} and a steady state twitch response at the beginning of each experiment. The slow change in baseline control twitch tension which continued throughout the experiment was taken into account when examining the effect of interventions.

A major difference between the different preparations was the anatomical site from which ventricular myocardium was excised in each species. All human tissue was obtained from the left ventricle, whereas both the guinea-pig and ferret tissue were taken from the right ventricle. Furthermore, a basal rate of 60 per minute may be physiological in human tissue but is much slower than the normal heart rates in the other two species (ferrets having heart rates of around 300 per minute). The choice of a uniform steady state stimulus frequency of 1Hz was considered justified for two reasons. Firstly, the use of an identical rate in each species removes one variable from the final analysis. Secondly, as discussed previously, tissue viability at high rates of stimulation would be impaired.

The viability of human myocardium in this study is attested to by the fact that biochemical interventions to both human and guinea–pig myocardium produced similar

inotropic responses (Table 57), in keeping with the magnitude of response expected with such interventions.

The reproducibility of mechanical restitution time constants in a single preparation throughout an experiment has been confirmed by Fry *et al* (1983). In experiments in which the muscle was deliberately made hypoxic, the time constants of mechanical restitution returned to control values on recovery of normal oxygen tensions, despite a persistent reduction of absolute developed tension. Furthermore, Fry *et al* (1983) have shown that the time constants of mechanical restitution are independent of the size and degree of fibrosis of the specimen. Thus, mechanical restitution can be regarded as a phenomenon related to the viable cells within a muscle and would appear to be independent of the total number of muscle fibres.

The technique of recording trans-membrane action potentials with glass micro-electrodes has been well described elsewhere (see Purves, 1981). There are, however, a number of problems with these techniques that warrant further discussion. Manipulation of the microelectrode and penetration into the cell required a certain amount of expertise which could only be acquired through experience. It was more difficult in some preparations than in others to obtain action potential recordings from. Frequently, although recordings could be made, a stable penetration was not achieved and serial recordings (as in restitution of slow action potential dV/dt max) could not be obtained. This was especially true of the guinea-pig papillary muscles in which it was more difficult to obtain stable electrode penetration than in human muscle. The technical problems associated with recording slow action potentials have already been referred to in *Results*. The high threshold of excitability of myocardium exposed to high [K^+] caused major difficulty in recording the upstroke velocity of the action potential. In order to differentiate stimulus artefact and phase one of the action potential a second micro-electrode was used as the reference electrode and was positioned close to the intracellular electrode. This did not overcome the problem in all cases, but stable recordings of slow action potential dV/dt max was possible in 16 out of 20 attempts (where initial penetration was successful).

While the maximum rate of rise of the slow action potential has been shown to provide a good approximation of the inward calcium current (Malécot and Trautwein, 1987), the use of this method has limitations and may be subject to contamination by the outward currents of the action potential.

The results of attempts to manipulate the rate of recovery of the 'slow' action potential dV/dt max were mixed and largely inconclusive due to the small numbers involved. Adrenalin and increased extracellular calcium had no consistent effect. Verapamil alone showed consistent effects (but n=3); the 'slow' action potentials being lower in amplitude and shorter in duration with reduced upstroke velocity and slowed dV/dt max recovery. Thus, both the magnitude and reactivation time constant of the slow inward current may be slowed by verapamil in this preparation.

INTERPRETATION OF RESULTS

Isometric Twitch Tension

The twitch tension parameters of human myocardium obtained from patients in all diagnostic categories differed from each of the two animal species. Human myocardium produced less tension per gram of tissue, time to peak tension was prolonged and peak rates of contraction and relaxation were reduced. The values of time to peak tension in human myocardium are similar to those obtained by others from trabeculae (mostly right ventricular) of normal transplant donor hearts handled under similar conditions, but at 30°C (Gwathmey *et al.* 1987). Developed tension was also similar to that measured by others in human atrial and ventricular myocardium measured at 30°C (Poole-Wilson *et al.* 1979).

In this study, time to peak tension in isolated guinea-pig and ferret myocardium is comparable to that found in rat (Capasso *et al.* 1981, Bing *et al.* 1971 and Cooper and Tomanek 1987), and cat, (Anderson, Manring, Arentzen *et al.* 1977). In the rabbit, time to peak tension appears to be intermediate (222ms) to the values obtained in animal and human experiments in this study (Shattock and Bers, 1987). Values in excess of 500ms may be seen in human myocardium from patients with end-stage heart failure (Gwathmey *et al.* 1987). In this study, however, there was no difference in any of the myocardial twitch tension parameters between any of the diagnostic groups (see Table 31). It is of course unlikely that any of these patients had impaired left-ventricular function to the degree of patients undergoing heart transplantation, since they would have been unsuitable for valve replacement surgery.

Three possible explanations may be responsible for the finding of reduced twitch tension and prolonged time to peak tension seen in human myocardium: 1) a true species difference is observed, 2) the difference in handling techniques applied to

human preparations has caused tissue damage, or 3) there is an intrinsic impairment of function which is undetected clinically.

Since there is no apparent correlation of isometric twitch tension and clinical indices of ventricular function or disease classification, the latter is an unlikely explanation. Furthermore, reduced isometric tension in human myocardium is a universal finding even in normal hearts. This is observed in isolated right ventricular trabeculae (Gwathmey *et al.* 1987) which presumably undergo less trauma in terms of dissection immediately prior to mounting in the tissue bath. One could therefore argue that it is an intrinsic property of human myocardium that it is capable of producing less isometric tension than other species. This might be related to other well described species differences such as variations in myosin isoenzymes (see Winegrad, 1984 for reveiw).

The maximum velocity of contraction seems to be influenced by the relative amounts of V_1 and V_3 myosin isoenzymes (Schwartz *et al*, 1981); with the V_3 isoenzyme being associated with a slower rate of force development. The lower mammals tend to have variable amounts of the three myosin isoenzymes V_1, V_2 and V_3, whereas in man the predominant isoenzyme is V_3. Almost certainly these differences explain the more highly significant species differences in time to peak tension observed in this study.

Mechanical Restitution

Certain similarities between mechanical restitution in different mammalian species has led to the proposal that this phenomenon represents a common fundamental cellular mechanism (Seed and Walker, 1988). However, important differences have been observed in the mechanical restitution of isolated myocardial preparations in different mammalian species (see *Introduction*); though most workers have failed to quantify mechanical restitution and direct comparison cannot be made. The phenomenon of mechanical restitution is thought to represent underlying cellular processes (Elzinga *et al*, 1981). In order to investigate these processes a quantitative description of the phenomenon is essential. In this study I have examined mechanical restitution in three mammalian species using identical experimental protocols.

Unlike twitch tension parameters, the results of mechanical restitution do not distinguish human from other mammalian species in the same way. So as not to include data from human tissue from disordered left ventricles the data has been divided according to diagnostic categories. It is apparent from the results in Table 31 that

variation exists between τ_1 between different diagnostic groups. Those patients with aortic stenosis tended to have a prolonged value for τ_1 (mean 603ms), and those with mitral stenosis had the shortest value (mean 260ms). (See below for a discussion of the changes that occur in different pathological states.)

If patients with pure mitral stenosis can be regarded as having normal left-ventricular function (supported by the fact that left ventricular systolic and end diastolic pressures and ejection fractions were normal) then there was no quantitative difference between the MRC in man and the ferret. Since there are obvious differences between the MRC in myocardium from different patients, it would be reasonable to confine the comparison of results from different species to that group of human subjects who were considered to have the most 'normal' myocardium.

All three species (human, ferret and guinea-pig) have been shown to have rapid recovery phase time constants (τ_1), with values between 190-260ms. The guinea-pig MRC is then characterized by a rapid decay time constant (τ_3) of approximately 29 seconds. Ferret and human myocardium, however, display a second, slower, recovery phase time constant (τ_2) of 3.0-4.5 seconds (which is absent in the guinea-pig) followed by a very slow decay (τ_3) of approximately 200 seconds.

Direct comparison of the mechanical restitution data obtained in these experiments with the results of others is difficult. This is largely due to the different preparations used and the lack of uniformity of stimulation rate and muscle bath temperature. A recovery of tension, reaching a maximum (or "optimum contractile response") (Pidgeon *et al.* 1980) at 700-800ms has been observed in the isolated myocardium of rabbit (Edman and Johannson 1976), isolated cat hearts (Pidgeon *et al.* 1980), intact dogs, (Pidgeon *et al.* 1980 and Elzinga *et al.* 1981) and in patients undergoing cardiac catheterisation (Seed *et al.* 1984). We have made similar observations in isolated guinea-pig myocardium. However, ferret (Wier and Yue 1986), rat (Ragnarsdóttir *et al.* 1982) and rabbit (Cave *et al.* 1990) appear to behave differently. Like the results of Wier and Yue (1986) in ferret papillary muscles, our data would suggest that a maximum response is seen in ferret and human myocardium after 4-5 seconds. In the rat a maximum value may not be reached for up to 60-120 seconds (Ragnarsdóttir *et al.* 1982).

A monoexponential function has been used to describe the process of mechanical restitution (Mahler and Rogel, 1970) and time constants have been described of 152ms in guinea-pig papillary muscles (Fry *et al.* 1983), 765ms in ferret papillary muscles

(Wier and Yue 1986), 606ms in isolated human myocardium (Fry *et al.* 1983), and 384ms in isolated dog hearts (Burkhoff *et al.* 1984).

In this study I present evidence to justify a biexponential recovery process in human and ferret myocardium (see *Results*). Having used this analytic approach, the similarity of the time constants of the rapid recovery phase (τ_1) in each species is notable. If we had assumed a monoexponential process, the time constant of human and ferret muscle would have been much longer and may have compared with the findings of others. Thus, the identification of recovery processes with similar time constants, in this study, endorses the theory that the underlying mechanism may be common to different species.

The principal difference between the MRC in different species appears to be in the time course of decay; ferret and human tissue having a much slower decay than the guinea-pig. Similarly in a study on rabbit trabeculae under identical experimental conditions and using the same method of analysis similar values of τ_1 and τ_3 are seen to those observed in human and ferret muscle (τ_1 = 190ms (Shattock, unpublished data) τ_3 = 224s (Cave *et al*, 1990))

In studies on isolated mammalian myocardium, using extracellular ion selective microelectrodes, post-rest decay of contraction has been shown to correspond to a net trans-sarcolemmal calcium efflux (Bers, 1985 and MacLeod and Bers, 1987). This phenomenon appears to vary between species, with the rat (which demonstrates post rest *potentiation* and has *no* decay of the MRC (Ragnarsdóttir *et al.* 1982)) having an *influx* of calcium during rest (Shattock and Bers, 1989). In this study human, ferret and guinea-pig myocardium show post-rest decay, which is much faster in the guinea-pig than the other species. The use of so-called "rapid cooling contractures" as an index of SR calcium content (Bers, 1989) reveals that the cellular efflux of calcium is associated with a depletion of sarcoplasmic reticulum calcium content. Thus, species differences in the rate and direction of calcium flux during diastole, might explain the differences in the rate of post-rest decay (τ_3) observed this study.

The second slow recovery phase (τ_2) is observed in the two species that exhibit a τ_3 in the region of 200 seconds. τ_2 is not seen in the guinea-pig that has a τ_3 of 29 seconds. While it would not be possible to speculate the nature of the cellular process underlying the slow recovery phase, it is possible that this process is present in the guinea-pig, but that analysis of the MRC is not sensitive enough to distinguish τ_2 from τ_3 which have a similar order of magnitude. In other words, there is insufficient evidence that the

apparent absence of a slow recovery phase in the guinea-pig represents a true species difference.

In summary, mechanical restitution is described by three distinct phases in the ferret and man. Rapid recovery has similar time constants in guinea-pig, ferret and man, suggesting a common underlying process. Post-rest decay, however, differs between species and may reflect different rates of trans-sarcolemmal calcium efflux.

Slow action potential dV/dt max

Magnitude

In these experiments, the maximum rate of rise of the action potential in human myocardium exposed to raised (14-18 mmol) external [K^+] was 4.4 ± 0.35 Vs^{-1}, compared to 126.6 ± 19.1 Vs^{-1} in 4mmol [K^+] . Similar values for slow action potential dV/dt max were obtained by others in single guinea-pig ventricular cells injected with 140mM caesium (Malécot and Trautwein, 1987). In the presence of adrenalin slow action potential dV/dt max was increased at 5.9 ± 0.47 Vs^{-1} which is similar to the values (6 to 12 Vs^{-1}) found by Schneider & Sperelakis (1975) in isolated perfused guinea-pig hearts exposed to isoprenaline in an external [K^+] of 27mM.

Kinetics of recovery of slow action potential dV/dt max

The reactivation time course of I_{si} was assessed in a derivative fashion by measuring the restitution of the upstroke velocity of the slow action potential. The time constant of recovery of slow action potential dV/dt max (τ_{SAP}) was 72.2±13.1 ms. Malécot and Trautwein (1987) have established a close proportionality between I_{si} and slow action potential dV/dt max, when there is no net current flow in the preparation, i.e. the conditions used here in field stimulation. A similar time course of reactivation of the slow inward current has also been observed with voltage-clamp techniques in isolated guinea-pig myocytes, using conditions similar to those employed in these experiments (Shimoni *et al.* 1987) and in rat myocytes (Mitchell *et al.* 1985) where the recovery time constant was around 100ms.

MODEL

Calcium ions are well known to play an important role in stimulus-response coupling in many different types of animal cell (for review see Rasmussen 1986a & 1986b). In the heart the circulation of calcium within and across the membrane of the myocardial cell is

central to the process of excitation-contraction coupling and is involved in the mechanism by which the heart can vary its force of contraction on a beat to beat basis (for reviews see Chapman, 1983, Morad & Goldman, 1973, Bowman *et al*, 1985, Braunwald *et al*, 1988, Colucci *et al*, 1986).

The force of contraction of the myocardial cell is ultimately dependent on the number of actin-myosin crossbridges formed, which is in turn dependent upon the concentration of calcium in the region of the myofilaments and their sensitivity to calcium. A rise in intracellular [Ca^{2+}] initiates contraction, but the precise source of this activator calcium is controversial. Calcium ions enter the cell during the plateau phase of the action potential through voltage-gated and time-dependent calcium channels. Additional sources of extracellular Ca^{2+} are via non-gated membrane ionic channels and via a bidirectional sodium-calcium exchanger, in which three sodium ions are exchanged for one calcium ion. The amount of calcium entering the cell during the action potential is thought to be insufficient to account for the rise in intracellular [Ca^{2+}] which occurs and is insufficient to cause activation of the myofilaments alone. It has therefore been postulated that calcium ions entering the cell via voltage-gated calcium channels induce a further increase in cytoplasmic [Ca^{2+}] by causing the stores of calcium within the sarcoplasmic reticulum to be released (the so-called calcium-induced calcium release) (Fabiato & Fabiato, 1977). Relaxation is associated with calcium uptake by intracellular storage sites, or removal from the cell via mechanisms such as the Na^{+}/Ca^{2+}exchanger. Ca^{2+} remaining within the cell may then be available for recirculation and release during subsequent depolarizations.

If the phenomenon of mechanical restitution is related to the cellular circulation of calcium, the existence of a number of distinct compartments involved in the handling of calcium during muscular contraction is implied (Lipsius *et al*, 1982). Activator calcium is released from intracellular stores and enters the cell during the action potential. This calcium is released into an area of the sarcoplasm in the region of the myofilaments. Studies using the photoprotein aequorin have demonstrated that the sarcoplasmic [Ca^{2+}] rises to a maximum at around the time of the maximum rate of rise of tension, and falls rapidly to a minimum by the time of peak tension (Chapman, 1983). This would suggest that Ca^{2+} is removed rapidly from the myofibrilar space. However, this calcium is clearly not taken up directly by the release stores; if this were so, a premature depolarisation would produce a maximal contraction. Since a premature depolarisation produces a sub-maximal mechanical response, it is presumed that at this time the release store has not taken up all the calcium released in the previous depolarisation. As the [Ca^{2+}] has already fallen in the region of the myofilaments, then there must be a third

site involved in the process of circulating calcium from the myofilaments back to the release site. In other words, calcium is released from a release store into the area of the myofilaments and taken up by a third uptake compartment from where it is returned to the release store, thus completing a cycle of calcium movement within the cell.

The amount of calcium available to the circulation described above is presumably a function of the net trans-sarcolemmal flux of Ca^{2+}. This in turn is dictated by the balance of previous calcium entry and loss from the cell and thus requires the inclusion of the cell membrane in the model (Figure 58).

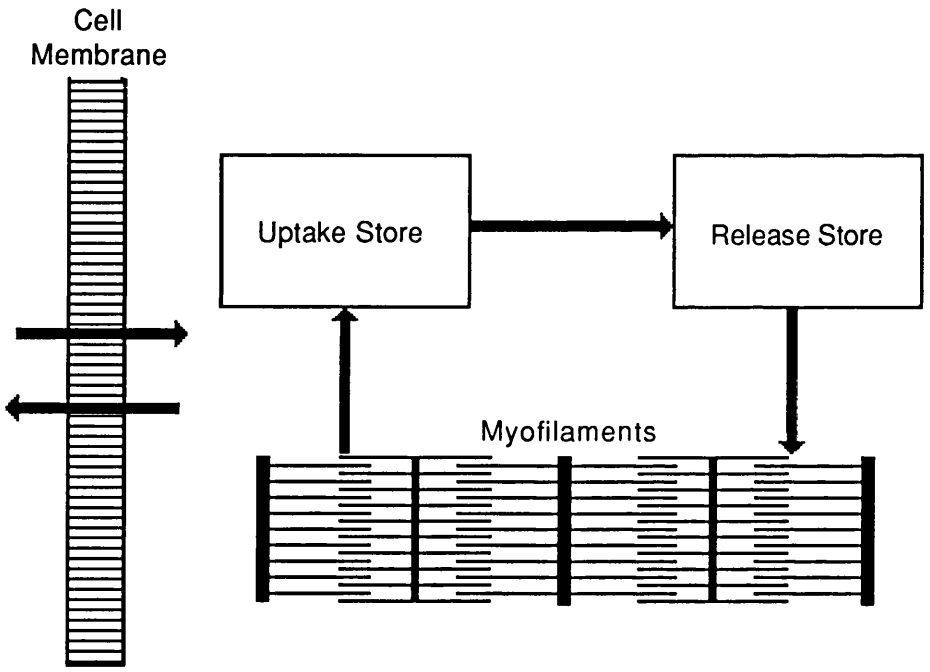

Figure 58. Diagram of simple model of intracellular calcium circulation. The arrows indicate the direction of calcium movement

According to this model, mechanical restitution is dependent on the availability of activator calcium as determined by the rate of uptake of calcium by the release store. This situation is complicated by the activator calcium entering the cell during the action potential. It is now generally accepted that that activator calcium is derived from both the intracellular release site (presumed to be the sarcoplasmic reticulum) and the voltage

dependent calcium current in the cell membrane (Chapman, 1983). The relative contributions of these two sources varies between species (Fabiato & Fabiato 1979).

Other factors influencing the strength of contraction include the sensitivity of the contractile proteins to Ca^{2+}, extracellular $[Ca^{2+}]$ and $[Na^{+}]$, trans-sarcolemmal Na^{+}/Ca^{2+} exchange and the capacity of other intracellular storage sites (such as the mitochondria) to sequester calcium (Chapman, 1983). These factors affect contractility by either changing the total amount of calcium available, or altering the calcium sensitivity of contractile proteins. Since they all tend to affect contractility over a relatively long time course they are unlikely to have effect within the brief period between beats. Indeed, measurement of the sarcoplasmic $[Ca^{2+}]$ with the photoprotein aequorin has shown that the variation of isometric force as a function of stimulus interval is mirrored by similar changes of sarcoplasmic $[Ca^{2+}]$ (Wier and Yue, 1986). It is therefore unlikely that beat-to-beat changes in contractility are due to changes in myofibrillar sensitivity. It would be more likely that the kinetics of recovery of contractility between beats is dependent upon the amount of calcium released, which may, in turn, depend on the rate of recovery of the voltage dependent calcium channels and on the rate of uptake of calcium into the release stores.

MECHANICAL RESTITUTION AND Ca^{2+} CIRCULATION

A basic assumption made in this study is that mechanical restitution can be described by exponential functions. The use of an exponential function is a convenient way to describe biological data and can be used to compare interventions within the same experiment and examine inter-experiment variability. It is not assumed that the underlying physiological processes obey first order kinetics.

The rapid recovery phase, τ_1

In guinea-pig and ferret myocardium and in human tissue obtained from patients with normal left-ventricular function, isometric force recovered after a previous contraction with an initial time constant (τ_1) of about 200ms. Several processes are likely to contribute to this phenomenon and the value of the time constant represents an empirical description of them. One explanation is that there is a delay in the transfer of Ca^{2+} between the intracellular uptake locus and the release site (Seed and Walker, 1988). It is also possible that the reactivation time of the second inward current, I_{si}, acting as a trigger to release intracellular Ca^{2+}, may be the rate limiting factor.

In order to investigate the contribution of these components two approaches have been taken; i) direct comparison of the reactivation time course of I_{si} with τ_1 and ii) measurement of τ_1 in the presence of agents expected to diminish the relative contribution of either I_{si} (verapamil) or the intracellular Ca^{2+} storage sites (ryanodine).

In human myocardium, the time constant of the slow action potential reactivation, τ_{SAP}, was consistently faster than τ_1 at normal extracellular [Ca^{2+}] and [Na^+] and showed no consistent correlation with the variability of the latter. Thus, in normal human and guinea-pig ventricular muscle there was no evidence that recovery of force is a direct consequence of second inward current refractoriness, implying that Ca^{2+} entering by this route does not directly activate the myofibrils to a significant extent.

Ryanodine (10μM) was noted not only to reduce isometric tension (37% of control in guinea-pig, 55% in human) but to decrease substantially τ_1 to a value not greatly different from that of τ_{SAP}. Ryanodine is supposed to prevent all but an insubstantial release of Ca^{2+} from the sarcoplasmic reticulum (Feher and Lipford, 1985). Under these conditions the reduced force may now be a result of direct activation from Ca^{2+} entering during the action potential. Thus, in the presence of ryanodine, the time constant, τ_1, reflects the time course of activation of I_{si}. This interpretation is consistent with the observation that mechanical restitution in the 4 day old rat is faster than in the adult rat and corresponds closely to electrical restitution in both neonatal and adult rats (Minelli *et al.* 1985). The source of activator calcium in the rat is known to change with its development (Fabiato and Fabiato, 1979). The foetal rat heart, like the frog, has no calcium induced release of calcium by the SR. After birth, the calcium induced calcium release mechanisms gradually develop. Similarly, in the cat the SR and T tubule system are poorly developed at birth and the time constant of restitution is faster in the neonate than in the adult (46 vs 300ms), (Maylie, 1982). A similar reduction of τ_1 has also been noted in the presence of 5mM caffeine (C.H.Fry and J.M.Walker, unpublished data), which also reduces the contribution of the SR to contractile activation and might, therefore, be expected to produce a result similar to ryanodine.

Verapamil (2.2nM) increased the value of τ_1 in both guinea-pig and human myocardium, as well as exerting a negative inotropic effect. This agent has been shown to reduce the the magnitude of I_{si} in cardiac muscle so that the contribution of intracellular stores in contractile activation would predominate. Thus, the increased value of τ_1 observed in the presence of verapamil will reflect the time course of intracellular recycling of Ca^{2+}, being unaffected by the contribution of transmembrane currents.

Thus it can be concluded that the time constant, τ_1, reflects at least two recovery processes, a fast reactivation of I_{si} and a slower intracellular recycling of activator Ca^{2+}. When one of these components is attenuated the value of τ_1 reflects the time course of the other. Thus, the value of τ_1 could be altered without changing the time constant of one of the recovery processes but merely by altering the value of its intercept (A). Any agent which alters both the magnitude of I_{si} and the amount of intracellular recycled Ca^{2+} could therefore have a variable net effect on the value of τ_1. This may explain the lack of consistent effect of alterations of the extracellular $[Ca^{2+}]$ which might be expected to affect both components. The observation that τ_1 is abbreviated by adrenalin and ouabain in human tissue but not in guinea-pig, might suggest that in human tissue the magnitude of the transmembrane current is increased relatively more than that of the recycled calcium in the intracellular pool. Consistent with these data, others have demonstrated an increase of I_{si} with cardiac glycosides (Weingart *et al*, 1978).

The decay phase, τ_3

Unlike the fast recovery phase, decay seems to differ markedly between species. Guinea-pig myocardium exhibited a decay phase some ten times faster than in human and ferret tissue. Slow post-rest decay has also been observed in rat (Ragnarsdóttir *et al.* 1982) and rabbit myocardium (Cave *et al*, 1990).

Shattock and Bers (1989) have demonstrated that in rat myocardium there is a net uptake of Ca^{2+} into the cell during rest whilst in the rabbit there a net efflux. A possible explanation for this is that the transmembrane flux of Ca^{2+} is linked to the Na^+ gradient across the cell membrane via a $3Na^+/Ca^{2+}$ counter-exchanger. If this is the case several situations would accentuate Ca^{2+} efflux; these include a low intracellular $[Na^+]$, a high intracellular $[Ca^{2+}]$ and a relatively negative membrane potential. If these situations prevailed then a rapid decay of post-rest tension would result. An increase of intracellular $[Na^+]$, a reduction of intracellular $[Ca^{2+}]$ and membrane depolarization would slow or even reverse the decay of tension during rest.

Several data support this hypothesis. In guinea-pig myocardium application of ouabain, which increases intracellular $[Na^+]$ (Fry, 1986), thus tending to encourage calcium influx via Na^+/Ca^{2+} exchange, and verapamil, which reduces intracellular $[Ca^{2+}]$ both prolonged τ_3. Conversely application of ryanodine drastically reduced τ_3. This result might also be explained by this hypothesis in that if intracellular storage is prevented by the ryanodine then the extrusion of Ca^{2+} from the cell will be accentuated. In human

myocardium similar results were observed with ouabain and ryanodine although verapamil was without effect.

In contrast to their effect on τ_1, an increase of the extracellular [Ca^{2+}] or reduction of the extracellular [Na^+] (C.H.Fry and J.M.Walker, unpublished data) prolong τ_3 in human myocardium. Both interventions would reduce Ca^{2+} efflux, and hence the rate of rest decay, one by reducing the transmembrane Ca^{2+} gradient, the other by coupling a Ca^{2+} influx to Na^+ efflux via a Na^+/Ca^{2+} exchange process.

The species variability in the value of τ_3 is also of interest. A large value will be a reflection of a high intracellular [Na^+], a low intracellular [Ca^{2+}] or a depolarized membrane. In rat myocardium, the relatively high intracellular [Na^+] (Shattock and Bers, 1989) may underlie the phenomenon. In human tissue the membrane potential (-83.0mV) is similar to that recorded in guinea-pig myocardium (-80.0mV) (C.H.Fry, unpublished data). Definitive measurements or intracellular ions have yet to be made in human tissue and correlated with the value of τ_3, but the result should corroborate or disprove this hypothesis.

The slow recovery phase time constant, τ_2

The mechanisms responsible for the second (slow) recovery time constant, τ_2, are obscure. Few interventions altered the value of this component and as the capacity is small it would be unlikely to exert a significant influence on the force-interval relationship. However, it is important to consider this component when calculating τ_1 because if it is ignored then the value of this rapid component will be overestimated and attenuate any alteration that might occur.

In summary, the rapid recovery time constant, τ_1, and the decay time constant, τ_3, associated with the mechanical restitution curve of mammalian myocardium can be manipulated by agents affecting Ca^{2+} metabolism. These interventions indicate a dependence of τ_1 on both the reactivation of I_{si} and the intracellular recycling of Ca^{2+}. The value of τ_1 may be influenced by the relative importance of these two factors. The decay constant, τ_3, is dependent on those mechanisms responsible for Ca^{2+} extrusion from the cell. These data are consistent with a Na^+/Ca^{2+} exchange playing a role in this context.

CLINICAL AND IN-VITRO COMPARISONS

In the forgoing discussion I have compared mechanical restitution in human myocardium with that in two other mammalian species. The similarities which occur (primarily in the value of τ_1) are restricted to myocardium obtained from patients with *"normal"* myocardium. A major objective of this study was to compare the *in-vitro* and *in-vivo* properties of human myocardium. It had been suggested by Fry *et al* (1983) in a smaller study, on 16 patients, that τ_1 in human myocardium is negatively correlated with the ciné-angiographic ejection fraction. In other words, τ_1 is prolonged when there is clinical evidence of left-ventricular failure. It is important to note, that the values of τ_1 in that study were greater than those in the present study and were derived from a two, rather than three, exponential model.

In the present study an attempt was made to compare the *in-vivo* (clinical and catheter) indices of left-ventricular function with *in-vitro* (isolated muscle) contractile properties. This area forms the basis of the important negative findings of this study (for detail see *Results*). In summary, there was no relationship between symptoms, drug history or catheter derived indices of contractility, and any of the measurements made on isolated myocardium obtained from the same patients.

The catheter measured indices of contractility were those of routine fluid filled catheter pressure measurements and angiographic volume estimations. It could be argued that these methods are relatively insensitive, and as such did not distinguish 'good' from 'failing' myocardium. While this is certainly a factor, another explanation is that most of the patients studied had well maintained left-ventricular function (ejection fraction 0.53±0.02); with valve lesions being the primary cause of symptomatic cardiac failure. (For review of the effects of left-ventricular volumes in valvular heart disease, see Yang *et al*, 1978.) Twelve patients in this study had ejection fractions of less than 45%, and seven of less than 40%. Separate analysis of this group showed no important differences in any of the isometric twitch and mechanical restitution parameters.

It has been shown that even in severe myocardial failure (muscle isolated from patients undergoing cardiac transplant) isometric twitch tension is normally preserved, but that both the twitch and calcium transient duration are prolonged (Gwathmey *et al*, 1987). In contrast with the present study Gwathmey's patients all had end-stage myocardial failure, and presumably grossly impaired ejection fractions.

The failure to find any relationship between myocardial failure and *in–vitro* measurements prompted investigation of the physiological basis for myocardial adaptive mechanisms in valvular heart disease. Abnormal pressure and volume loads have been shown to produce well defined effects on myocardial mass and left-ventricular volume (Dodge and Baxley, 1969), but the cellular basis for these adaptive processes in man remains incompletely understood. In this study there was no relationship between the left-ventricular end-diastolic volume index and any of the *in-vitro* parameters measured. Furthermore, myocardium from patients with predominantly regurgitant lesions did not appear to differ from that from patients with no evidence of pressure or volume overload. A conclusion of this study is therefore that volume overload, while causing significant increase in left-ventricular end-diastolic volume, is not associated with abnormal isometric twitch profiles or mechanical restitution.

The results obtained from different diagnostic groups show distinct abnormalities in myocardium obtained from patients with aortic stenosis, raising the possibility that the hypertrophic response to pressure overload may be involved in the mechanism of these abnormalities.

HYPERTROPHY

A major objective of this study was to examine the *in-vitro* properties of hypertrophic human myocardium. For this purpose a group of patients with valvular aortic stenosis was studied and comparison was made with patients with other valve lesions. As already discussed, there was no difference between the *in-vitro* parameters of other diagnostic categories. This section of the discussion will therefore be confined to the results obtained from myocardium from patients with aortic stenosis as compared with all other patients. That biopsies in aortic stenosis were obtained only from the left-ventricular outflow tract and from either the LV outflow and papillary muscles in all other cases is unlikely to have affected the results, since there was no difference in the *in-vitro* parameters measured from the two sites.

The hypertrophic response of myocardium to increased loads is a normal physiological response to the increased demands of physical growth which occur during childhood and adolescence (Grossman, 1980). In pathological states associated with left ventricular pressure-overload, ventricular wall thickness increases in parallel to systolic pressure with the result that wall stress is normalized (Grossman *et al*, 1975). Thus,

systolic ventricular function is preserved in patients with mild aortic stenosis (Gunther & Grossman, 1979), but in later stages ventricular function becomes depressed (Spann *et al*, 1980 and Krayenbuehl *et al*,1982). Ross (1985) has described four distinct phases in the natural history of left ventricular overload: 1) early hypertrophy secondary to mild or moderate overload, 2) compensated hypertrophy associated with severe chronic overload, 3) reversible impaired ventricular performance with severe overload (so-called afterload mismatch) and 4) irreversible myocardial disease. Most subjects of this study had relatively well preserved left ventricular function and compared well with the control group of patients without aortic stenosis, suggesting that most were within what Ross would call phase 2. Four patients had left ventricular ejection fractions less than 40% and three of these were NYHA symptom class IV. It is likely, therefore, that these patients were within Ross' phase 3 or 4.

There are two major differences observed in the *in-vitro* performance of myocardium from patients with aortic stenosis. Firstly, the time course of development of twitch tension is prolonged in these patients, but peak isometric tension is no different from the control group. Secondly, mechanical recovery of the myocardium between beats (τ_1) is slower in patients with aortic stenosis. Furthermore, the time constant of the fast recovery phase (τ_1) is correlated both to the degree of aortic stenosis and to the degree of left ventricular hypertrophy. There is an additional suggestion that the recovery of the slow inward current (τ_{SAP}) (as measured by slow action potential dV/dt max) is slower in patients with aortic stenosis, and there is a positive correlation between τ_{SAP} and left ventricular wall thickness in patients both with and without aortic stenosis.

Abnormalities of twitch tension (prolonged time to peak tension associated with normal isometric twitch tension) in myocardium from patients with aortic stenosis are similar to the observations of others in rats (Bing *et al*, 1971) with surgically induced left ventricular hypertrophy, and in cats (Anderson, Manring, Arentzen *et al*, 1977) with right ventricular hypertrophy. Isolated myocardium from dilated hypertrophic hearts of transplant recipients show a similar pattern of unimpaired peak tension and prolonged time to peak tension (Gwathmey *et al*, 1987).

The effect of hypertrophy on the MRC is qualitatively similar to the results of others on the papillary muscles of cats with right ventricular hypertrophy (Anderson, Manring, Arentzen *et al*, 1977). In each study myocardial function is generally preserved, yet abnormalities of the force-interval relationship suggest some alteration in the cellular handling of calcium in hypertrophic muscle. Mechanical restitution in human subjects with aortic stenosis differs from controls in two ways. Firstly, τ_1 is slower, which

suggests either a reduced rate of calcium uptake by the SR or reduced rate of recovery of membrane currents, or a combination of both. Secondly, the MRC of these patients is shifted upwards and tension at long intervals overshoots steady state values more than controls, suggesting that the slower recovery process is associated with an increased capacity of the system. It was also interesting to note that the four patients who were more severely ill, with impaired left ventricular function, had values for τ_1 generally at the upper end of the range (685ms, 1600ms, 526ms and 394ms).

From studies on a model of pressure overload hypertrophy in the ferret using the light emitting protein, aequorin, it has been suggested that the rate of calcium uptake and possibly the rate of release of calcium from intracellular stores is decreased in hypertrophy (Gwathmey & Morgan, 1985). Furthermore, the observation of a biphasic calcium transient in myocardium obtained from human transplant recipients has been interpreted as reflecting abnormal calcium handling by both the sarcolemma and the sarcoplasmic reticulum (Gwathmey *et al*, 1987).

Hemwall *et al* (1984) showed that slow action potentials in cats with right ventricular hypertrophy were significantly smaller in amplitude and duration than controls, suggesting an abnormality of sarcolemmal calcium transport. Twitch tension was reduced in the papillary muscles of the cats in that study, so the discrepancy between these and the contractile properties of human myocardium may reflect the different species and models used. However, in this study there is a suggestion of slowing of the slow inward current recovery in hypertrophic human myocardium; the significance of any differences possibly being concealed by the small numbers involved.

Direct evidence of altered calcium handling in myocardial hypertrophy is provided by studies on isolated SR. In a model of left ventricular hypertrophy in the rabbit (Sordahl *et al*, 1973) the rate of uptake and capacity of the SR for calcium is reduced. SR function is similarly impaired in patients with cardiac failure (Lentz *et al*, 1978 and Limas *et al*, 1987), but the relationship between hypertrophy and SR function in man is unknown. In the rat, SR function appears to be dependent on the degree of hypertrophy, being enhanced in mild hypertrophy (Limas *et al*, 1980), and impaired in more severe degrees of hypertrophy (Limas & Cohn, 1977). According to *the model* described above, the results of this study on hypertrophic myocardium in man may be interpreted as demonstrating both an increased capacity of intracellular calcium release sites and a reduced rate of uptake of calcium to the release loci.

In summary, isolated hypertrophic human myocardium may be distinguished by a prolonged time to peak tension and a slow recovery of twitch tension between beats. These results are consistent with the hypothesis that abnormalities of mechanical restitution are related to altered cellular calcium handling involving the function and capacity of the sarcoplasmic reticulum and possibly the recovery of sarcolemmal membrane currents.

MECHANICAL ALTERNANS

Mechanical alternans, or its bedside clinical counterpart, pulsus alternans, is described as an alternation of strong and weak contractions in the presence of a regular rhythm. First described by Traube in 1872, the mechanism for this phenomenon remains incompletely understood. It is distinguished from pulsus bigeminus, which is alternate strong and weak contraction as a result of alternate sinus and ectopic beats with varying RR intervals. The phenomenon of mechanical alternans is recognised as being a sign of depressed myocardial function (see Braunwald, 1988). It is most common in heart failure secondary to an increased resistance to left-ventricular ejection (e.g. systemic hypertension and aortic stenosis) but also occurs in coronary artery disease and dilated cardiomyopathy. It tends to occur with the combination of depressed contractility and a tachycardia, and is often accentuated during the first few beats following a premature ventricular beat.

There has been controversy over the exact mechanism of mechanical alternans, essentially surrounding the relative roles of changes in ventricular loading and contractility. Initially it was thought that changes in stroke volume were a result of beat–to–beat changes in end-diastolic volume (Wenckebach, 1902); a theory augmented by an angiographic study by Gleason and Braunwald (1962) on a patient with pulsus alternans and a study on canine heart preparations by Mitchell *et al*, (1963). However, more extensive investigations in man (Swanton *et al*, 1976) and dogs (Guntheroth *et al*, 1969) have shown a lack of relationship between loading and alternations in contractility. McGaughey *et al* (1985) in a study in the isolated canine heart showed a difference in end-systolic pressure-volume relationship between the large and small beats of mechanical alternans, consistent with an alternation in contractility. It should be emphasised, however, that the relationship between alternations in stroke volume, pre-load, after-load and contractility is complex and that changes in loading inevitably influence stroke volume even if changes in contractility are primarily responsible.

Confirmation that alternation in contractility occurs was provided by a study on an isometric papillary muscle preparation (Nayler & Robertson, 1965) which demonstrated mechanical alternans in the absence of significant changes in end-diastolic tension. In a study in open chest dogs Mahler and Rogel (1970) demonstrated mechanical alternans in segments of myocardium held isometrically between two limbs of a force transducer. They showed a positive correlation between the time constant of mechanical recovery of a beat and the force of contraction of its preceding beat. Thus an equation describing mechanical alternans was derived and was found to predict the results of their experiments on dog hearts.

Mechanical alternans is frequently observed in preparations of isolated myocardium. This was true in this study and occurred particularly in myocardium obtained from more severely ill patients, usually recovering rapidly following mounting of the preparation. In some cases recovery did not occur and no steady state peak isometric twitch tension could be established, making it impossible to construct mechanical restitution curves.

The study of mechanical alternans was not an initial aim of this study. However, the emergence of an abnormality of the force interval relationship in myocardium from patients with left-ventricular pressure overload raised the question as to whether this could provide an explanation for the mechanism of mechanical alternans in such patients. An inevitable consequence of mechanical restitution is that a finite time is required for full recovery of contractility between beats. This would suggest that at heart rates above a certain value (i.e. with a cycle length shorter than the time required for full recovery) restitution would be incomplete. According to *the model* of cellular calcium circulation suggested above, this would be a consequence of a reduced amount of Ca^{2+} released by the myofibrils returning to SR release sites in time for the subsequent beat. Assuming the Ca^{2+}, which are unable reach the SR release sites in time, are not lost from the cell, then they would be available for release during the next beat together with the reduced amount recirculated from the preceding smaller beat. Since the cycle length has dictated the amount of Ca^{2+} which can be recirculated between beats, it will appear that any surplus Ca^{2+} recycles every other beat.

This is illustrated in Figure 59 in which the normal state is indicated in the upper diagram. Here, all Ca^{2+} released by the myofibrils are recirculated to the next beat. In the lower diagram the cycle length is shorter and there is insufficient time for full recirculation. Beat 2 is therefore sub-maximal. Ca^{2+} released from beat 2 is then recirculated to beat 3 together with additional Ca^{2+} which is now available from beat 1.

The implication of this theory is that mechanical alternans would occur in situations where either the cycle length was short or when mechanical restitution was slowed. That mechanical alternans can occur during tachycardia even in the normal heart (Saunders & Ord, 1962) is consistent with the hypothesis. If correct, the process should be self perpetuating and mechanical alternans would be more likely to occur at higher heart rates and in myocardium with a prolonged recovery time constant. The system is analogous to an oscillator with a time lag between the input and output.

It has been shown that mechanical restitution is slowed in myocardium from patients with increased afterload resistance. This observation may therefore explain the increased incidence of pulsus alternans in such patients, and why this occurs at lower heart rates than in patients with normal hearts.

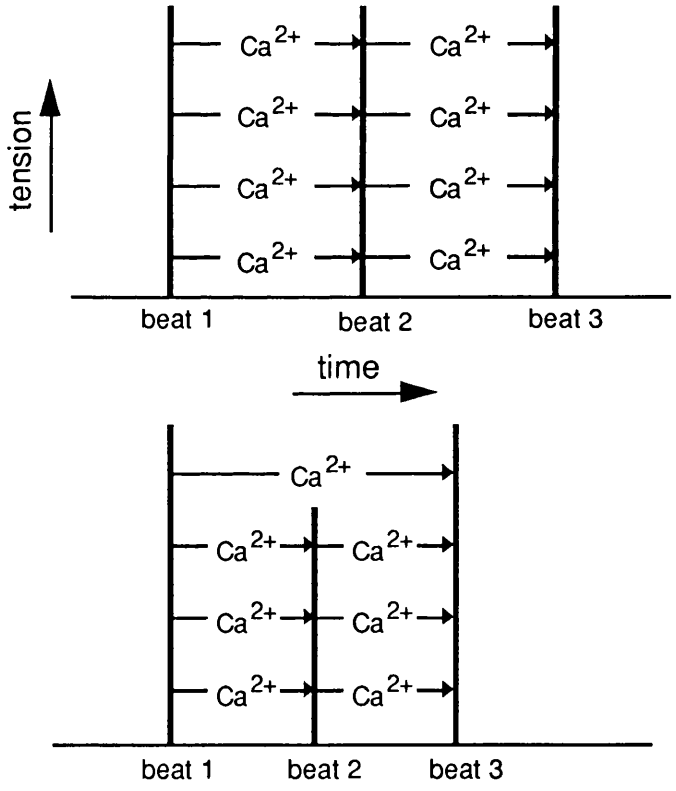

Figure 59. Calcium recirculation in mechanical alternans. See text for explanation.

SUMMARY AND CONCLUSIONS

The central theme of this study was to investigate the *in-vitro* mechanical properties of isolated human ventricular myocardium and to compare these findings with clinical and *in-vivo* parameters. The initial aim was to examine myocardium from patients undergoing valve replacement and to compare the results obtained from myocardium with different degrees of pressure and volume overload. The results have shown that the mechanical physiology of hypertrophied myocardium (that obtained from patients with aortic stenosis) differs from that of myocardium from other patients. In hypertrophy the time to development of peak isometric tension is prolonged, whereas the amount of tension produced is unaltered. It has also been shown that the rate of recovery of tension between beats (mechanical restitution) is slowed in hypertrophy. This finding provides a possible explanation for the higher incidence of pulsus alternans in patients with increased ventricular afterload.

In order compare mechanical restitution curves these were described as multiple exponential processes. A curve fitting procedure was used to ascertain the number of exponential processes in each case, to assess the goodness-of-fit and to provide the exponential time constants.

The investigation into the mechanisms underlying mechanical restitution took two forms:

Firstly, a comparison between human myocardium and that of two other mammalian species revealed important species differences. In man and the ferret mechanical restitution (which includes both the recovery and decay processes) is best described by two recovery phases (a fast followed by a slow phase) and a slow decay phase. In the guinea-pig, there is a single rising phase followed by a decay phase. The initial recovery phase in each species had similar time constants, suggesting similar underlying mechanisms. The decay phase, however, was much slower in man and the ferret than in the guinea-pig.

Secondly, a number of interventions were performed in order to manipulate cellular calcium handling at different sites and to examine the effects of these on mechanical restitution. In addition the role of recovery of the slow inward current was examined by measuring dV/dt max of the slow action potential. The results of these studies were consistent with the hypothesis that the cellular control of calcium is intimately involved in the mechanisms underlying mechanical restitution; that the recovery of releasable calcium within the sarcoplasmic reticulum, and to a lesser extent the recovery of the

slow inward current, underlie the recovery phase; and that net cellular calcium balance (usually efflux) is responsible for the decay phase.

From the manner in which mechanical restitution is altered in human hypertrophic myocardium these data are consistent with the hypothesis that the calcium capacity of the sarcoplasmic reticulum is increased and that the rate of uptake of calcium is reduced.

There was a failure, in this study, to identify any consistent relationship between the clinical and catheterisation data and *in-vitro* data in patients. One explanation for this is that the sensitivity of the *in-vivo* methods used was inadequate to distinguish degrees of myocardial failure.

This novel analytical approach to the mechanical restitution curve has provided a new insight into the underlying mechanisms, allowed comparison between different species and elucidated cellular physiological abnormalities which occur in human pathological states.

FUTURE INVESTIGATIONS

A number of further questions are posed by this study:

Can these or similar observations on the force-interval relationship in isolated myocardium be made in patients, and if so do they have clinical relevance or a predictive value in assessment of the hypertrophic response in aortic stenosis?

Can the explanations given for the processes underlying mechanical restitution be verified by direct measurement of intra-cellular ions and membrane currents?

Finally, there is always the doubt that the so-called normal human myocardium was not normal. It would be interesting to examine mechanical restitution in myocardium from hearts donated for transplantation and furthermore to compare these, say, with myocardium from patients with end-stage heart failure (the excised hearts).

APPENDIX

I. CIRCUIT DIAGRAMS

Differentiator Circuit Design

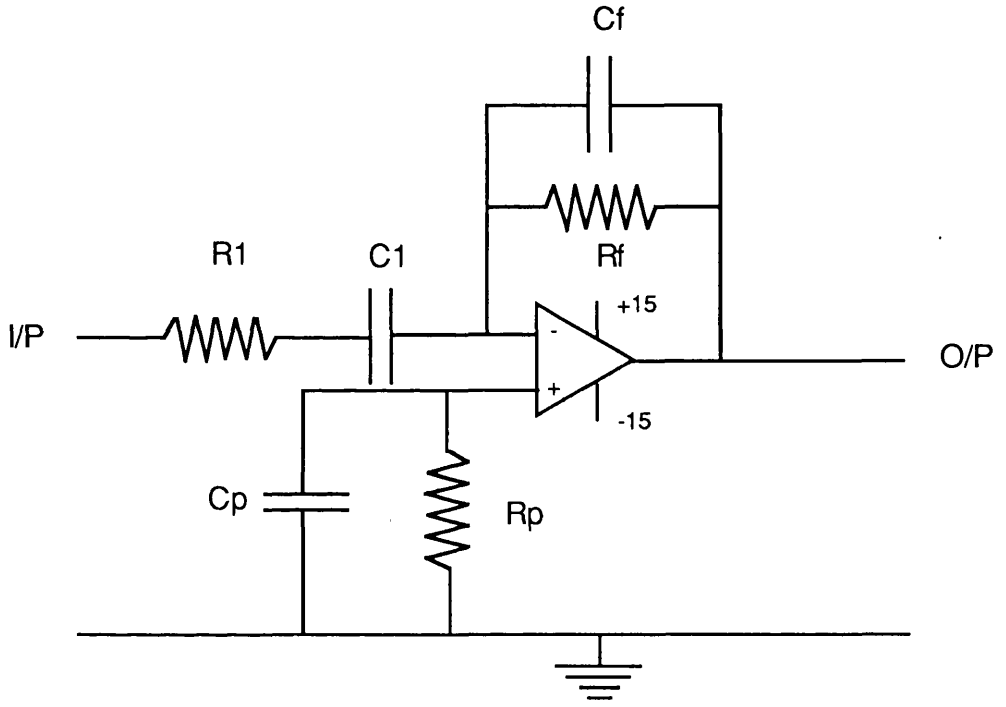

General circuit diagram for a differentiator

The parameters for the different differentiator circuits were as follows:

	Operational Amp.	Rf	Cf	R1	C1	Rp	Cp
1. Tension.	Type 351	10kΩ	4.7nF	330Ω	1μF	10kΩ	10μF
2. Slow Action Potential.	Type 741 S	22kΩ	1.0nF	10kΩ	1.0μF	22kΩ	10μF
3. Normal Action Potential.	Type 741 S	22kΩ	1.0nF	470kΩ	0.05μF	22kΩ	0.47μF

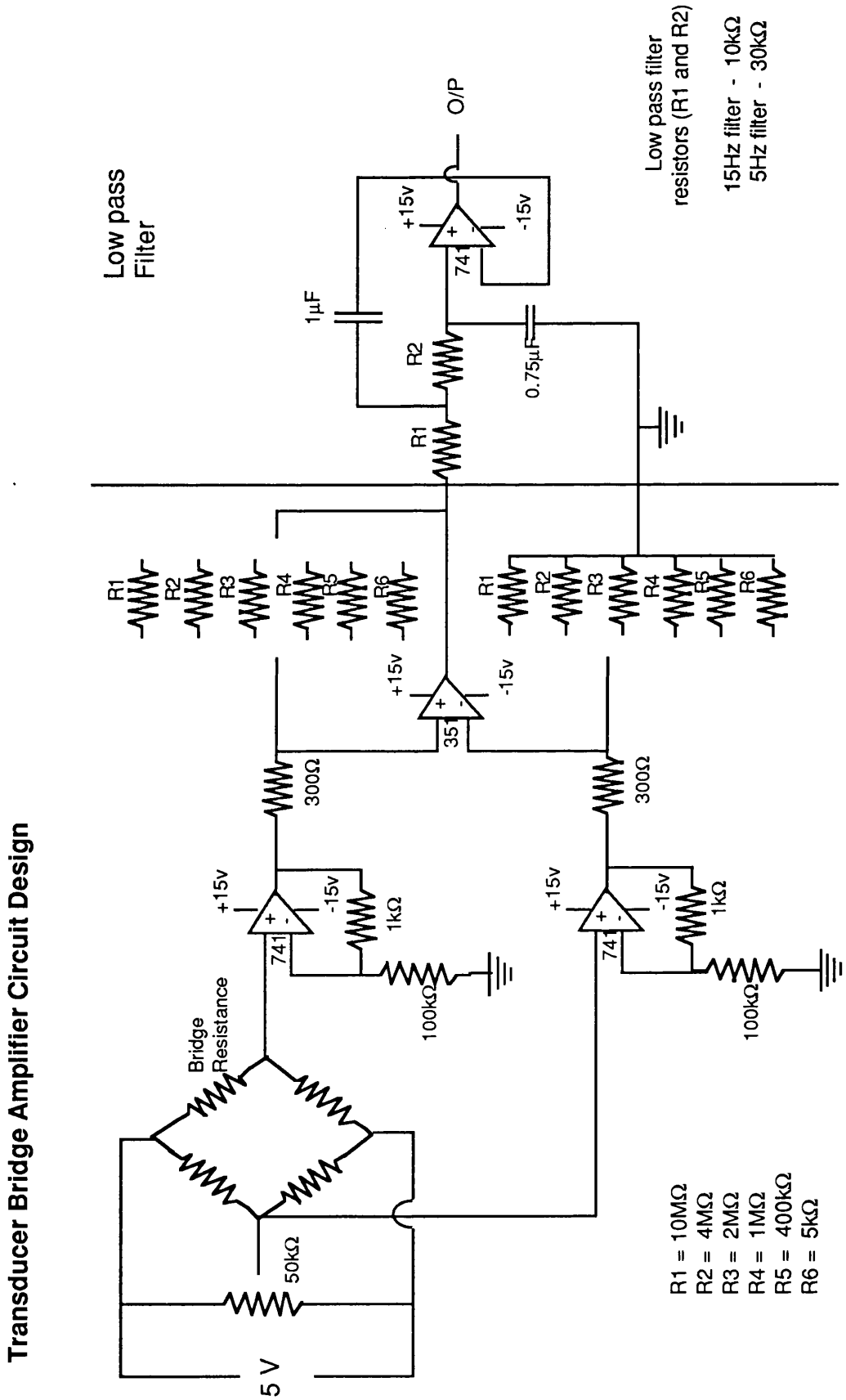
Transducer Bridge Amplifier Circuit Design
Bridge Resistance
50kΩ
5 V
741
+15v
-15v
1kΩ
100kΩ
300Ω
351
Low pass Filter
1μF
R1
R2
0.75μF
O/P
Low pass filter resistors (R1 and R2)
15Hz filter - 10kΩ
5Hz filter - 30kΩ
R1 = 10MΩ
R2 = 4MΩ
R3 = 2MΩ
R4 = 1MΩ
R5 = 400kΩ
R6 = 5kΩ

Microelectrode head-stage pre-amplifier circuit design

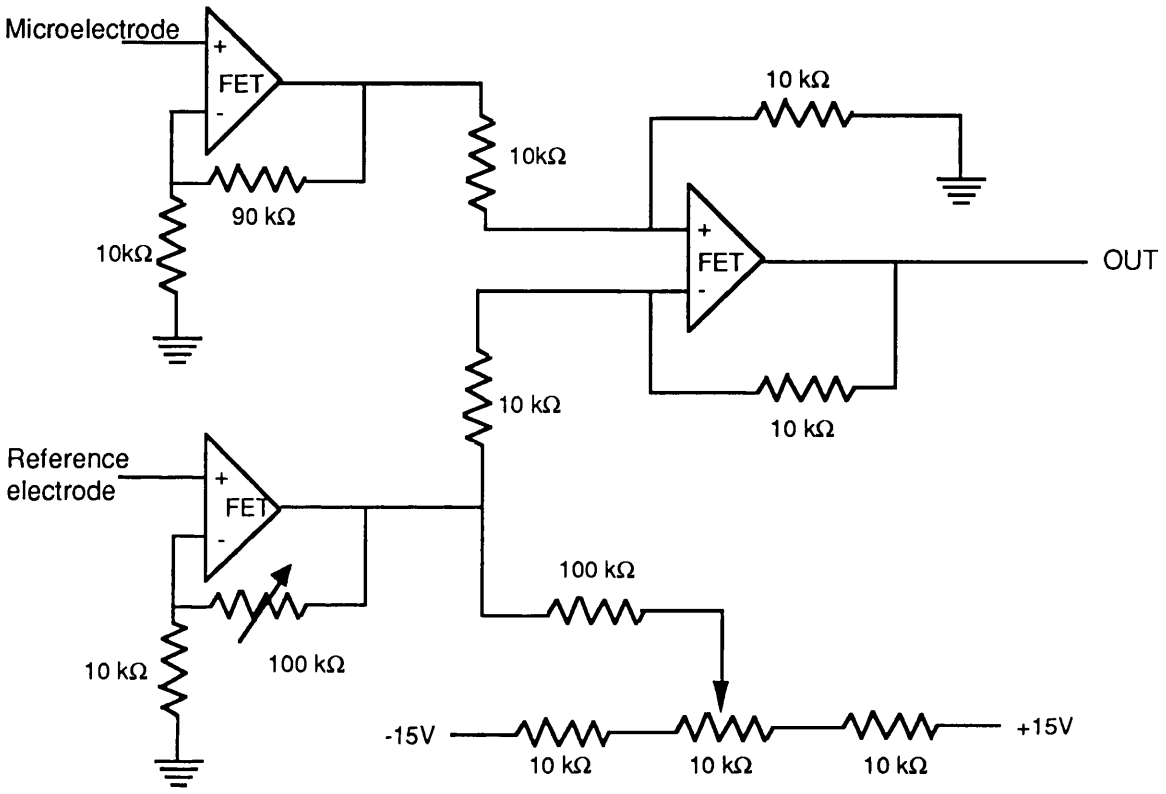

Flip-flop circuit design

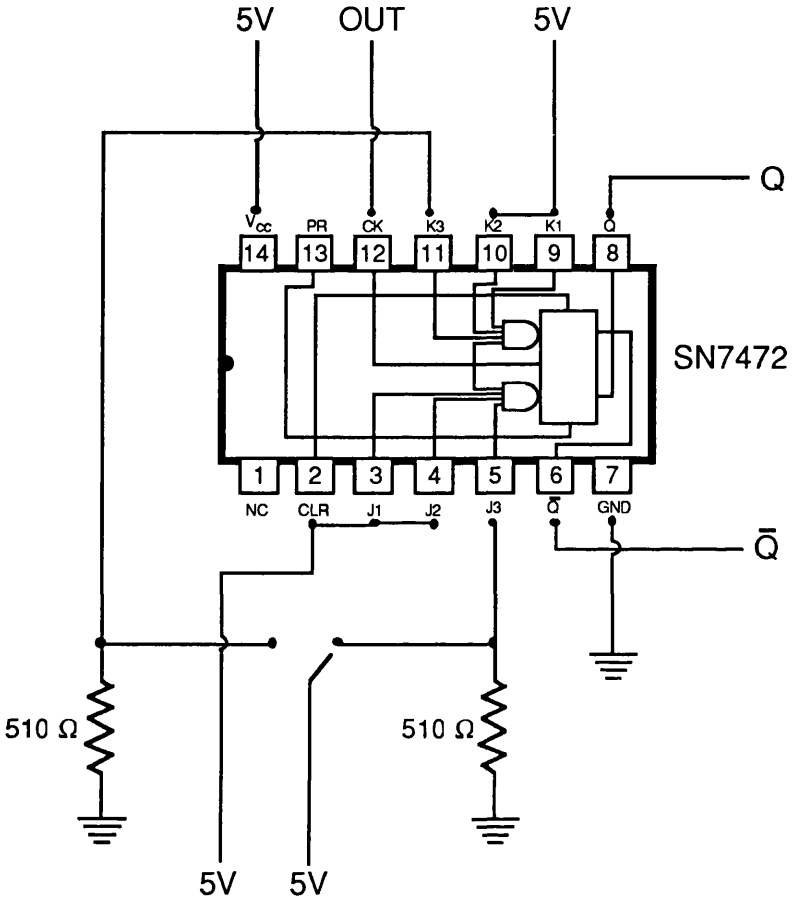

INPUT J	K	Q	$\bar{Q}$	OUTPUT
0	1	0	1	0
1	0	0	1	1
0	1	1	0	0
1	0	1	0	1

Integrated circuit:

Texas Instruments SN7472/9N72. J-K flip-flop with AND inputs.

II. SPREADSHEET

Curve Stripping Spreadsheet Template

The following is a guide to the operation and construction of the spreadsheet template designed for multiple exponential curve stripping.

Using Jazz™ release 1A (Lotus™ Development Corp., USA) on an Apple® Macintosh® microcomputer.

Data is first entered into cells of columns A and B. Column A contains the value of normalized twitch tension (ectopic/steady state). Column B contains the corresponding ectopic interval (in milliseconds).

Column C contains a column beginning with the following formula:

```
LN(ABS(A1-$D$9))
```

where
- $D$9 = fixed reference to value of cell D9
- D9 = the user defined value of the decay curve asymptote
- LN = the natural logarithm of (x)
- ABS = the absolute value of (x)
- A1 = relative reference to the corresponding cell in column A (containing the normalized twitch tension)

A graph plotting the data points in columns A and B is then displayed and the user defines the points which describe the decay curve and identifies the ectopic interval at which it would be reasonable to begin a logarithmic transform. Accordingly the values of the ectopic intervals (column B) are copied together with the natural logarithmic transform (column C) and pasted into a second spreadsheet where standard least squares linear regression analysis is performed. The linearity of the transformed data may be inspected on a displayed plot. At this stage the asymptotic value (D9) may be modified to achieve the best linear fit.

The values of the intercept and slope thus obtained are then pasted into cells D4 and D5 respectively.

D6 then displays the decay time constant using the formula:

-1/D9 (τ_3)

Columns J to R contain formulae and are not required to be seen by the user. The formulae are as follows:

J = EXP($D$4+(-B1/$D$6))+$D$9

where EXP = e raised to the power of (x)

K = ABS(J1-A1)

L = J1-M1

M = EXP($F$4+(-B1/$F$6))

N = ABS(K1-M1)

O = EXP($H$4+(-B1/$H$6))

P = L1-O1

Q = IF(ISNUMBER(A1),(A1-P1)^2,"/")

(returns a value of (A1-P1)squared if there is a numerical value in A1; otherwise returns text string "/")

R = IF(ISNUMBER(A1),(A1-L1)^2,"/")

Column J is automatically plotted over the data points, showing where the data deviates from the fitted decay curve.

Column E contains the natural logarithmic transform of the difference between the data (in column A) and the fitted decay curve:

E = LN(K1)

Column E together with the corresponding valves in column B are then pasted across to the other spreadsheet for least squares regression analysis. The plot derived from this shows the user whether the relationship is linear (single rising exponential) or not. Invariably, there is some linearity of the data at longer ectopic intervals, even if all the data is not linearly related. If the overall relationship is non-linear all data points beyond the initial linear relationship can be removed and the regression equation for the remaining points derived. The values for intercept and slope thus obtained are then

pasted onto the original spreadsheet in cells F4 and F5 respectively. F6 then provides the time constant of this rising exponential with the formula:

F6 = -1/F5

(τ_2 in a three exponential model, τ_1 in a two exponential model)

Column M plots this second fitted curve over the data together with the fitted decay curve. Any divergence of of the data from this fitted curve may be seen by the user.

Column G then gives the natural logarithmic transform of the difference between second fitted curve and the residual data.

If appropriate an initial rapid recovery phase is fitted by pasting values from column G together with corresponding values in column B into the linear regression spreadsheet. Values for the intercept and slope are then pasted into cells H4 and H5 respectively. Cell H6 provides the time constant of the fast rising exponential.

H6 = -1/H5 (τ_1)

Finally, this fitted curve is automatically superimposed onto the data plot together with the other two fitted exponential curves.

The goodness-of-fit of the exponential function can be ascertained by inspection of the following cells.

T8 = COUNT ($A$1..$A$40)
(number of data points)

T9 = IF(ISERR(Q1),SUM($R$1..$R40),SUM($Q$3..$Q$41))
(sum of squares of differences)

V8 = AVG($A$1..$A$40)
(mean)

V9 = ($T$9/$T$8)/$V$8
(variance)

The matrix S3..V9 can be used to print out a description of the fitted curve together with the composite plot by using the *Hotview* facility. The following formulae and text entry are required to complete this:

S4 - "Intercept"

S5 - "Slope"

S6 - "Tau"

S8 - "n"

S9 - "Sum of Squares"

U8 - "Mean"

U9 - "Variance"

T3 - "Curve 1"

T4 = $H$4

T5 = $H$5

T6 = $H$6 (τ_1)

U3 - "Curve 2"

U4 = $F$4

U5 = $F$5

U6 = $F$6 (τ_2)

V3 - "Curve 3"

V4 = $D$4

V5 = $D$5

V6 = $D$6 (τ_3)

REFERENCES

Abbott BC, Mommaerts WFHM (1958) A study of inotropic mechanisms in the papillary muscle preparation. *J Gen Physiol.* **42:** 533-551.

Anderson PAW, Manring A, Arentzen CE, ScottRankin J, Johnson EA (1977) Pressure-induced hypertrophy of cat right ventricle: an evaluation with the force-interval relationship. *Circ Res.* **41:** 582-588.

Anderson PAW, Manring A, Johnson EA (1973) Force-frequency relationship. -a basis for a new index of contractility. *Circ Res.* **33:** 665-671.

Anderson PAW, Manring A, Johnson EA (1977) The force of contraction of isolated papillary muscle: a study of the interaction of its determining factors. *J Mol Cell Cardiol.* **9:** 131-150.

Anderson PAW, Manring A, Serwer GA, Woodrow Benson D, Edwards, SB, Armstrong BE, Sterba RJ, Floyd, RD (1979) The force-interval relationship of the left ventricle. *Circulation.* **60:** 334-348.

Anderson PAW, Scott Rankin J, Arentzen CE, Anderson RW, Johnson EA (1976) Evaluation of the force-frequency relationship as a descriptor of the inotropic state of canine left ventricular myocardium. *Circ Res.* **39:** 832-839.

Banchero N (1987) Cardiovascular responses to chronic hypoxia. *Ann Rev Physiol.* **49:** 465-476.

Bers D (1989) SR Ca loading in cardiac muscle preparations based on rapid cooling contractures. *Am J Physiol.* **256:** C109-C120.

Bers DM (1985) Ca influx and sarcoplasmic reticulum Ca release in cardiac muscle activation during post rest recovery. *Am J Physiol.* **248:** H366-H381.

Bing OHL, Matsushita S, Fanburg BL, Levine BL, Levine HJ (1971) Mechanical properties of rat cardiac muscle during experimental hypertrophy. *Circ Res.* **28:** 234-245.

Bowditch HP (1871) Über die Eigenthümlichkeiten der Reizbarkeit, welche die Muskelfasem des Herzens zeigen. *Arbeiten Physiologischer Anstalt von Leipzig.* **6:** 139-176.

Bowman WC, Rodger IW, Shahid M (1985) Modification of calcium ion exchange and its relation to myocardial contractility. In: *Control and Manipulation of Ca Movement,* ed Parratt JR, Raven Press, New York. 213-238.

Braunwald E (1988) In: *Heart Disease, a textbook of cardiovascular medicine.* Ed. Braunwald E. WB Saunders, Philadelphia, USA.

Braunwald E, Sonnenblick EH, Ross J (1988) Mechanisms of cardiac contraction and relaxation. In: *Heart Disease, a textbook of cardiovascular medicine.* Ed. Braunwald E. WB Saunders, Philadelphia, USA. 383-425.

Braveny P, Kruta V (1958) Dissociation de deux facteurs: Restitution et potentiation dans l'action de l'intervalle sur l'amplitude de la contraction du myocarde. *Archives Internationales de Physiologie et de Biochemie.* **66:** 633-652.

Burkhoff D, Yue D, Franz M, Hunter W, Sagawa K (1984) Mechanical restitution of isolated perfused canine left ventricles. *Am J Physiol.* **246:** H8-H16.

Capasso JM, Strobeck JE, Sonnenblick EH (1981) Myocardial mechanical alterations during gradual onset long-term hypertension in rats. *Am J Physiol.* **241:** H435-H441.

Cave AC, Shattock MJ, Hearse DJ (1990) Functional and metabolic recovery of the heterotopically transplanted rabbit heart is complete 24 hours post transplantation. *J. Mol. Cell. Cardiol*: In press.

Chapman CB, Baker O, Reynolds J, Bonte FJ (1958) Use of biplane cinefluorography for measurement of ventricular volume. *Circulation.* **18:** 1105-1117.

Chapman RA (1983) Control of cardiac contractility at the cellular level. *Am J Physiol.* **245:** H535-H552.

Chilian WM, Marcus ML (1987) Coronary vascular adaptations to myocardial hypertrophy. *Ann Rev Physiol.* **49:** 477-487.

Clark WA, Chizzonite RA, Everett AW, Rabinowitz M, Zak R (1982) Species correlations between cardiac isomyosins. A comparison of electrophoretic and immunological properties. *J Biol Chem.* **257:** 5449-5454.

Colucci WS, Wright RF, Braunwald E (1986) New positive inotropic agents in the treatment of congestive heart failure. mechanisms of action and recent clinical developments (first of two parts). *New Eng J Med.* **314:** 290-299.

Cooper G IV (1987) Cardiocyte adaptation to chronically altered load. *Ann Rev Physiol.* **49:** 501-518.

Cooper G IV, Tomanek RJ (1987) Model dependent behaviour of pressure hypertrophied myocardium. *Cardiovasc Res.* **21:** 342-351.

Cooper G IV, Tomanek RJ, Ehrhardt JC, Marcus ML (1981) Chronic progressive pressure overload of the cat right ventricle. *Circ Res.* **48:** 488-497.

Dodge HT, Baxley WA (1969) Left ventricular volume and mass and their significance in heart disease. *Am J Cardiol.* **23:** 528-537.

Donald TC, Unnoppetchara K, Peterson D, Hefner LL (1972) Effect of initial muscl length on Vmax in isotonic contraction of cardiac muscle. *Am J Physiol.* **223:** 262-267.

Edman KAP, Jóhannson M (1976) The contractile state of rabbit papillary muscle in relation to stimulation frequency. *J Physiol.* **254:** 565-581.

Elzinga G, Lab MJ, Noble MIM, Papadoyannis DE, Pidgeon J, Seed A, Wohlfart B (1981) The action-potential duration and contractile response of the intact heart related to the preceding interval and the preceding beat in the dog and cat. *J Physiol.* **314:** 481-500.

Fabiato A, Fabiato F (1977) Calcium release from the sarcoplasmic reticulum. *Circ Res.* **40:** 119-129.

Fabiato A, Fabiato F (1979) Calcium-induced release of calcium from the sarcoplasmic reticulum of skinned cells from adult human, dog, cat, rabbit, rat and frog hearts and from fetal and new-born rat ventricles. *Ann NY Acad Sci.* **307:** 491-522.

Feher JJ, Lipford GB (1985) Mechanism of action of ryanodine on cardiac sarcoplasmic reticulum. *Biochem Biophys Acta.* **813:** 77-87.

Fouad FM (1987) Left ventricular diastolic function in hypertensive patients. *Circulation.* **75(suppl I):** I-48 - I-55.

Fouad FM, Tarazi RC, Gallagher JH, MacIntyre WJ, Cook SA (1980) Abnormal left ventricular relaxation in hypertensive patients. *Clin Sci.* **59:** 411s-414s.

Fry CH (1986) Measurement and control of intracellular magnesium ion concentration in guinea-pig and ferret ventricular myocardium. *Magnesium.* **5:** 306-316.

Fry CH, Walker JM, Webb-Peploe MM, Williams BT (1983) Restitution of contractility in-vitro, of human and guinea-pig myocardium. *J Physiol.* **339:** 26-27P.

Gettes LS, Reuter H (1974) Slow recovery from inactivation of inward currents in mammalian myocardial fibres. *J Physiol.* **240:** 703-724.

Gleason WL, Braunwald E (1962) Studies on Starling's Law of the Heart. VI. Relationships between left ventricular end-diastolic volume in man with observations on the mechanism of pulsus alternans. *Circulation.* **25:** 841-848.

Gorlin R, Gorlin SG (1951) Hydraulic formula for calculation of the area of the stenotic mitral valve, other cardiac valves and central circulatory shunts. *Am Heart J.* **41:** 1-29.

Grossman W (1980) Cardiac hypertrophy: useful adaptation or pathologic process?. *Am J Med.* **69:** 576-584.

Grossman W, Jones D, McLaurin LP, (1975) Wall stress and patterns of hypertrophy. *J Clin Invest.* **56:** 56-64.

Gunther S, Grossman W (1979) Determinants of ventricular function in pressure-overload hypertrophy in man. *Circulation.* **59:** 679-688.

Guntheroth WG, Morgan BC, McGough GA, Scher AM (1969) Alternate deletion and potentiation as the cause of pulsus alternans. *Am Heart J.* **78:** 669-681.

Gwathmey JK, Copelas L, MacKinnon R, Schoen FJ, Feldman MD, Grossman W, Morgan JP (1987) Abnormal intracellular calcium handling in myocardium from patients with end-stage heart failure. *Circ Res.* **61:** 70-76.

Gwathmey JK, Morgan JP (1985) Altered calcium handling in experimental pressure overload hypertrophy in the ferret. *Circ Res.* **57:** 836-843.

Hanrath P, Mathey DG, Siegert R, Bleifeld W (1980) Left ventricular relaxation and filling pattern in different forms of left ventricular hypertrophy: an echocardiographic study. *Am J Cardiol.* **45:** 15-23.

Harigaya S, Schwartz A (1969) Rate of calcium binding and uptake in normal animal and failing human cardiac muscle membrane vesicles (relaxing system) and mitochondria. *Circ Res.* **25:** 781-794.

Hemwall E, Duthinh V, Houser S (1984) Comparison of slow response action potentials from hypertrophied myocardium. *Am J Physiol.* **246:** H675-H682.

Hill AV (1928) The diffusion of oxygen and lactic acid through tissues. *Proc Roy Soc.* **104:** 39-96.

Hill AV (1938) Heat of shortening and dynamic constants of muscle. *Proc Roy Soc.* **126:** 136-195.

Hirota Y (1980) A clinical study of ventricular function. *Circulation.* **62:** 756-763.

Hughes SW, Cooper IC, Katritis D, Webb-Peploe MM (1988) Left-ventricular volume and valve gradient analysis using an Apple Macintosh computer. In: *Medical Applications of Microcomputers.* Springer Verlag, London. 101-111.

Huston TP, Puffer JC, MacMillan Rodney W (1985) The athletic heart syndrome. *New Eng J Med.* **313:** 24-33.

Inouye I, Massie B, Loge D, Topic N, Silverstein D, Simpson P, Tubau J (1984) Abnormal left ventricular filling: an early finding in mild to moderate systemic hypertension. *Am J Cardiol.* **53:** 120-126.

Jack JSB, Noble D, Tsien RW (1976) In: *Electric current flow in excitable cells.* Clarendon Press, Oxford

Katz AM (1990) Cardiomyopathy of overload, a major determinant of prognosis in congestive cardiac failure. *New Eng J Med.* **322:** 100-110.

Kennedy JW, Trenholme SE, Kasser IS (1970) Left ventricular volume and mass from a single-plane cineangiocardiogram. A comparison of anterposterior and right anterior oblique methods. *Am Heart J.* **80:** 343-352.

Koch-Weser J (1963) Effect of rate changes on strength and time course of contraction of papillary muscle. *Am J Physiol.* **204:** 451-457.

Koch-Weser J, Blinks JR (1963) The influence of the interval between beats on myocardial contractility. *Pharmacological Rev.* **15:** 601-652.

Kohlhart M, Mnich Z, Wais U, Maier G (1978) Studies on the time-dependent response of the cardiac Ca-mediated action potential due to variations of the external calcium concentration. *Basic Res Cardiol.* **73:** 257-272.

Krayenbuehl HP, Hess O, Hirzel H (1982) Pathophysiology of the hypertrophied heart in man. *Eur Heart J.* **3 (supp A):** 125-131.

Krayenbuehl HP, Hess OM, Monrad ES et al (1989) Left ventricular myocardial structure in aortic valve disease before, intermediate, and late after aortic valve replacement. *Circulation.* **79:** 744-755.

Krayenbuehl HP, Hess OM, Schneider J, Turina M (1983) Physiologic or pathologic hypertrophy. *Eur Heart J.* **4 (suppl A):** 29-34.

Lecarpentier Y, Waldenström A, Clergue M, Chemla D, Oliviero P, Martin JL, Swynghedauw B (1987) Major alterations in relaxation during cardiac hypertrophy induced by aortic stenosis in guinea pig. *Circ Res.* **61:** 107-116.

Lentz, RW, Harrison CE, Dewey JD, Barnhorst DA, Danielson GK, Pluth JR (1978) Functional evaluation of cardiac sarcoplasmic reticulum and mitochondria in human pathologic states. *J Mol Cell Cardiol.* **10:** 3-30.

Limas CJ, Cohn JN (1977) Defective calcium transport by cardiac sarcoplasmic reticulum in spontaneously hypertensive rats. *Circ Res.* **40:** I.62 - I.69.

Limas CJ, Olivari M, Goldenberg IF, Levine TB, Benditt DG, Simon A (1987) Calcium uptake by cardiac sarcoplasmic reticulum in human dilated cardiomyopathy. *Cardiovascular Res.* **21:** 601-605.

Limas CJ, Spier SS, Kahlon J (1980) Enhanced calcium transport by sarcoplasmic reticulum in mild cardiac hypertrophy. *J Mol Cell Cardiol.* **12:** 1103-1116.

Lindenmayer GE, Sordahl LA, Harigaya S, Allen JC, Besch HR, Schwartz A (1971) Some biochemical studies on subcellular systems isolated from fresh recipient human cardiac tissue obtained during transplantation. *Am J Cardiol.* **27:** 277-283.

Lipsius SL, Fozzard HA, Gibbons WR (1982) Voltage and time dependence of restitution in heart. *Am J Physiol.* **234:** H68-H76.

MacLeod KT, Bers DM (1987) Effects of rest duration and ryanodine on changes of extracellular [Ca] in cardiac muscle from rabbits. *Am J Physiol.* **253:** C398-C407.

Mahler Y, Rogel S (1970) Interrelation between restitution time-constant and alternating myocardial contractility in dogs. *Clin Sci.* **39:** 625-639.

Malécot CO, Trautwein W (1987) On the relationship between Vmax of slow responses and Ca-current availability in whole-cell clamped guinea pig heart cells. *Pflügers Arch.* **410:** 15-22.

Malhotra A, Penpargkul S, Schaible T, Scheuer J (1981) Contractile proteins and sarcoplasmic reticulum in physiologic cardiac hypertrophy. *Am J Physiol.* **241:** H263-H267.

Maylie JG (1982) Excitation-contraction coupling in neonatal and adult myocardium of cat. *Am J Physiol.* **242:** H834-H843.

McGaughey MD, Maughan WL, Sunagawa K, Sagawa K (1985) Alternating contractility in pulsus alternans studied in the isolated canine heart. *Circulation.* **71:** 357-362.

McKee PA, Castelli WP, McNamara PM, Kannel WB (1971) The natural history of congestive heart failure: The Framingham Study. *New Eng J Med.* **285:** 1441-1446.

Minelli R, Poggesi C, Reggiani C, Tanzi F (1985) Electrical and mechanical restitution in the rat isolated cardiac papillary muscle during post-natal growth. *J Physiol.* **369:** 83P.

Mitchell JH, Sarnoff SJ, Sonnenblick EH (1963) The dynamics of pulsus alternans: alternating end-diastolic fibre length as a causative factor. *J Clin Invest.* **42:** 55-63.

Mitchell MR, Powell T, Terrar DA, Twist VW (1983) Characteristics of the second inward current in cells isolated from rat ventricular muscle. *Proc Roy Soc Lond.* **219:** 447-469.

Mitchell MR, Powell T, Terrar DA, Twist VW (1985) Influence of a change in stimulation rate on action potentials, currents and contractions in rat ventricular cells. *J Physiol.* **364:** 113-130.

Morad M, Goldman Y (1973) Excitation-contraction coupling in heart muscle: membrane control of development of tension. *Prog Biophys Mol Biol.* **27:** 257-313.

Morgan HE, Gordon EE, Kira Y, Chua BHL, Russo LA, Peterson CJ, McDermott PJ, Watson PA (1987) Biochemical mechanisms of cardiac hypertrophy. *Ann Rev Physiol.* **49:** 533-543.

Nayler WG, Robertson PGC (1965) Mechanical alternans and the staircase phenomenon in dog papillary muscle. *Am Heart J.* **70:** 494-498.

Niedergerke R (1956) The 'staircase' phenomenon and the action of calcium on the heart. *J Physiol.* **134:** 569-583.

NYHA (1964) Criteria committee, New York Heart Association; *Diseases of the heart and blood vessels: nomenclature and criteria for diagnosis. (6th edition)* Little and Brown Co, Boston. 114.

Paulus WJ, Brutsaert DL (1982) Relaxation abnormalities in cardiac hypertrophy. *Eur Heart J.* **3 (supp A):** 133-137.

Pidgeon J, Lab M, Seed A, Elzinga G, Papadoyannis D, Noble MIM (1980) The contractile state of cat and dog heart in relation to the interval between beats. *Circ Res.* **47:** 559-567.

Poole-Wilson PA, Galindez E, Fry CH (1979) Effect of ouabain in therapeutic concentrations on K^+ exchange and contraction of human and rabbit myocardium. *Clin Sci.* **57:** 415-420.

Purves RD (1981) *Microelectrode methods for intracellular recording and ionophoresis.* Academic Press, London.

Ragnarsdóttir K, Wohlfart B, Johannsson M (1982) Mechanical restitution of the rat papillary muscle. *Acta Physiol Scand.* **115:** 183-191.

Rasmussen, H (1986a) The calcium messenger system (first of two parts). *New Eng J Med.* **314:** 1094-1101.

Rasmussen, H (1986b) The calcium messenger system (second of two parts). *New Eng J Med.* **314:** 1164-1170.

Reuter H (1979) Properties of two inward membrane currents in the heart. *Ann Rev Physiol.* **41:** 413-424.

Reuter H (1984) Ion channels in cardiac cell membranes. *Ann Rev Physiol.* **46:** 473-484.

Ross J (1985) Afterload mismatch in aortic and mitral valve disease: implications for surgical therapy. *JACC.* **5:** 811-817.

Sasayama S, Franklin D, Ross J (1977) Hyperfunction with normal inotropic state of the hypertrophied left ventricle. *Am J Physiol.* **232(4):** H418-H425.

Sasayama S, Ross J, Franklin D, Bloor C, Bishop S, Dilley RB (1976) Adaptations of the left ventricle to chronic pressure overload. *Circ Res.* **38:** 172-178.

Saunders DE, Ord JW (1962) The haemodynamic effects of paroxysmal supraventricular tachycardia in patients with the Wolf-Parkinson-White syndrome. *Am J Cardiol.* **9:** 223-236.

Schaible TF, Ciambrone GJ, Capasso JM, Scheuer J (1984) Cardiac conditioning ameliorates cardiac dysfunction associated with renal hypertension in rats.. *J Clin Invest.* **73:** 1086-1094.

Schaper J, Schaper W (1983) Ultrastructural correlates of reduced cardiac function in human heart disease. *Eur Heart J.* **4 (suppl A):** 35-42.

Scheuer J, Buttrick P (1987) The cardiac hypertrophic responses to pathologic and physiologic loads. *Circulation.* **75(suppl I):** I-63 - I-68.

Schneider JA, Sperelakis N (1975) Slow Ca^{2+} and Na^{+} responses induced by isoproterenol and methylxanthines in isolated perfused guinea pig hearts exposed to elevated K^{+}. *J Mol Cell Cardiol.* **7:** 249-273.

Schwartz K, Lecarpentier Y, Martin J, Lompre A, Mercadier J, Swynghedauw B (1981) Myosin enzymatic distribution correlates with speed of myocardial contraction. *J Mol Cell Cardiol.* **13:** 1071-1075.

Seed WA, Noble MIM, Walker JM, Miller GAH, Pidgeon J, Redwood D, Wanless R, Franz MR, Schoettler M, Schaefer J (1984) Relationships between beat-to-beat interval and the strength of contraction in the healthy and diseased human heart. *Circulation.* **70:** 799-805.

Seed WA, Walker JM (1988) Relation between beat interval and force of the heartbeat and its clinical implications. *Cardiovascular Res.* **22:** 303-314.

Seldinger SI (1953) Catheter replacement of the needle in percutaneous arteriography: a new technique. *Acta Radiol.* **39:** 368-376.

Sellars, RD, Levy MJ, Amplatz K, Lillehei CW (1964) Left retrograde cardioangiography in acquired cardiac disease. Technic, indications and interpretations in 700 cases. *Am J Cardiol.* **14:** 437-447.

Selzer A (1987) Changing aspects of the natural history of valvular aortic stenosis. *New Eng J Med.* **317:** 91-98.

Shattock MJ, Bers DM (1989) Rat vs rabbit ventricle: calcium flux and intracellular sodium assessed by ion selective microelectrodes. *Am J Physiol.* **256:** C813-C822.

Shattock MJ, Bers DM (1987) Inotropic response to hypothermia and the temperature dependence of ryanodine action in isolated rabbit and rat ventricular muscle: implications for excitation-contraction coupling. *Circ Res.* **61:** 761-771.

Shattock MJ, Bullock G, Manning AS, Young M, Hearse DJ (1983) Limitations of the isolated papillary muscle as an experimental model: a metabolic, functional and ultrastructural study. *Clin Sci.* **64:** 4p.

Shimoni Y, Spindler AJ, Noble D (1987) The control of calcium current reactivation by catecholamines and acetylcholine in single guinea-pig ventricular myocytes. *Proc Roy Soc Lond.* **230:** 267-278.

Smith V, Schulman P, Karimeddini MK, White W, Meeran MK, Katz AM (1985) Rapid ventricular filling in left ventricular hypertrophy: II. Pathologic hypertrophy. *JACC.* **5:** 869-874.

Sonnenblick EH (1962) Force-velocity relations in mammalian heart muscle. *Am J Physiol.* **202:** 931-939.

Sonnenblick EH, Braunwald E, Morrow AG (1965) The contractile properties of human heart muscle. Studies on myocardial mechanics of surgically excised papillary muscle. *J Clin Invest.* **44:** 966-977.

Sordahl LA, McCollum WB, Wood WG, Schwartz A (1973) Mitochondria and sarcoplasmic reticulum function in cardiac hypertrophy and failure. *Am J Physiol.* **224:** 497-502.

Spann J, Covell JW, Eckberg DL, Sonnenblick E, Ross J, Braunwald E (1972) Contractile performance of the hypertrophied and chronically failing cat ventricle. *Am J Physiol.* **223(5):** 1150-1157.

Spann JF, Bove AA, Natarajan G, Kreulen T (1980) Ventricular performance, pump function and compensatory mechanism in patients with aortic stenosis. *Circulation.* **62:** 576-582.

Swanton RH, Jenkins BS, Brooksby IAB, Webb-Peploe MM (1976) An analysis of pulsus alternans in aortic stenosis. *European J Cardiol.* **4:** 39-47.

Swinscow TDV (1983) Statistics at square one. *British Medical Association, London.*

Traube L (1872) Ein fall von pulsus bigeminus nebst Bemerkungen über die Leberschwellungen bei Klappenfehler und über acute Leberatrophic. *Bericht Klin Wochenschrift.* **9:** 185-188.

Tritthart H, Volkmann R, Weiss R, Fleckenstein A (1973a) Calcium mediated action potentials in mammalian myocardium. *Naunyn-Schmiedeberg's Arch Pharmacol.* **280:** 239-252.

Tritthart R, Kaufmann R, Volkmer HP, Bayer R, Krause H (1973b) Ca-movement controlling myocardial contractility. I. Voltage, current and time dependence of mechanical activity under voltage clamp conditions (cat papillary muscles and trabeculae). *Pflügers Arch.* **338:** 207-231.

Weber KT, Janicki JS, Pick R, Abrahams C, Shroff SG, Bashey RI, Chen RM (1987) Collagen in the hypertrophied, pressure-overloaded myocardium. *Circulation.* **75(suppl I):** I-40 - I-47.

Weidmann, S (1955) The effect of the cardiac membrane potential on the rapid availability of the sodium-carrying system. *J Physiol.* **127:** 213-224.

Weingart R, Kass RS, Tsien RW (1978) Is digitalis inotropy associated with enhanced slow inward calcium current? *Nature.* **273:** 389-392.

Wenckebach KF (1902) Zur analyse des unregelmässigen Pulses: IV.Ueber den pulsus alternans. *Z Klin Med.* **44:** 218-225.

Wier W, Yue DT (1986) Intracellular calcium transients underlying the short-term force-interval relationship in ferret ventricular myocardium. *J Physiol.* **376:** 507-530.

Wikman-Coffelt J, Parmley WW, Mason DT (1979) The cardiac hypertrophy process: analyses of factors determining pathological vs. physiological development. *Circ Res.* **45:** 697-707.

Williams JF Jr, Potter RD (1974) Normal contractile state of hypertrophied myocardium following pulmonary constriction in the cat. *J Clin Invest.* **54:** 1266-1272.

Winegrad, S. (1984) Regulation of cardiac contractile proteins: correlations between physiology and biochemistry. *Circ Research.* **55:** 565-574.

Wisenbaugh T, Allen P, Cooper G, Holzgrefe H, Beller G, Carasello B (1983) Contractile function, myosin ATPase activity and isoenzymes in the hypertrophied pig left ventricle after a chronic progressive pressure overload. *Circ Res.* **53:** 332-341.

Yang SS, Bentivoglio LG, Maranhão V, Goldberg H (1978) . In: *From cardiac catheterisation data to hemodynamic parameters.* FA Davis, Philadelphia, USA.

Yue DT, Burkhoff D, Franz MR, Hunter WC, Sagawa K (1985) Postextrasystolic potentiation of the isolated canine left ventricle: relationship to mechanical restitution. *Circ Research.* **56:** 340-350.